Structural analysis and multidisciplinary design of flexible fluid loaded composite canard

by

Yang Yang

A dissertation submitted to the graduate faculty

in partial fulfillment of the requirements for the degree of

DOCTOR OF PHILOSOPHY

Major: Aerospace Engineering

Program of Study Committee:
Vinay Dayal, Major Professor
Jerry Vogel
Thomas McDaniel
James Bernard
Adrian Sannier

Iowa State University

Ames, Iowa

2005

Graduate College
Iowa State University

This is to certify that the doctoral dissertation of

Yang Yang

has met the dissertation requirements of Iowa State University

Signature was redacted for privacy.

Major Professor

Signature was redacted for privacy.

For the Major Program

To

my parents,

Mr. Wenyi Yang and Ms. Baohui Liang

TABLE OF CONTENTS

ABSTRACT

Mechanical performance of a composite canard subject to static aerodynamic loads was numerically studied in the present research. The canard was modeled as a symmetrically laminated curved panel, consisting of 8 plies of T300/5208 graphite/epoxy composite laminate. Modeling of this structure-fluid interaction system involves the coupling of two formulations: the solid classically treated in FEM formulation, and the fluid described by potential panel method in CFD. A structure-fluid iterative loop was implemented to simulate the relationship between the deformed aircraft wing and aerodynamic load. The outcome of the structural analysis indicated that the ply orientation have a significant effect on the mechanical performance of the composite laminates such that various design objectives can be achieved just by selecting the proper arrangement of ply orientation and thickness. Three numerical optimization techniques were applied respectively in the structural optimization design which aims at achieving the best structural performance and material efficiency while satisfying certain constraints. Gradient-based CONMIN converged quickly but only provided local optimum values. Probabilistic algorithm GA was capable of achieving the global/near-global optimums but the searching process was time-consuming. HYBRID, an automated hybridization process which combined GA and CONMIN together, has been implemented so that a single run of the algorithm gives a global optimum at reasonable computational cost. A structurally optimized design of the composite canard with lighter weight and higher stiffness has been obtained. A morphing design was performed on this structurally optimized composite panel to improve its maneuverability. An advanced design of composite canard with high structural efficiency and good maneuverability has been obtained by adjusting the ply angles. The strain energy of the host structure decreased which helps reduce the mechanical energy loss and improve the performance of the embedded or bonded actuators/sensors. The improved mechanical performance of the advanced design indicates that the adaptive laminated composite structures enhance the possibility of achieving a multi-functional structure for high performance structural applications.

CHAPTER 1 INTRODUCTION

Composite materials are a new class of materials that combine two or more separate components into a form suitable for structural applications. While each component retains its identity, the new composite material displays desirable macroscopic properties superior to its parent constituents, particularly in terms of mechanical properties and economic value. The use of composites has increased rapidly over the last few years and there is every indication that this will continue.

The attraction of composites primarily stems from their ability to replace the traditional lightweight/high-strength materials such as metals and woods, with an even lighter-weight/higher-strength alternative. Compared to alternative materials, composites have a lower density at equal or greater strength properties. Depending on the application, lighter weight can improve performance, reduce energy needs, simplify handling and speed up installation. Additionally, composites offer new design flexibilities, improved corrosion and wear resistance, low thermal conductivity, increased fatigue life, and most significantly, the possibility of optimal design through the variation of stacking pattern and fiber orientations. These properties can be tailored to meet specific application requirements.

As the aerospace industry increases the usage of composites in primary structures, more and more components are being replaced by composite materials, such as canards, propellers, stiffeners used to stiffen the aircraft skin, wing boxes, etc.. The developments of composite structures have received considerable attention because the structure components made from lightweight / high-strength composite materials are very suitable for aerospace application. In this study, a composite canard of BEECHCRAFT Starship 1 (model 2000) [1] was modeled as a uniform-thickness laminated composite panel with the similar geometry dimensions. The objectives of this work are to analyze the mechanical performances of this laminated composite structure subject to transverse aerodynamic pressures and optimize the existing design to improve the structural efficiency and maneuverability. The major tasks of this dissertation are introduced in this chapter.

1.1 Structure-fluid interaction problem

Deformations of an aircraft during flight may have severe consequences on the aerodynamic performance, maneuverability, and handling qualities. For this reason, the influence of structural deformation on the aerodynamic load distribution and vice versa needs to be considered. Research on structure-fluid interaction in the field of numerical aeroelastic simulation has strongly increased recently. Beckert [2] has proposed a scheme for coupling fluid and structural models in space based on finite interpolation elements. Girodroux-Lavigne et al. [3] have described a computation work for the prediction of static aeroelastic configurations using advanced time-domain structure-fluid coupling method.

This study has coupled efforts on Computational Solid Mechanics, where Finite Element Method (FEM) is applied, with Computational Fluid Dynamics (CFD) based on Potential Flow Panel Method in an interdisciplinary manner. The modeling of this structure-fluid interaction system involves the coupling of two formulations: the solid classically treated in FEM formulation, and the fluid described by potential panel method in CFD. The coupling between the structure and flow requires taking into account the changes of aerodynamic forces due to the deflection of the loaded canard structure. The structural deflections and stresses caused by the aerodynamics loads are calculated through a finite element procedure. The finite element model of the canard is updated after each aerodynamic analysis to include the changes in pressure loads acting on the structural surface. Then the changes of the nodal deflections were taken into account when the aerodynamics loads were recalculated.

The structure-fluid interaction can be considered as a coupling between the aerodynamic forces and the moving structure. The calculations of the aerodynamic forces are dependent of the structural model. The structural and aerodynamic calculations need to exchange some information between them. Therefore, the coupling operator has been introduced, which transfers the loads issued from the aerodynamic simulation on the structural model, and then transfers the deformed shape or structural nodes displacements back to the aerodynamic grid. The same mesh has been taken in CFD calculation as in FEM, in order to transfer all the data between the structural and aerodynamic calculations without extra difficulties.

1.2 Structural analysis

Structural analysis on the laminated composite canard was performed by using FEM and CFD techniques based on Mechanics of Laminated Composite. A finite element program FEMCOMP combined with an aerodynamic subroutine is applied to calculate the deflections, strains, and stresses of the composite canard. For the flow computations, the velocity field for each solution is obtained by applying the Biot-Savart law for all velocity filaments in the system and the corresponding pressures are obtained by applying the Bernoulli equation. The literature background of the structural analysis is introduced briefly as following:

FEM is a numerical method which was developed in 1956 for the analysis of structural problems. Over the years, the finite element technique has been so well established that it is considered to be the best method for solving complex engineering problems [4, 5, 6]. It works reasonably well for calculating structural characteristics and structural responses. Today, the increased performance of computers and new explicit finite element software developments are leading industry to consider the opportunity of using them to aid in design studies. Many studies have shown that the development of finite element techniques for composite structures with their complex behavior is an ambitious but achievable goal which requires basic research activities.

Mechanics of Laminated Composite [7, 8, 9, 10] have been employed as a major part of the theoretical basis of the structural analysis. First-order Shear Deformation Theory (FSDT) of laminate composite plate [11] is incorporated into the literature basis of this structural analysis instead of the Classic Lamination Theory (CLT) because the simplification of the assumed plane stress conditions and neglecting the stress components in transverse direction in CLT is dangerous in the case of laminated composite structure. Since the matrix material is of relatively low shearing stiffness as compared to the fibers, a reliable prediction of the response of these laminated plates must account for interlaminar (transverse) shear deformation or cross-sectional warping of individual layers. Failure and delamination are significantly influenced by transverse shear stresses [12, 13]. Rolfes [14] has mentioned that FSDT copes with assuming the transverse normal stress to be zero and accounts for transverse shear deformation. This is very reasonable since the ratio of the Young's modulus to the Shear modulus for composites can be much higher than for isotropic materials. Noor and Burton [15] have presented extensive surveys on shear deformation theories and computational models relating to laminated plates. Pagano [16] has provided an exact three-dimensional elasticity solution for rectangular cross-ply plates for a simply supported boundary condition.

In this work, Fortran program FEMCOMP was implemented based on FEM, FSDT, CFD potential flow method, and the Mechanics of Laminated Composite. A structure-fluid iterative loop was included to simulate the relationship between the deformed aircraft wing and aerodynamic load. The mechanical performance of the cantilever laminated composite panel under the aerodynamic pressure has been calculated by using FEMCOMP. The relationship between the aerodynamic pressure and deflection of the canard was one of the attractions of this study when calculating the loads on the panel. The pressure results in deflections of the canard. This in turn affects the performance of the aerodynamic loads. A feedback loop of canard behavior and overall pressure distribution in a fluid field was implemented to achieve more accurate and stable results. A suitable failure criterion was applied at the end of the structural analysis to maintain the appropriate margin of safety.

1.3 Optimization using CONMIN, GA and HYBRID methods

Composite laminated structures are widely chosen as the subject of the research on the optimization due to their design flexibilities with respect to ply angles and layer thickness. The optimal designs of laminated plates have been investigated by several researchers. Kim et al. [17] have studied the optimal stacking sequence design of symmetrically laminated plates under in-plane loading to maximize load-bearing, using the Tsai-Wu failure criterion as an objective function. Kam and Chang [18] have worked on the optimal ply arrangements for maximizing stiffness using global optimization technique. Kim and Sin [19] have developed a algorithm for optimizing laminated plate stacking sequences and determining thicknesses, which incorporates discrete ply angles and considers the uncertainties of material properties in a two-step optimization process.

Although extensive research efforts have been devoted to the optimization design of composite laminated plates with various objectives and constraints, some specific requirements of aircraft wing design need further research. Two of the considerations are, the handling of the structure-fluid phenomena, and searching for the efficient optimization method. Three numerical optimization techniques incorporated with FEMCOMP which served as the evaluator of the objective function are applied respectively to improve the existing design in this study. Since the ply orientation and thickness have a significant effect on the performance of the laminated composite canard, in theory, various design objectives can be achieved just by selecting the proper ply orientation and thickness. In aerospace engineering, weight is one of the most important design parameters. Thus, the weight of the canard is considered as the objective value with respect to the ply orientations and plate thickness. This structural optimization aims at achieving the best structural performance and material efficiency while satisfying certain constraints.

First of all, a gradient-based optimizer CONMIN (Constraint Minimization) is applied on the optimization problem to achieve the optimal designs of the structural model. CONMIN was originally implemented by Vanderplaats and the detailed instructions of CONMIN can be found in [20, 21]. The basic algorithm of CONMIN is the method of feasible directions, which incorporates the constraints on the optimization problem directly into the search strategy. Gradient-based algorithms use the iterative improvement technique; the technique is applied to a single point in the search space. During a single iteration, a new point is selected from the neighborhood of current point. If the new point provides a better value of the objective function, the new point becomes the current point. The method terminates if no further improvement is possible.

In general, compared to non-gradient-based algorithms, gradient-based optimizers are capable of reaching an optimum design very quickly, which is one of the greatest advantages of gradient based algorithms. However, engineering optimization problems have often to deal with non-smooth and/or non-convex design spaces and multiple, local minima and saddle points often exist. Consequently some gradient-based optimization techniques get stuck in local optima. It is demonstrated that the gradient-based algorithms provide local optimum values only and these values depend on the selection of the starting point. To increase the chances of success, gradient based algorithms usually are executed for a number of different starting points.

Compared to gradient-based optimization, non-gradient-based optimizers allow to perform the optimum search in a zone of design space significantly larger than in the gradient-based optimization case. Genetic algorithms (GAs) are numerical search procedures derived from the natural genetics and rely on the application of Darwin's principle of survival of the fittest. When a population of biological creatures is allowed to evolve over generations, individual characteristics that are useful for survival tend to be passed onto future generations. GAs maintain a population of potential solutions – other methods process a single point of the search space. In general, the attained design will really be the true global optimum [22].

Since introduced by John Holland [23] at the University of Michigan in 1975, GAs have increasingly been applied in a variety of fields, including medicine, business, and engineering. Goldberg [24] provided an excellent introduction to the use of GAs in search and optimization. GAs have been used extensively in the optimal design of composite laminates. Le Riche and Haftka [25, 26] have performed the structural optimization studies on composite laminates regarding the adjustments of the stacking sequence and thickness using GAs. Muc and Gurba [27] described the concept of using GAs procedure in layout optimization of composite structures and the attention was focused on the applicability of GAs in conjunction with FEM computation of objective functions. On the computation aspect, McMahon et al. [28] have implemented a Fortran 90 GA module which is used to define genetic data types and fitness functions, and to provide a general framework for solving composite laminate structure design problems.

Due to the special consideration of structure-fluid phenomenon in the design of a composite canard, a Fortran program based on GAs is applied on the optimization problem for laminated composite canard in conjunction with structural analysis program FEMCOMP to obtain the global optimums. Again, ply angles and thickness served as the continuous design variables and the weight of the canard is the optimization objective.

GAs have proved to be an effective approach for solving optimization problems. However, there are many existing situations in which the standard GA does not perform well. For a typical GA convergence procedure, initially the solution quality improves very rapidly. But obtaining further improvements soon becomes very difficult, and the majority of the computation time is spent in the later part of the process in which very small improvement is obtained slowly. Despite GAs' superior search ability, it is not able to meet the high expectation that theory predicts for the quality and efficiency of the solution. In general, local search techniques have the advantage of solving the problem quickly, though their results are strongly dependent on the initial starting point; therefore they can easily be trapped in a local optimum. On the other hand, GA samples a large search space, climbs many peaks in parallel, and is likely to lead the search towards the most promising area. However, a GA faces difficulties in fine tuning. It has been widely accepted that a conventional GA is only capable of identifying the high performance region at an affordable time and display inherent difficulties in performing local search for numerical applications [29, 30]. Another problem with GAs is the premature convergence which occurs because of the loss of diversity in the population and it is a commonly encountered problem when the search goes on for several generations [24, 31]. And also, there is no guarantee of convergence to global optima because of GAs' poor exploitation capabilities.

If one can make use of the advantages of both local search and GAs techniques, the optimization algorithm can be improved both effectively and efficiently. Michaelewics [22] suggested that the GAs should be used as a preprocessor to perform the initial search, once the high performance regions of the search space are identified by a GAs, it may be useful to invoke a local search routine to optimize the members of the final population. Many methods of hybridization have been proposed. Kim and Myung [32] developed a two-phase evolutionary programming (TPEP) method, first standard EP method is applied for the initial search and modified EP with limited population (best individual of the first search) has been adopted. However, this method was not able to find the optimal solution for difficult constrained non-linear optimization problems consistently. Baskar et al. [33] improved TPEP by implementing a direct search optimization technique to increase the solution quality and reduce the computational expense. Lin and Lee [34] inserted a local improvement into a standard GA and the real calculation required in the local search is replaced by a regression model which improved the computation efficiency. Chelouah and Siarry [35] proposed a continuous hybrid algorithm combining GA and Nelder-Mead simplex algorithm for continuous multimodal optimization problems which showed better efficiency but seemed not to have a proper criteria for transferring the search from GA to the local optimization algorithms.

In the present work, a hybrid genetic algorithm was developed which consists of a global search using GA to decrease the design space followed by a gradient-based local optimization search to locate the exact optimum. The global search uses the exact analysis in which all redundant iterative loops are omitted. The gradient-based search only focuses on the reduced design space containing the optimum as obtained from the global search. In this way, the good characteristics of gradient method (efficiency, exactness) and GAs (robustness, global optimum) are combined.

1.4 Morphing design

Many aerospace engineers are exploring innovative technologies that will determine the future of flight, which may have the capability to respond to changes in speed or environmental conditions by altering or morphing their shape. NASA-Langley Research Center also proposed the Aircraft Morphing Program which was an attempt to couple research across a wide range of disciplines to integrate smart technologies into high payoff aircraft applications [36].

Morphing structures using distributed induced sensors and strain actuators through closed loop control systems to change shapes are termed adaptive/smart structures. Morphing wings are adaptable to the fluid flow around them structurally and geometrically, thereby changing the wing structural parameters in order to provide the best performance under any flight conditions. An adaptive structure involves distributed actuators and sensors and one or more microprocessors that analyze the responses from the sensors and use integrated control theory to command the actuators to apply localized strains/displacements to alter system response [37]. It has the capability to respond to a changing external environment as well as to a changing internal environment. Applications of adaptive structures to aerospace systems are expanding rapidly.

The adaptive composite structures have enhanced the possibility to carry out shape control, vibration isolation and control, and noise reduction as described in [38]. Laminated composite panel with induced actuators is one of the basic elements of adaptive structures.

Some studies on the design of the adaptive laminated model have been performed [39, 40, 41] and most of the discussion focused on how to develop the theoretical structural finite element model for adaptive structures which have embedded piezoelectric actuators/sensors patches. However, the mechanical energy losses which affect the performance of the adaptive structure severely needs to be considered carefully. On the other hand, the high mechanical energy losses also have influence on the delamination of the composite laminate structure.

Therefore, the energy reduction of the host structure is considered as the objective of the morphing optimization in the present work. The minimization of the strain energy which is produced in the deformed adaptive canard helps to reduce the 'self-heating' which can severely affect the performance of the actuator. In order to achieve the advance composite canard design, the morphing design is performed based on the structural optimization and the host structure, composite laminated canard. The gradient-based optimizer CONMIN is used again to carry out the morphing design of the composite canard.

The primary goal of this dissertation is to study the mechanical performance of the composite canard subject to aerodynamic loads in a structure-fluid phenomenon, to compare the characteristics of gradient-based optimization method and non-gradient-based GAs and develop an improved hybridization optimization method, and finally, to achieve an optimum composite laminated design which has both structural efficiency and excellent maneuverability from the structural optimization and morphing design. This research is restricted to numerical analyses and no models were fabricated. Chapter 2 gives an introduction to the theoretical background of the structural analysis; Chapter 3 performs the FEM analysis on the structure-fluid interaction problem; Chapter 4 and 5 provide the optimization designs using CONMIN and GA respectively; Chapter 6 develops a hybridized optimization method; Chapter 7 carries out the morphing design on the structurally optimized canard; Chapter 8 presents the conclusions of this research work.

CHAPTER 2 THEORETICAL ASPECTS

This chapter is concerned with the theoretical aspects of anisotropic composite materials, finite element method, and potential flow method. The structural analysis on the laminated composite canard is performed based on the theories described in this chapter.

2.1 Theories of composite laminate

Conventional metallic materials are nearly isotropic. That is, the properties associated with an axis passing through a point in the material are generally independent of the orientation of the axis. By comparison, the properties of composites are anisotropic since their properties are essentially dependent on orientation. A composite material is heterogeneous at the constituent material level, with properties possibly changing from point to point. Composite laminate is fiber-oriented in the desired directions and bonded together in a structural unit since the unidirectional lamina is not a good structural component due to poor transverse properties. The virtually limitless combinations of ply materials, ply orientations, and ply stacking sequences are offered by laminated construction.

Composite structures are generally fabricated in the form of laminates consisting of multiple laminae, or plies, considerably enhance the design flexibility inherent in composite structures.

Since each kind of composite has characteristic material property symmetries, it is possible to simplify the general anisotropic stress-strain relationships. In particular, the symmetry possessed by the unidirectional lamina simplifies it to an orthotropic material. An orthotropic material has three material symmetry planes in three mutually perpendicular directions at a point.

2.1.1 The stress-strain relationship for the generally orthotropic lamina

In the analysis of laminates having multiple laminae it is often necessary to know the stress-strain relationships for the generally orthotropic lamina in nonprincipal (off-axis) coordinate (1, 2, 3) and global coordinate (x, y, z), as shown in Fig. 2.1 [9, 10].

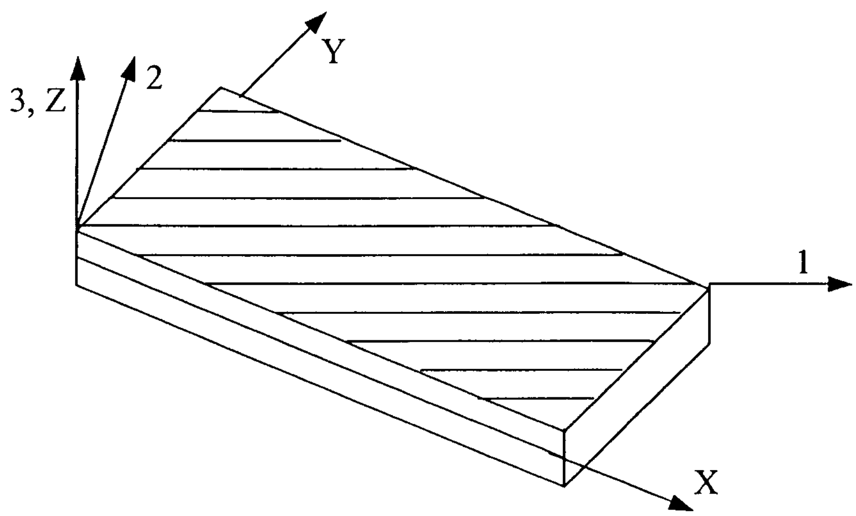

Fig. 2.1: Global and local coordinates of a lamina

The transformation equations for the stresses in the 1, 2 coordinate system is written in matrix form as

$$\begin{Bmatrix} \sigma_x \\ \sigma_y \\ \sigma_{xy} \end{Bmatrix} = \begin{bmatrix} \cos^2\theta & \sin^2\theta & -2\cos\theta\sin\theta \\ \sin^2\theta & \cos^2\theta & 2\cos\theta\sin\theta \\ \cos\theta\sin\theta & -\cos\theta\sin\theta & \cos^2\theta - \sin^2\theta \end{bmatrix} \begin{Bmatrix} \sigma_1 \\ \sigma_2 \\ \sigma_{12} \end{Bmatrix} \tag{2.1}$$

The stress-strain relationship of a lamina in the 1, 2 coordinate system are given by

$$\begin{Bmatrix} \sigma_1 \\ \sigma_2 \\ \sigma_{12} \end{Bmatrix} = \begin{bmatrix} Q_{11} & Q_{12} & 0 \\ Q_{21} & Q_{22} & 0 \\ 0 & 0 & Q_{66} \end{bmatrix} \begin{Bmatrix} \varepsilon_1 \\ \varepsilon_2 \\ \varepsilon_{12} \end{Bmatrix}, \quad \begin{Bmatrix} \sigma_4 \\ \sigma_5 \end{Bmatrix} = \begin{bmatrix} Q_{44} & Q_{45} \\ Q_{45} & Q_{55} \end{bmatrix} \begin{Bmatrix} \varepsilon_4 \\ \varepsilon_5 \end{Bmatrix} \tag{2.2}$$

where the Q_{ij} are the components of the lamina stiffness matrix, which are related to the engineering constants by

$$
\begin{aligned}
Q_{11} &= \frac{E_1}{1-\nu_{12}\nu_{21}} \\
Q_{12} &= \frac{\nu_{12}E_2}{1-\nu_{12}\nu_{21}} = Q_{21} \\
Q_{22} &= \frac{E_2}{1-\nu_{12}\nu_{21}} \\
Q_{66} &= G_{12}
\end{aligned}
\tag{2.3}
$$

The tensor strains transform the same way as the stresses, and the stress-strain relation in the global coordinate system can be written as

$$
\begin{Bmatrix} \sigma_x \\ \sigma_y \\ \sigma_{xy} \end{Bmatrix} = \begin{bmatrix} \overline{Q}_{11} & \overline{Q}_{12} & \overline{Q}_{16} \\ \overline{Q}_{12} & \overline{Q}_{22} & \overline{Q}_{26} \\ \overline{Q}_{16} & \overline{Q}_{26} & \overline{Q}_{66} \end{bmatrix} \begin{Bmatrix} \varepsilon_x \\ \varepsilon_y \\ \varepsilon_{xy} \end{Bmatrix}, \quad \begin{Bmatrix} \sigma_{yz} \\ \sigma_{xz} \end{Bmatrix} = \begin{bmatrix} \overline{Q}_{44} & \overline{Q}_{45} \\ \overline{Q}_{45} & \overline{Q}_{55} \end{bmatrix} \begin{Bmatrix} \varepsilon_{yz} \\ \varepsilon_{xz} \end{Bmatrix}
\tag{2.4}
$$

where the $\overline{Q}_{ij}$ are the components of the transformed lamina stiffness matrix which are defined as follows:

$$
\begin{aligned}
\overline{Q}_{11} &= Q_{11}\cos^4\theta + Q_{22}\sin^4\theta + 2(Q_{12}+2Q_{66})\sin^2\theta\cos^2\theta \\
\overline{Q}_{12} &= (Q_{11}+Q_{22}-4Q_{66})\sin^2\theta\cos^2\theta + Q_{12}(\cos^4\theta + \sin^4\theta) \\
\overline{Q}_{22} &= Q_{11}\sin^4\theta + Q_{22}\cos^4\theta + 2(Q_{12}+2Q_{66})\sin^2\theta\cos^2\theta \\
\overline{Q}_{16} &= (Q_{11}-Q_{12}-2Q_{66})\cos^3\theta\sin\theta - (Q_{22}-Q_{12}-2Q_{66})\cos\theta\sin^3\theta \\
\overline{Q}_{26} &= (Q_{11}-Q_{12}-2Q_{66})\cos\theta\sin^3\theta - (Q_{22}-Q_{12}-2Q_{66})\cos^3\theta\sin\theta \\
\overline{Q}_{66} &= (Q_{11}+Q_{22}-2Q_{12}-2Q_{66})\sin^2\theta\cos^2\theta + Q_{66}(\sin^4\theta + \cos^4\theta) \\
\overline{Q}_{44} &= Q_{44}\cos^2\theta + Q_{55}\sin^2\theta \\
\overline{Q}_{45} &= (Q_{55}-Q_{44})\cos\theta\sin\theta \\
\overline{Q}_{55} &= Q_{55}\cos^2\theta + Q_{44}\sin^2\theta
\end{aligned}
\tag{2.5}
$$

where θ is the angle (measured counter-clockwise) between the x-y and 1-2 axes (see Fig. 2.1).

2.1.2 Classical Lamination Theory

In Classical Lamination Theory (CLT), it is assumed that the individual laminae are perfectly bonded together so as to behave as a unitary, nonhomogeneous, anisotropic panel. The displacements across lamina interfaces are assumed to be continuous, with no interfacial slip. Each ply is assumed to be in a state of plane stress and that interlaminar stresses are neglected. CLT will not be discussed in detail in this work. A complete set of equations is given as follows:

$$\begin{Bmatrix} N_x \\ N_y \\ N_{xy} \\ M_x \\ M_y \\ M_{xy} \end{Bmatrix} = \begin{bmatrix} A_{11} & A_{12} & A_{16} & B_{11} & B_{12} & B_{16} \\ A_{12} & A_{22} & A_{26} & B_{12} & B_{22} & B_{26} \\ A_{16} & A_{26} & A_{66} & B_{16} & B_{26} & B_{66} \\ B_{11} & B_{12} & B_{16} & D_{11} & D_{12} & D_{16} \\ B_{12} & B_{22} & B_{26} & D_{12} & D_{22} & D_{26} \\ B_{16} & B_{26} & B_{26} & D_{16} & D_{26} & D_{66} \end{bmatrix} \begin{Bmatrix} \varepsilon_x^0 \\ \varepsilon_y^0 \\ \gamma_{xy}^0 \\ \kappa_x \\ \kappa_y \\ \kappa_{xy} \end{Bmatrix} \tag{2.6}$$

where ε_x^0, ε_y^0 and ε_{xy}^0 are the strains on the middle surface;

κ_x, κ_y and κ_{xy} are the curvatures of the middle surface;

N_x, N_y, and N_{xy} are the forces per unit length;

M_x, M_y, and M_{xy} are the moments per unit length;

the laminate extensional stiffnesses are given by

$$A_{ij} = \int_{-t/2}^{t/2} (\overline{Q}_{ij})_k dz = \sum_{k=1}^{N} (\overline{Q}_{ij})_k (z_k - z_{k-1}) \tag{2.7}$$

the laminate coupling stiffnesses are given by

$$B_{ij} = \int_{-t/2}^{t/2} (\overline{Q}_{ij})_k z dz = \frac{1}{2} \sum_{k=1}^{N} (\overline{Q}_{ij})_k (z_k^2 - z_{k-1}^2) \tag{2.8}$$

the laminate bending stiffnesses are given by

$$D_{ij} = \int_{-t/2}^{t/2} (\overline{Q}_{ij})_k z^2 dz = \frac{1}{3} \sum_{k=1}^{N} (\overline{Q}_{ij})_k (z_k^3 - z_{k-1}^3) \tag{2.9}$$

where z_{k-1} is the distance from middle surface to inner surface of the kth lamina, z_k is the corresponding distance from middle surface to outer surface of the kth lamina, as shown below in Fig.2.2.

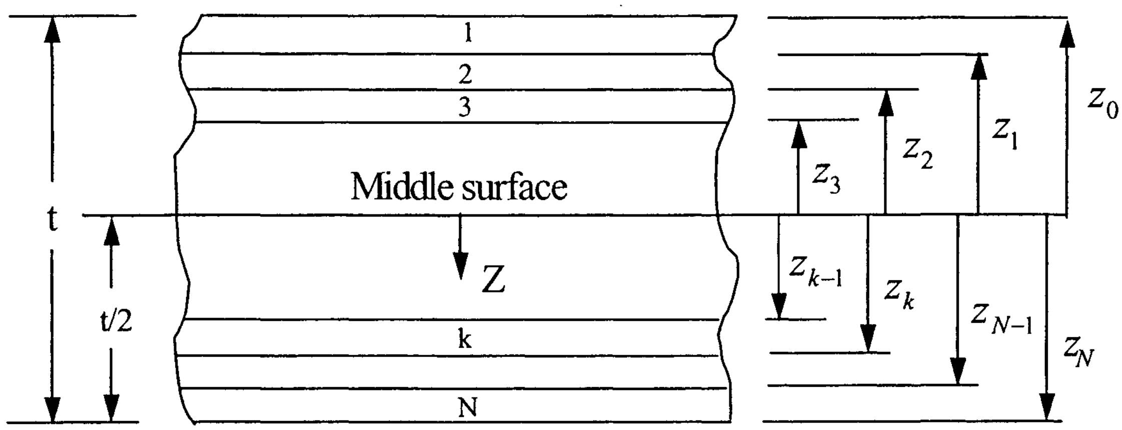

Fig. 2.2: Laminate geometry and ply numbering system

Quasi-isotropic laminates. In structural analysis, only symmetric quasi-isotropic laminate is considered which is also defined as the starting point of the optimization of ply orientations. It has both geometric and material property symmetry about the middle surface. Quasi-isotropic laminate consists of three or more identical orthotropic laminae which are oriented at the same angle relative to adjacent laminae. The extensional stiffness matrix [A] is identical to one for an isotropic material, but the stiffness matrix [D] do not necessarily have isotropic form. The extensional force-deformation relationships for the quasi-isotropic laminated are given by

$$\begin{Bmatrix} N_x \\ N_y \\ N_{xy} \end{Bmatrix} = \begin{bmatrix} A_{11} & A_{12} & 0 \\ A_{12} & A_{11} & 0 \\ 0 & 0 & (A_{11} - A_{12})/2 \end{bmatrix} \begin{Bmatrix} \varepsilon_x^0 \\ \varepsilon_y^0 \\ \gamma_{xy}^0 \end{Bmatrix} \tag{2.10}$$

Since there is equal probability of fibers oriented in any direction, or there is a continuous variation in fiber orientation, directionality would disappear in quasi-isotropic laminate. Quasi-isotropic laminates represent the minimum performance which is expected from a composite laminate

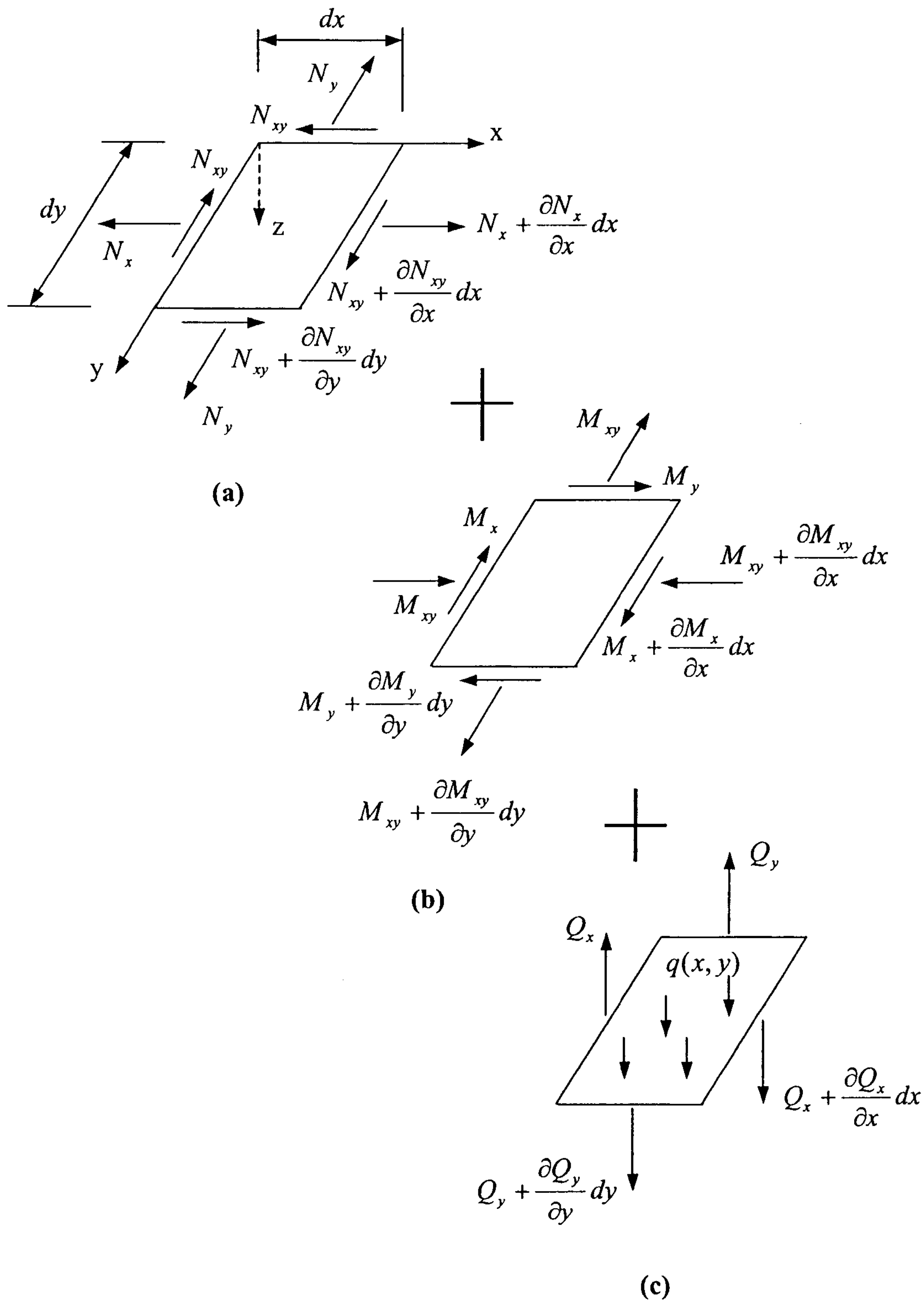

Fig. 2.4: Stress resultants and external loads acting on laminate. (From Halpin [10])

2.1.3 First-order Shear Deformation Theory (FSDT) of laminated plate

Since most of the aerospace structures are thin-walled, the stress analysis is often carried out assuming plane stress conditions and neglecting the stress components in transverse direction. While this simplification is reasonable for structure made of homogenous isotropic materials, it could be dangerous in the case of laminated composite structures. Experimental investigations have shown that failure can occur in a transverse shearing mode when certain combinations of in-plane compression and in-plane shear are acting. This failure is significantly influenced by transverse shear stresses. Furthermore, the development and progression of delaminations, which are eventually the most severe type of damage in laminated composites, is very much affected by transverse stresses.

CLT and FSDT are widely used for the analysis of layered composite structures. While CLT is based on the assumption of a single lamina under plane stress, FSDT copes with assuming the transverse normal stress to be zero and accounts for transverse shear deformation. This is very reasonable since the ration of the Young's modulus to the Shear modulus can be much higher for composites than for isotropic materials.

Reddy [11] presented a generalization about FSDT of laminated composite plate, where the displacement field is assumed to be of the form

$$
\begin{aligned}
u(x,y,z,t) &= u_0(x,y,t) + z\phi_1(x,y,t) \\
v(x,y,z,t) &= v_0(x,y,t) + z\phi_2(x,y,t) \\
w(x,y,z,t) &= w_0(x,y,t)
\end{aligned}
\tag{2.11}
$$

where

u_0 and v_0 are the tangential displacements of the middle surface along the x and y directions, respectively;

w_0 is the transverse displacement at the middle surface and the same as the transverse displacement of any point having the same x and y coordinates because the transverse normal strain ε_z is negligible;

(u, v, w) denote the displacements along the (x, y, z) directions of a point $(x, y, 0)$ on the midplane;

(ϕ_1, ϕ_2) are the rotations of the transverse normals about the y and x axes, see Fig. 2.3.

For the classical theory, it is assumed that

$$\phi_1 = -\frac{\partial w}{\partial x} \text{, and } \phi_2 = -\frac{\partial w}{\partial y} \tag{2.12}$$

The strain-displacement relations can be obtained as following

$$\begin{aligned}
\varepsilon_x &= \frac{\partial u}{\partial x} + z\frac{\partial \phi_1}{\partial x} \\
\varepsilon_y &= \frac{\partial v}{\partial y} + z\frac{\partial \phi_2}{\partial y} \\
\varepsilon_z &= 0 \\
\varepsilon_{yz} &= \phi_2 + z\frac{\partial w}{\partial y} \\
\varepsilon_{xz} &= \phi_1 + z\frac{\partial w}{\partial x} \\
\varepsilon_{xy} &= \frac{\partial u}{\partial y} + \frac{\partial v}{\partial x} + z(\frac{\partial \phi_1}{\partial y} + \frac{\partial \phi_2}{\partial x})
\end{aligned} \tag{2.13}$$

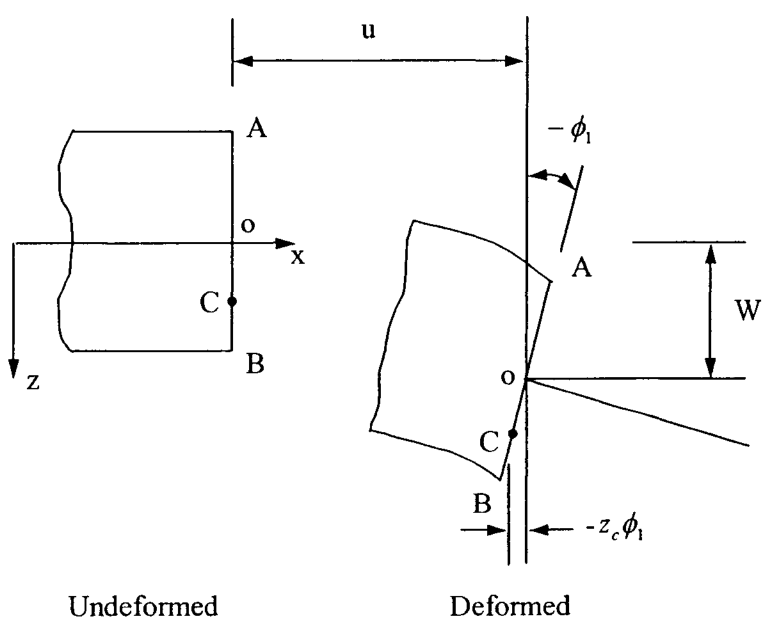

Fig. 2.3: Geometry of deformation in the x-z plane for the FSDT analysis

2.1.4 Analysis of small transverse deflections

The analysis of transverse deflections of laminates has its basis in CLT. It is convenient to use an infinitesimal element, as shown in Fig. 2.4 from Halpin [10]. In-plane stress resultants are shown in Fig. 2.4 (a), moment resultants are shown in Fig. 2.4 (b), and transverse shear stress resultants are shown in Fig. 2.4 (c).

In the diagrams, we assume that the transverse deflections are small, so that the out-of-plane components of the in-plane resultants N_x, N_y, and N_{xy} are negligible. $q(x, y)$ is a distributed transverse load. The transverse shear stress resultants Q_x and Q_y are similarly defined as

$$Q_x = \int_{-t/2}^{t/2} \tau_{xz} dz \tag{2.14}$$

$$Q_y = \int_{-t/2}^{t/2} \tau_{yz} dz \tag{2.15}$$

The differential equations of static equilibrium of the plate in terms of stress and moment resultants according to Newton's second law are

$$\frac{\partial N_x}{\partial x} + \frac{\partial N_{xy}}{\partial y} = 0 \tag{2.16}$$

$$\frac{\partial N_y}{\partial y} + \frac{\partial N_{xy}}{\partial x} = 0 \tag{2.17}$$

$$\frac{\partial Q_x}{\partial x} + \frac{\partial Q_y}{\partial y} + q(x, y) = 0 \tag{2.18}$$

where $Q_y = \dfrac{\partial M_y}{\partial y} + \dfrac{\partial M_{xy}}{\partial x}$ and $Q_x = \dfrac{\partial M_x}{\partial x} + \dfrac{\partial M_{xy}}{\partial y}$

By substituting the laminate force-deformation equations, strain-displacement relations, and the curvature-displacement equations in Eqs. (2.16), (2.17), and (2.18), the corresponding equilibrium equations in terms of displacement can be derived as following

$$
\begin{aligned}
&A_{11}\frac{\partial^2 u_0}{\partial x^2}+2A_{16}\frac{\partial^2 u_0}{\partial x\partial y}+A_{66}\frac{\partial^2 u_0}{\partial y^2}+A_{16}\frac{\partial^2 v_0}{\partial x^2}+(A_{12}+A_{66})\frac{\partial^2 v_0}{\partial x\partial y}+A_{26}\frac{\partial^2 v_0}{\partial y^2}\\
&-B_{11}\frac{\partial^3 w}{\partial x^3}-3B_{16}\frac{\partial^3 w}{\partial x^2\partial y}-(B_{12}+2B_{66})\frac{\partial^3 w}{\partial x\partial y^2}-B_{26}\frac{\partial^3 w}{\partial y^3}=0
\end{aligned}
\tag{2.19}
$$

$$
\begin{aligned}
&A_{16}\frac{\partial^2 u_0}{\partial x^2}+(A_{12}+A_{66})\frac{\partial^2 u_0}{\partial x\partial y}+A_{26}\frac{\partial^2 u_0}{\partial y^2}+A_{66}\frac{\partial^2 v_0}{\partial x^2}+2A_{26}\frac{\partial^2 v_0}{\partial x\partial y}+A_{22}\frac{\partial^2 v_0}{\partial y^2}\\
&-B_{16}\frac{\partial^3 w}{\partial x^3}-(B_{12}+2B_{66})\frac{\partial^3 w}{\partial x^2\partial y}-3B_{26}\frac{\partial^3 w}{\partial x\partial y^2}-B_{22}\frac{\partial^3 w}{\partial y^3}=0
\end{aligned}
\tag{2.20}
$$

$$
\begin{aligned}
&D_{11}\frac{\partial^4 w}{\partial x^4}+4D_{16}\frac{\partial^4 w}{\partial x^3\partial y}+2(D_{12}+2D_{66})\frac{\partial^4 w}{\partial x^2\partial y^2}+4D_{26}\frac{\partial^4 w}{\partial x\partial y^3}+D_{22}\frac{\partial^4 w}{\partial y^4}\\
&-B_{11}\frac{\partial^3 u_0}{\partial x^3}-3B_{16}\frac{\partial^3 u_0}{\partial x^2\partial y}-(B_{12}+2B_{66})\frac{\partial^3 u_0}{\partial x\partial y^2}-B_{26}\frac{\partial^3 u_0}{\partial y^3}\\
&-B_{16}\frac{\partial^3 v_0}{\partial x^3}-(B_{12}+2B_{66})\frac{\partial^3 v_0}{\partial x^2\partial y}-3B_{26}\frac{\partial^3 v_0}{\partial x\partial y^2}-B_{22}\frac{\partial^3 v_0}{\partial y^3}=q(x,y)
\end{aligned}
\tag{2.21}
$$

The in-plane displacements u_0 and v_0 are coupled with transverse displacements, w, when the coupling stiffness, B_{ij}, are present in above equations. For symmetric laminates with $B_{ij}=0$, Eq. (2.21) alone becomes the governing equation for transverse displacements. These governing partial differential equations must be solved subject to the appropriate boundary conditions.

2.1.5 Laminate strength analysis

For the determination of strength of any material it is a common practice to estimate the stress at the time and the location when failure occurs. According to Tsai and Hahn [8], for composite materials, the failure phenomenon is rather complex. The unidirectional composites have highly directionally dependent strength. The longitudinal strength is much more than that of the transverse and shear strengths, so all three stress components have to be examined before judgment on the cause of failure. The reason is that in longitudinal direction the strength depends on fiber properties while the transverse and shear strength depends on matrix properties.

To determine the strength, we need a failure criterion for the unidirectional plies. The strength of a laminated composite will be based on the strength of the individual plies within a laminate. As the loads applied to the laminate increase, successive ply failure will result. The first ply failure (FPF) will be followed by other ply failures until the last ply failure which would be the ultimate failure of the laminate.

Quadratic interaction criterion. The quadratic failure criterion is a widely used approach to determine the failure of unidirectional composite. It is based on the on-axis stress or strain as the basic variable with different tensile and compressive strengths.

$$F_{ij}\sigma_i\sigma_j + F_i\sigma_j = 1 \tag{2.22}$$

where F 's are strength parameters. When the equation is satisfied, failure results.

Eq. (2.22) can be explained in the form given below

$$\begin{aligned} &F_{11}\sigma_1^2 + 2F_{12}\sigma_1\sigma_2 + F_{22}\sigma_2^2 + F_{66}\sigma_6^2 + 2F_{16}\sigma_1\sigma_6 \\ &\qquad + 2F_{26}\sigma_2\sigma_6 + F_1\sigma_1 + F_2\sigma_2 + F_6\sigma_6 = 1 \end{aligned} \tag{2.23}$$

In the natural coordinate system, the shear strength should be unaffected by the direction or sign of the shear stress component. But sign reversal for the normal stress components has a significant effect on the strength of the composite. So, the terms that contain first-order shear stress are deleted from the equation. Then we get

$$F_{11}\sigma_1^2 + 2F_{12}\sigma_1\sigma_2 + F_{22}\sigma_2^2 + F_{66}\sigma_6^2 + F_1\sigma_1 + F_2\sigma_2 = 1 \tag{2.24}$$

where F_{11}, F_{22}, F_{66}, F_1, and F_2 can be measured by performing simple longitudinal tensile, compressive, and shear tests and transverse tensile and compressive tests. F_{12}, which is related to the interaction between two normal stress components, can be determined by a complex biaxial test. Such tests are not easy to perform, hence in place of this test, it is assumed that the orthotropic failure criterion in Eq. (2.24) is a generalization of the von Mises criterion with,

$$F_{12}^* = -\frac{1}{2} \tag{2.25}$$

The strength parameters F 's are fixed for a given material. When imposed stress components are substituted into Eq. (2.24), a positive numerical value is produced. If the value is equal to unity, the failure criterion is satisfied, and failure will occur under the given stress components. If the imposed stress components are smaller, the value of left-hand side is less than unity, failure will not occur.

Strength ratios. For increasing the information given by the failure criterion, we can use a different variable, strength R, which not only defines the upper bound where the allowable or ultimate exist, but also indicates the quantitative measure of the safety margin,

$$\sigma_{i(a)} = R\sigma_i \qquad \varepsilon_{i(a)} = R\varepsilon_i \tag{2.26}$$

where stress or strain components without remarks are those applied or imposed; subscript (a) means the allowed or the ultimate stress or strain.

Some features of R are described below,

1. when applied stress or strain is zero, $R = \infty$
2. when the stress or strain is safe, $R > 1$
3. when the allowable or ultimate stress or strain is reached, $R = 1$
4. R can not be less than unity which has no physical reality

Rewriting Eq. (2.22) with the allowable stresses,

$$F_{ij}\sigma_{i(a)}\sigma_{j(a)} + F_i\sigma_{i(a)} = 1 \tag{2.27}$$

Substituting Eq. (2.26) to (2.27)

$$[F_{ij}\sigma_i\sigma_j]R^2 + [F_i\sigma_i]R - 1 = 0 \tag{2.28}$$

or

$$aR^2 + bR - 1 = 0 \tag{2.29}$$

The solution of this quadratic equation gives two strength ratios,

$$R, R' = \pm\sqrt{(b/2a) + (1/a)} + (b/2a) \tag{2.30}$$

Usually, only R is useful.

2.2 Finite element method

In engineering, a complicated real life problem is replaced by a simpler simulation for which a solution can be obtained. For most practical problems, an approximate solution is sought rather than the exact one because of the financial considerations and the limitation of the existing mathematical tools. It is often possible to improve and refine the approximate solution by spending more computational efforts in FEM. The limitations on this refinement are time and computer capacity. The general applicability of the finite element method makes it a powerful and versatile tool for a wide range of problems, especially for engineering analyses.

2.2.1 General description of FEM

In the finite element method, the actual continuum is represented as finite elements. These elements are considered to be interconnected at nodes and maintain the continuity between elements. The nodes usually lie on the element boundaries where adjacent elements are connected. It is called finite element discretization. Since the actual variation of the field variable inside the continuum is not known, it is assumed that the variation of the field variable inside a finite element can be approximated by a simple function. These approximating functions for the whole continuum are written. The new unknowns are the nodal values of the field variable. The solution to the approximate displacement field is obtained by minimizing the total potential of the elements. This results in a set of linear equations which can be written in matrix formulation. The solution of these equations over the structure provides with the nodal values of the field variables. Once these are known, the approximating functions define the field variable throughout the assemblage of elements. To extend the concept to the structures field, the terminology has to be modified, such as, structure in place of continuum or domain, displacement in place of field variable, stiffness matrix in place of characteristic matrix, and element strains in place of element resultants.

The solution of governing differential equation over every element is approximated by a linear combination of unknown parameters (undetermined values at the nodes of the element) and pre-selected interpolating of approximate function (shape function). The number of unknowns and the number of equations are equal to the total number of degree of freedom in the entire domain. The solution $u(x)$ can be written as

$$u(x) \approx U_e(x) = \sum_{j=1}^{n} U_j^e \psi_j^e(x) \tag{2.31}$$

where U_e is the finite element interpolation of u on a typical element Ω_e, U_j^e is the value of U_e at the j-th node (unknown parameter), and $\psi_j^e(x)$ are the interpolating polynomials.

Procedure of finite element analysis. The procedure of FEM for a structural problem can be stated in the following steps:

1. *Discretization of the structure*

   Divide the structure to be analyzed into subdivisions and model it with suitable finite elements. The number, type, size and arrangement of the elements have to be decided.

2. *Selection of a proper interpolation model*

   Some suitable solution within an element is assumed to approximate the unknown solution because the displacement solution of a complex structure under any specified load conditions cannot be predicted exactly. The assumed solution should be simple from computational point of view and satisfy certain convergence requirements. In general, the solution or the interpolation model is taken in the form of a polynomial.

3. *Derivation of element stiffness matrices and load vectors*

   From the assumed displacement model, the stiffness matrix $[K^{(e)}]$ and the load vector $P^{(e)}$, of element "e" are to be derived by using either equilibrium conditions or a suitable variational principle.

4. *Assemblage of element equations to obtain the overall equilibrium equations*

   Since the structure may be composed of several finite elements, the individual element stiffness matrices and load vectors are assembled maintaining continuity and equilibrium equations resulting in

   $$[K]\{u\} = \{F\} \tag{2.32}$$

   where $[K]$ is the assembled stiffness matrix, $\{u\}$ is the vector of nodal displacements after boundary conditions are applied and $\{F\}$ is the vector of nodal forces for the complete structure.

5. *Solution for the unknown nodal displacements*

   The overall equilibrium equations are modified to account for the boundary conditions of the problem.

   For linear problems, u can be solved easily. But for nonlinear problems, the stiffness matrix $[K]$ and/or the load vector $\{F^e\}$ have to be updated several times to get the solution.

6. *Computation of element strains and stresses*

   From the known nodal displacements u, the element strains can be computed by using kinematic relations. Then stresses can be computed using the material stiffness properties.

The whole procedure is implemented by Fortran language to calculate the deformations, stresses, and strains of the composite laminated plate under aerodynamic loading.

2.2.2 Shear deformable plate element

The discretization of the domain into subregions is equivalent to replacing the domain having an infinite number of degrees of freedom by a system having finite number of degrees of freedom. The shapes, sizes, number and configurations of the elements have to be chosen carefully such that the original body or domain is simulated as closely as possible without extensive computational effort.

A rectangular linear (4 nodes) plate element is presented here. The displacements $(u_1, u_2, u_3, \phi_1, \phi_2)$ are interpolated by expression of the form,

$$u_i = \sum_{j=1}^{n} u_j^i \psi_j(\xi_1, \xi_2), \qquad i = 1,2,3, \tag{2.33}$$

$$\phi_i = \sum_{j=1}^{n} \phi_i^j \psi_j(\xi_1, \xi_2), \qquad i = 1,2$$

Where ψ_j are the interpolation functions, and u_i^j and ϕ_i^j are the nodal values of u_i and ϕ_i, respectively; n is the number of the nodes per element. The ξ_1 and ξ_2 coordinate system is called the natural coordinate system in Fig. 2.5.

The interpolation function for this four nodes element is linear and given as

$$\psi_1 = \frac{1}{4}(1-\xi_1)(1-\xi_2) \qquad \psi_2 = \frac{1}{4}(1+\xi_1)(1-\xi_2) \tag{2.34}$$

$$\psi_3 = \frac{1}{4}(1+\xi_1)(1+\xi_2) \qquad \psi_4 = \frac{1}{4}(1-\xi_1)(1+\xi_2)$$

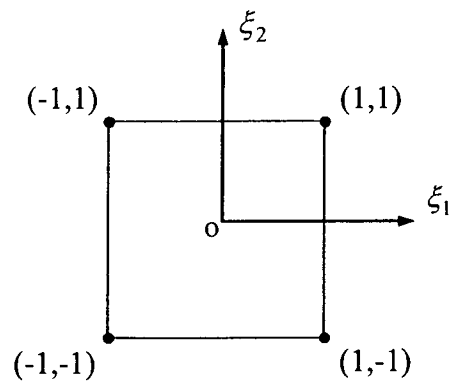

Fig. 2.5: Four-node plate element geometry in local coordinate system

After the interpolation functions are defined, all the integration can be performed in the natural coordinate system. The elements are mapped to the global coordinate system to formulate the global stiffness matrix. Boundary conditions are applied on the assembled equations. They are solved for the nodal values of displacements.

2.2.3 Finite element formulation

Substituting the displacements of Eq. (2.33) into the virtual work principle, the finite element form of the static version of the governing equation of motion is obtained

$$[K]\{\Delta\} = \{F\} \tag{2.35}$$

where $\{\Delta\}$ is the vector of nodal values of displacements $(u_1, u_2, u_3, \phi_1, \phi_2)$. $[K]$ is the stiffness matrix and $\{F\}$ is the imposed force vector.

These equations cannot be solved for $\{\Delta\}$ because the matrix $[K]$ is singular and its inverse doesn't exist. In the case of solid mechanics, it means that the loaded body or structure is free to undergo unlimited rigid body motion unless some support constraints are imposed to keep the body or structure in equilibrium under the loads. Appropriate boundary conditions have to be applied to Eq. (2.35). The number of degrees of freedom to be specified is dictated by the physics of the problem.

2.2.4 Calculation of stresses and strains

Once the nodal displacements have been obtained, the strains are evaluated in each element by differentiating the displacement. The continuity of displacement is ensured at the boundaries of the elements in the displacement-based finite element model, but not of strains. Strains are continuous within an element. Stains and stresses may jump across element boundary, and cause a less accurate solution for stresses. This jump can be reduced by using smaller elements sizes or more complex element types.

Strains can be calculated in global coordinate system. But we need to transform strains and stresses to the local coordinate, since the failure criteria used in this study requires that stresses remain in the local coordinate system. The strains for the laminate are calculated over the elements. Then, based on the assumption that the strains are continuous over individual plies, the ply strains are calculated. Next, these off-axis strains are changed to on-axis strains using the relations

$$\begin{Bmatrix} \varepsilon_1 \\ \varepsilon_2 \\ \varepsilon_6 \end{Bmatrix} = \begin{bmatrix} \cos^2\theta & \sin^2\theta & \cos\theta\sin\theta \\ \sin^2\theta & \cos^2\theta & -\cos\theta\sin\theta \\ -\cos\theta\sin\theta & 2\cos\theta\sin\theta & 2(\cos^2\theta - \sin^2\theta) \end{bmatrix} \begin{Bmatrix} \varepsilon_x \\ \varepsilon_y \\ \varepsilon_{xy} \end{Bmatrix} \tag{2.36}$$

The stresses can then be calculated for each ply in the local coordinate system, using Eq. (2.1) for the calculation on each ply.

2.3 Potential flow panel method

Wing lift forces and/or pressure fields generated by the interaction between the wing and free stream flow are defined by means of a potential flow panel method procedure. The flow field is assumed to be incompressible, steady, and irrotational. Velocity potential fields generated in the potential flow simulations are composed of a superposition of rectilinear free stream and vortex components. Source components are not used since the wing is assumed to be a thin lifting surface. This is a reasonable assumption since thickness plays an insignificant role in lift generation. The wing lifting surface is represented by a series of quadrilateral panels each of which supports a constant strength vortex filament along the outer boundary, thus creating a series of ring vortices. A wake panel and corresponding ring vortex that extends from the trailing edge of the lifting surface to infinity behind the wing is used to develop the wing wake. Vortex strengths for each solution are obtained by satisfying no-flow-through boundary conditions at the center of each wing based ring vortex and a Kutta condition at the trailing edge which guarantees proper flow from the wing to the wake behind the wing. The velocity field for each solution is obtained by applying the Biot-Savart law for all velocity filaments in the system and the corresponding pressures are obtained by applying the Bernoulli equation.

CHAPTER 3 MULTIDISCIPLINARY ANALYSIS ON A COMPOSITE CANARD

Modern aircraft design is a multidisciplinary process in which a large number of disciplines and design variables are involved due to the complexity of aerospace systems. The efficient coordination of various disciplinary analysis capabilities and effective communication among the design departments which are strongly separated by disciplines are required. The interest in this methodology causes an increase in the number of interdisciplinary couplings and also makes it become hard for the designer to estimate the consequences of changing certain subsystems. In this section, an interdisciplinary analysis is applied on a composite canard by integrating two disciplines, the aerodynamics discipline evaluated the pressure distribution, and the structures discipline calculated the canard deformations and stresses resulting from the air pressure.

A finite element analysis (FEA) program FEMCOMP was implemented in Fortran based on the Mechanics of Laminated Composite and FEM discussed in Chapter 2. In this chapter, the structural analysis is performed on the composite canard by using FEMCOMP, which coupled two disciplines, structure and aerodynamics. The integrated structure-fluid software FEMCOMP is employed to analyze the mechanical behaviors – the deflections, stresses, and strains of the composite canard under the aerodynamic loads, and then evaluate the modified designs during the optimization process in the following chapters.

3.1 Description of structure – fluid interaction problem

The canard (a horizontal stabilizer in front of the wing) of Beechcraft Starship 2000 has been selected as the model of the numerical study. Beechcraft Starship 2000 is a pressurized, all-composite twin-engine business turboprop, which is also an aircraft based on the advanced composite technology. The typical parameters that govern the physical envelope of the canard are shown in Fig.3.1.

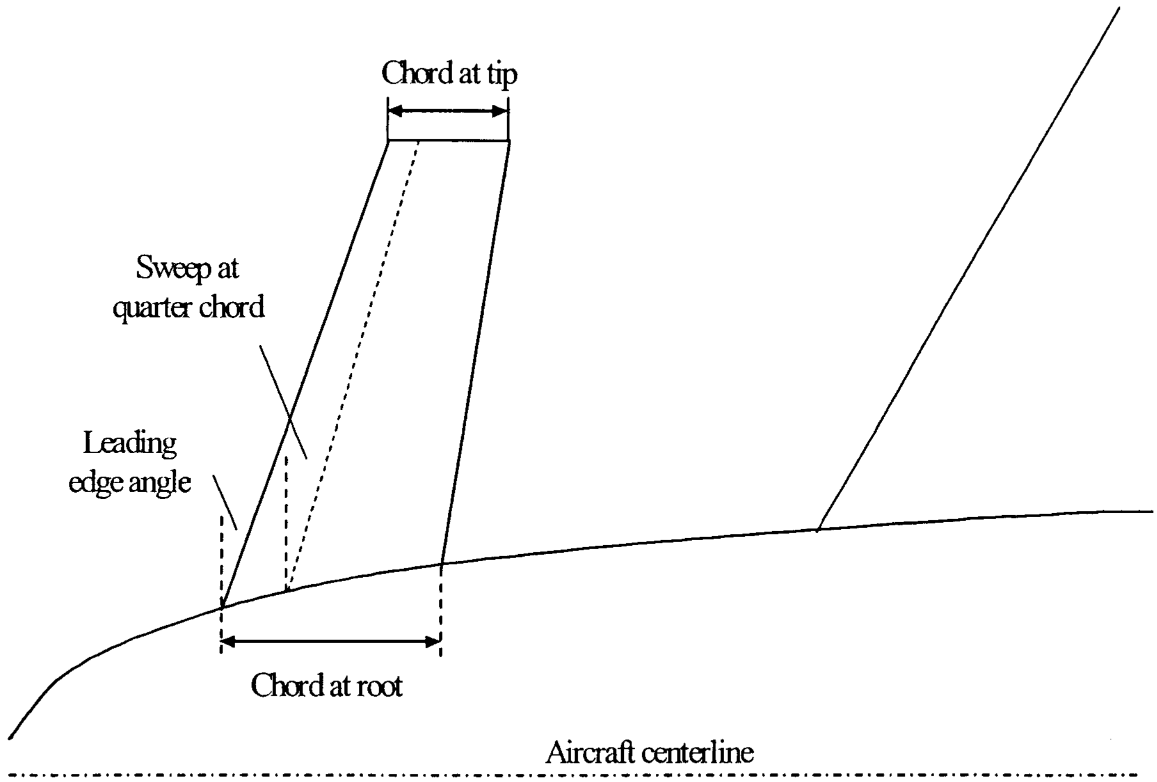

Fig. 3.1: Half-Canard View

In order to accurately predict structure-fluid interaction phenomena, this study has coupled efforts on Computational Structural Mechanics, where FEM is applied, with CFD in an interdisciplinary manner. The modeling of this structure-fluid interaction system involves the coupling of two formulations: the solid, classically treated in FEM formulation; the fluid, described by potential panel method in CFD. The coupling between the structure and flow requires taking into account the changes of aerodynamic forces due to the canard deflection. The structural displacements and stresses caused by the aerodynamics loads were calculated through a finite element procedure. The finite element model of the canard was updated after each aerodynamic analysis to include the changes in pressure loads acting on the structural surface. Then the changes of the nodal deflections were taken into account when the aerodynamics loads were recalculated.

The structure interaction can be considered as a loose coupling between the aerodynamic forces and the moving structure. The calculations of the aerodynamic forces are independent of the structural model. The structural and aerodynamic calculations need to exchange some information between them. Therefore the coupling operator has been introduced, which transfers the loads issued from the aerodynamic simulation on the structural model, and then transfers the deformed shape or structural nodes displacements back to the aerodynamic grid. The same mesh has been taken in CFD calculation as in FEM, in order to transfer all the data between the structural and aerodynamic calculations.

3.2 Structural analysis of composite canard

Advanced composite materials are widely used in aircraft and space systems due to their advantages of high stiffness- and high strength-to-weight ratios. However, the analysis of multi-layered structures is a complex task compared to conventional single layer metallic structures due to the exhibition of coupling among torsion and bending strains; weak transverse shear rigidities; and discontinuity of the mechanical characteristics along the thickness of the laminates.

Since the matrix material is of relatively low shearing stiffness as compared to the fibers, a reliable prediction of the response of the composite canard must account for interlaminar (transverse) shear deformation or corss-sectional warping of individual layers. FSDT has been proposed as the proper theory to solve the interlaminar shear deformation problem, which assumes constant transverse shear deformation through the entire thickness of the laminate [42]. In the present work, the structural analysis of the composite canard is carried out based on first order shear deformation laminate theory, which has been discussed in Chapter 2. The out-of-plane shear stresses in this multilayered composite panel are considered as primary variables of the problem.

This chapter presents the initial structural analysis of a composite canard by integrating two disciplines. First, the aerodynamics discipline evaluated the pressure distribution on the surface of the canard. Second, the structures discipline calculated the canard deformations and stresses resulting from the air pressure. The aerodynamic loads were kept as a distributed pressure load and applied directly to the geometry mode. These fields were then applied to the corresponding geometric surfaces as normal loads. The application of the aerodynamics loads on the structural model was the most important step of the coupling procedure. The load distribution and the geometry nodal positions were stored in certain vectors, which exported by the aerodynamics discipline.

The deflections, stresses and strains were calculated as a basic evaluation of the mechanical performances with a certain stacking sequence. The effect of the thickness of the panel was also checked. Two more different stacking sequences were chosen and the mechanics performances were evaluated for each stacking sequence and compared with the initial design.

3.2.1 Formulation of finite element analysis

Model description. In the process of structural analysis, the canard was modeled as a curved laminated composite panel (see Fig. 3.2) with uniform thickness, consisting of 8 plies of T300/5208 graphite/epoxy composite laminae. The curvature of the laminated panel was defined based on the geometries of actual aircraft canard. The maximum height of the camber is taken as 5% of the length of the chord, which is located in the middle of each chord. During the numerical analysis, the composite panel was grided in aerodynamic subroutine to obtain the actuate pressure. Then, the same mesh was applied in FEM part as in aerodynamics calculations in order to reduce the computational cost. This also simplifies the interface implementation work between the aerodynamics subroutines and solid mechanics subroutines. The parameters of interest were the out-of plane displacement and the stresses in the laminate.

Element type. Based on FSDT, the composite canard is modeled as a laminated shell with 5 degrees of freedom. Since the curvature of the canard is significantly small, four-noded shear deformable plate elements using linear shape functions were employed in the finite element analyses in order to simplify the calculations and reduce the computational cost.

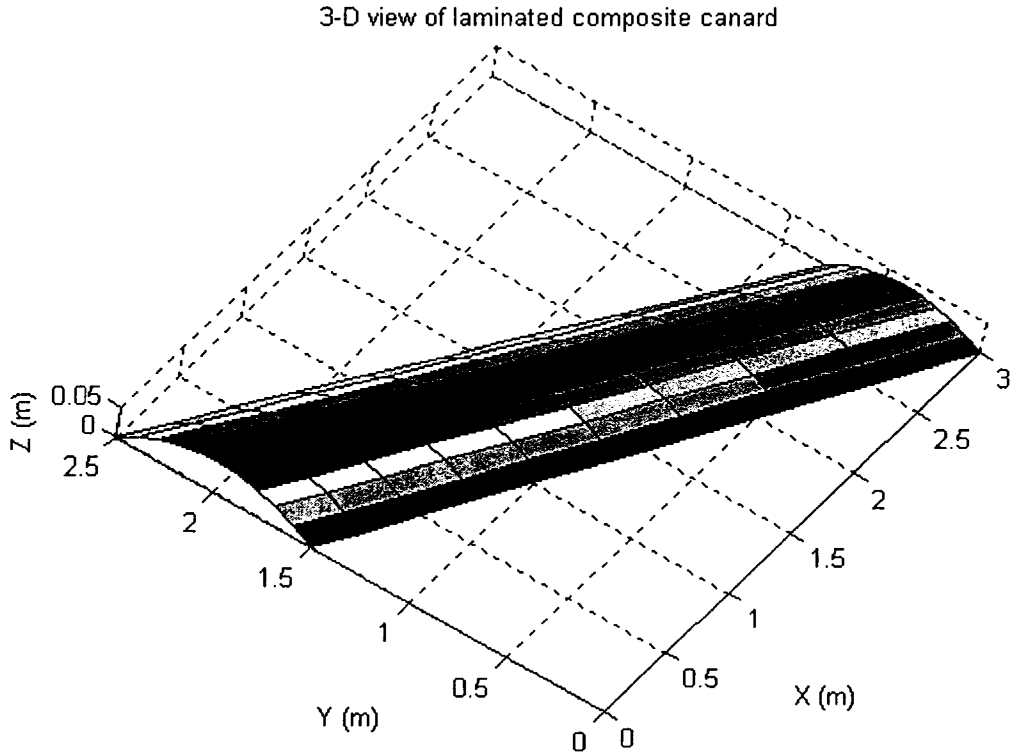

(a) Composite canard in 3-D coordinates

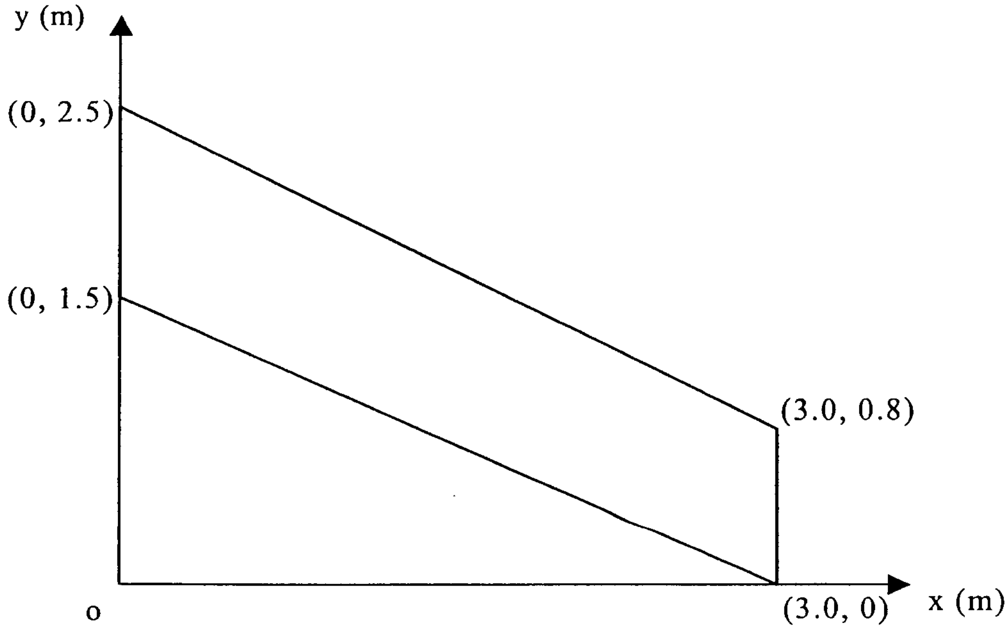

(b) Composite canard in x-y coordinates

Fig. 3.2: Laminated composite canard

Mesh. A 9×10 element non-uniform mesh is chosen in this part, 10 nodes in x direction and 11 nodes in y direction, as shown in Fig. 3.3. This results in a total of 90 elements. This mesh was originally used in the calculation of aerodynamic loads. Since the aerodynamic loading and the deformation of the panel affect each other, there is a need to account for the deflection of the canard under the aerodynamic forces. An iterative loop between the aerodynamics subroutines and structure subroutines was implemented to achieve the more accurate aerodynamic loads and deformations of the panel.

In this case, if a different mesh is taken in the subroutines of FEM, it will be necessary to process a load mapping between aerodynamic coordinates and structural coordinates. It could be very difficult to map the loads from aerodynamics field to structural field or map the deflections from finite elements back to aerodynamic elements in the iterative loop within the allowable computation cost. Hence the same grid was chosen in solid FEM program to simplify the processing of loads mapping. Four-node plate elements using linear shape function were used as the finite element type.

Boundary conditions. Three edges of the canard are set to be free and the remaining side is fixed in all degrees of freedom, as shown in Fig. 3.4.

Loading. Aerodynamic pressure loads are applied on the composite canard in transverse direction, as shown in Fig. 3.4. An aerodynamic program coded in Fortran and based on the potential flow panel method is used to determine the corresponding aerodynamic loads under the specified angle of attack and incident velocity which are listed in the Table 3.1.

Table 3.1: Properties of air

Properties of air	
Angle of attack α	1°
Incident velocity of air	120 m/sec
Density of air	1.2251 Kg/m^3

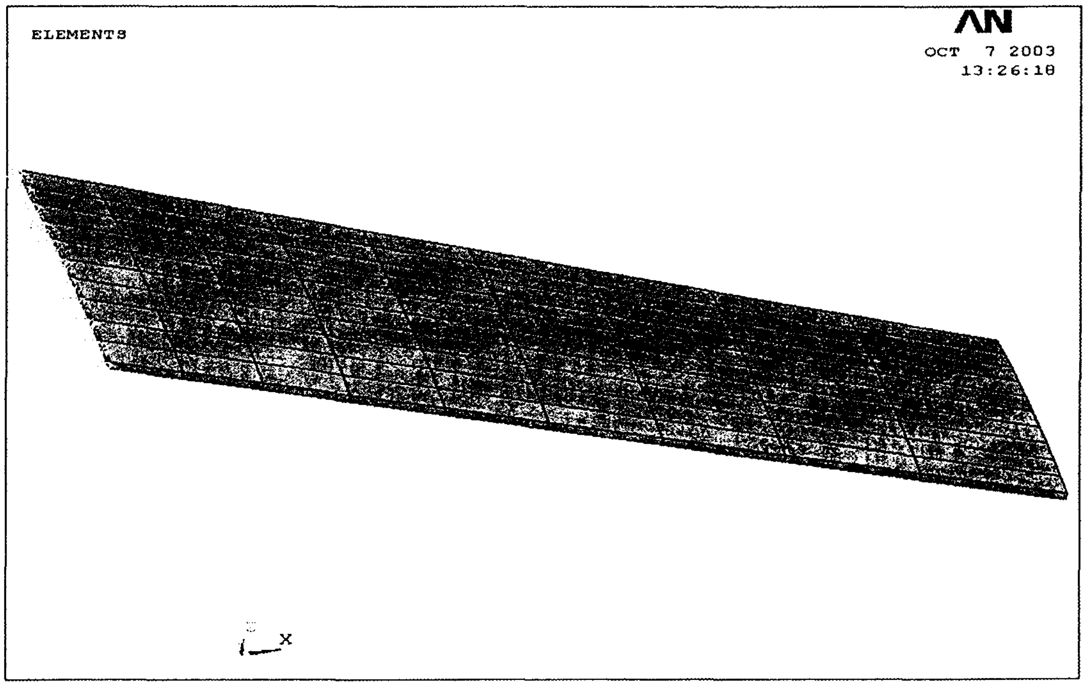

(a). Meshed laminated panel

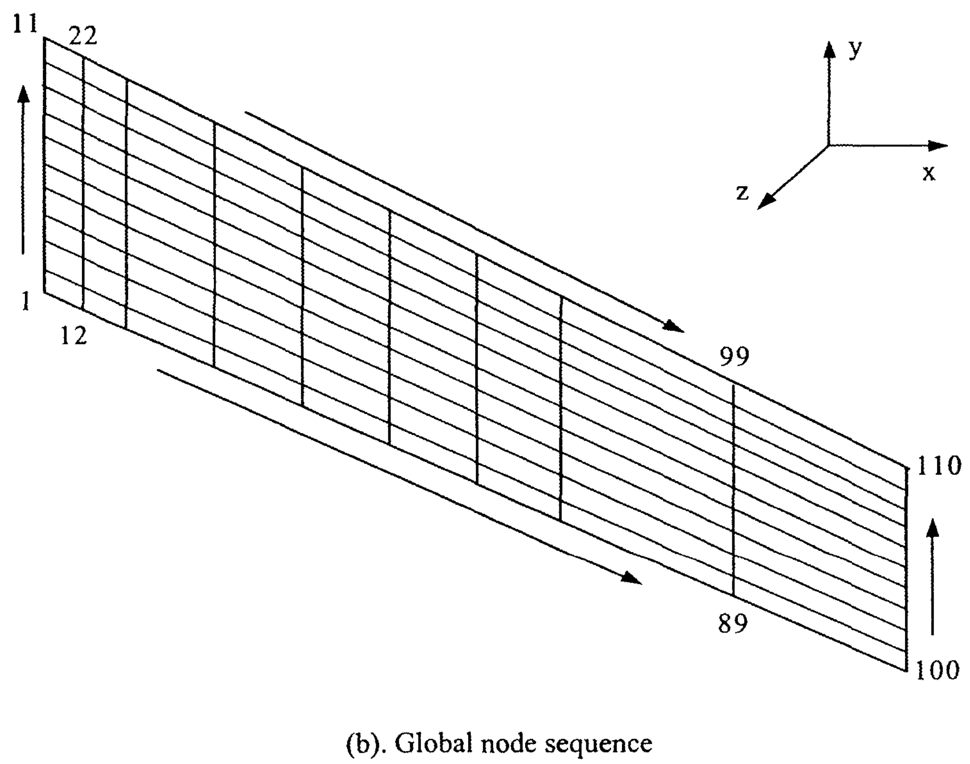

(b). Global node sequence

Fig. 3.3: FEM mesh of composite canard

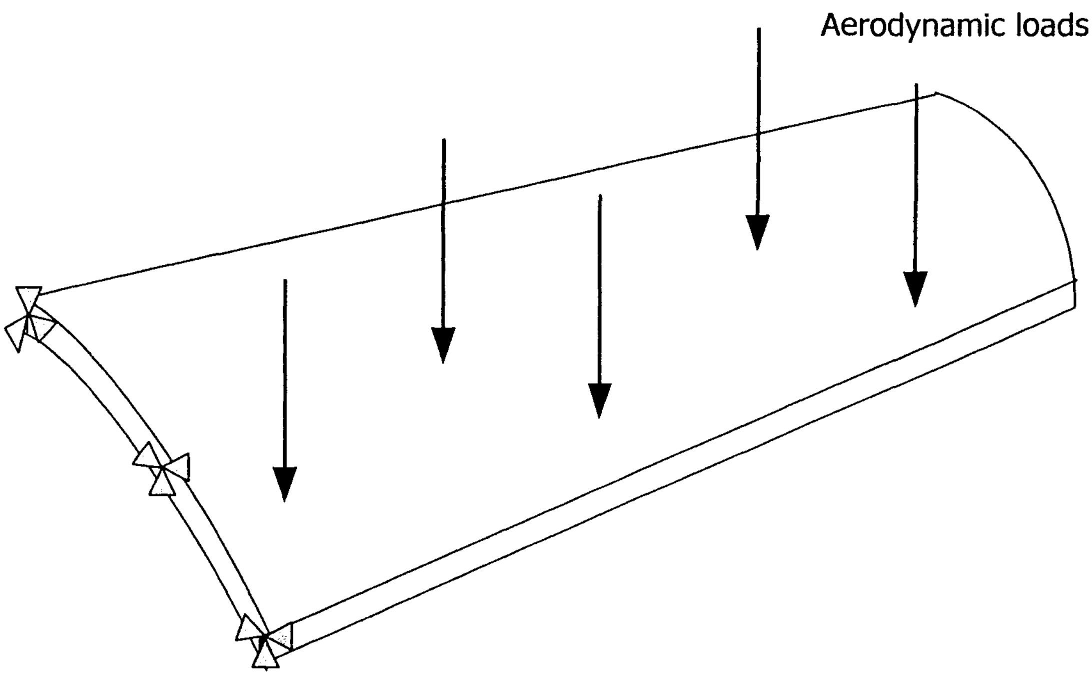

Fig. 3.4: Boundary conditions of the canard

Material properties. The selection of the material generally depends on the characteristics of the proposed operating environment; moisture exposure, loading, manufacturing, inspection, etc.. In this case, for a composite canard design, T300/5208 Graphite/epoxy was selected with the properties in Table 3.2.

Table 3.2 Material properties

T300/5208 graphite/epoxy	
E_{11}	181.00 GPa
E_{22}	10.30 GPa
$G_{12} = G_{13}$	7.17 GPa
ν_{12}	0.28
G_{23}	3.4 GPa
Density	1600 Kg/m^3

The composite panel has a uniform thickness of 0.05m, and consisting of 8 same thickness Graphite/epoxy plies.

A quasi-isotropic laminate with stacking sequence $[\,0^\circ / 45^\circ / -45^\circ / 90^\circ\,]_s$ was considered as the ply arrangement. The canard design with this stacking sequence is referred to as Canard #1.

3.2.2 Software implementation

An integrated code FEMCOMP has been implemented in Fortran and Fortran 90 based on Mechanics of Composite Materials [10], FSDT [11], FEM [4, 5, 6], and potential flow method. Within FEMCOMP a standard isoparametric four-node plate element with full and reduced integration rules (linear 2×2 Gauss-quadrature) is used. The architecture of FEMCOMP is shown in Fig. 3.5. The iterative calculations converged when the terminate criteria was satisfied.

The aerodynamic forces and moments acting on the panel are a function of the positions of each node in fluid coordinates, free stream velocity, and angle of attack. The aerodynamic loads are calculated based on the angle of attack and free stream velocity. These loads are applied to the canard and the deflection is calculated by FEA subroutines. This deflection then is used to determine the new locations of each node on the panel. The new coordinate positions are used to recalculate aerodynamic loads, which are reapplied on the composite panel to calculate the next positions of each node. This iterative procedure is repeated until the difference between two subsequent positions of the same node is insignificant, as shown in Eq.(3.1).

$$\frac{|d_i - d_{i-1}|}{|d_{i-1}|} \le 0.01 \qquad (3.1)$$

d_i and d_{i-1} are the subsequent positions of the same node in the iterative loop. The results converged if the difference is within 1% of the previous location. Once equilibrium between the load and deformation is achieved, strains and stresses of the laminated composite canard are calculated and the strength of the composite panel is checked by applying Quadratic Interaction Criterion.

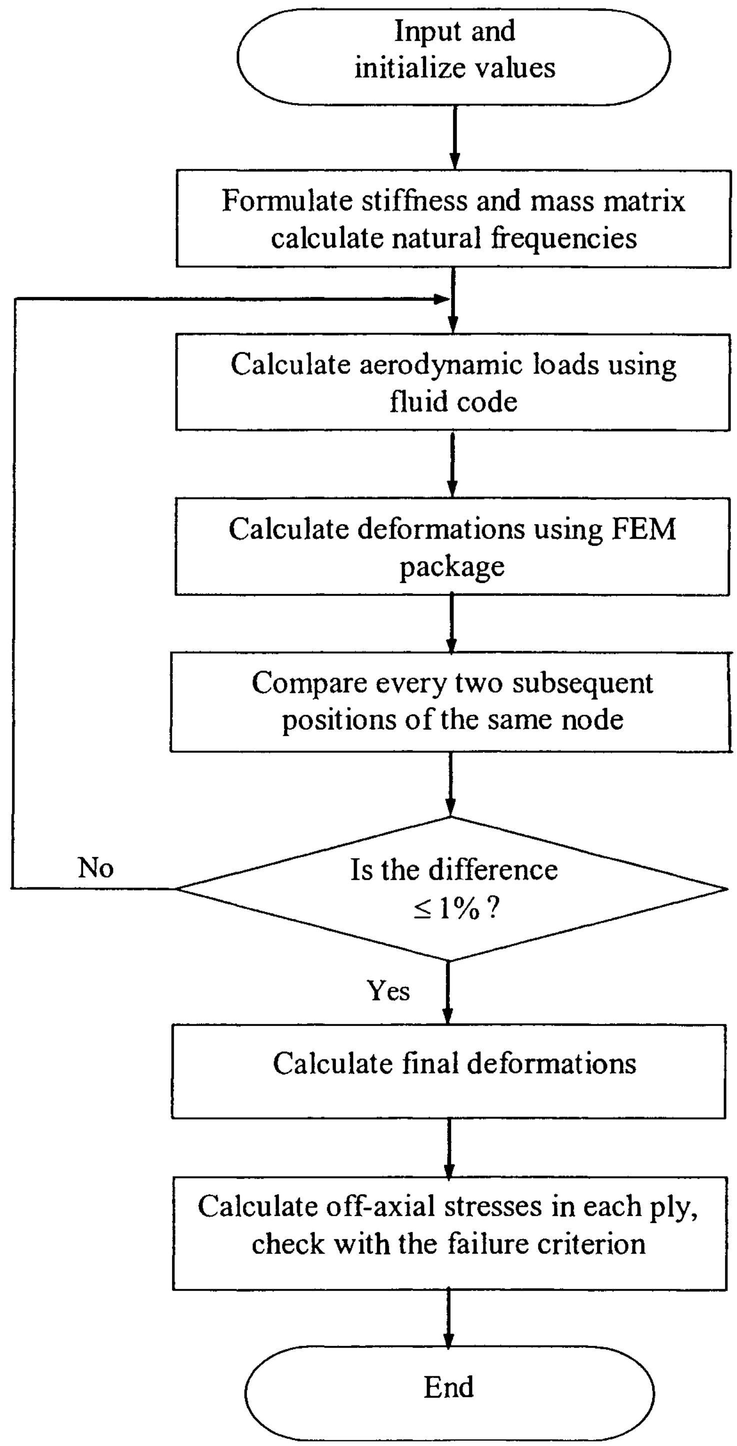

Fig. 3.5: Flowchart of FEMCOMP

3.3 Results

The results of the structural analysis of the laminated composite canard are presented in this section. The mechanical performance and the through-thickness distributions of transverse shear stresses inside the laminated panel are presented. Two more multilayered composite panels were analyzed in order to assess the effect of the stacking sequence on the mechanical performance. The results are discussed subsequently.

3.3.1 Results of analysis on Canard #1

After the first calculation step was completed, the maximum out-of-plane deflection of the composite panel made with the stacking sequence $[0°/45°/-45°/90°]_s$ was 0.1356 m, which occurred at Node 100 (right bottom tip, see Fig.3.3) and was opposite to the positive z direction. Since the terminate criterion was not satisfied after this computation, the program kept running and the system coordinates were updated from step to step. Once the program converged, the final maximum displacement is 0.1829 m, which is located at Node 100 and in negative z direction. Fig.3.6 (a) shows the final deflection of the loaded canard; (b) shows the comparisons of positions of unloaded canard and loaded canard at the first and the last iterative steps. The final stable deflection of the canard was obtained after iterative calculations. It took 84 iterative cycles to achieve the stable configuration. The twisting in the cross section suggests that the canard is subject to moment load which is caused by a pressure differential across the canard.

The results also demonstrated the existence of the interactive effects between structure and fluid. The structure-fluid interaction can be considered as a loose coupling between the aerodynamic forces and the moving structure. The calculations of the aerodynamic forces are independent of the structural model. The structural and aerodynamic calculations need to exchange some information between them.

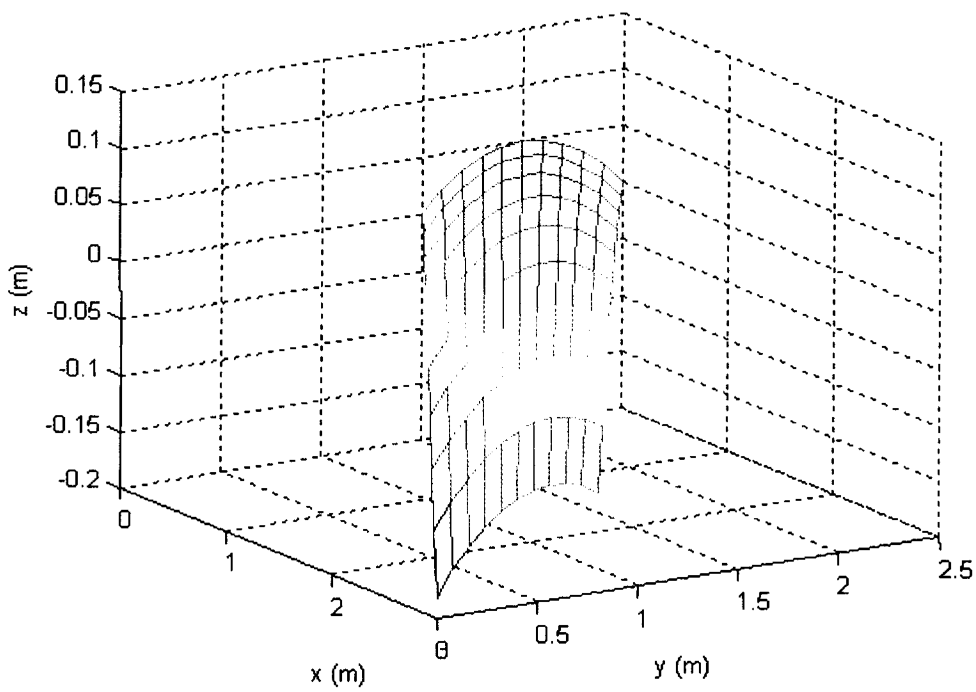

(a) Final deflection of loaded canard

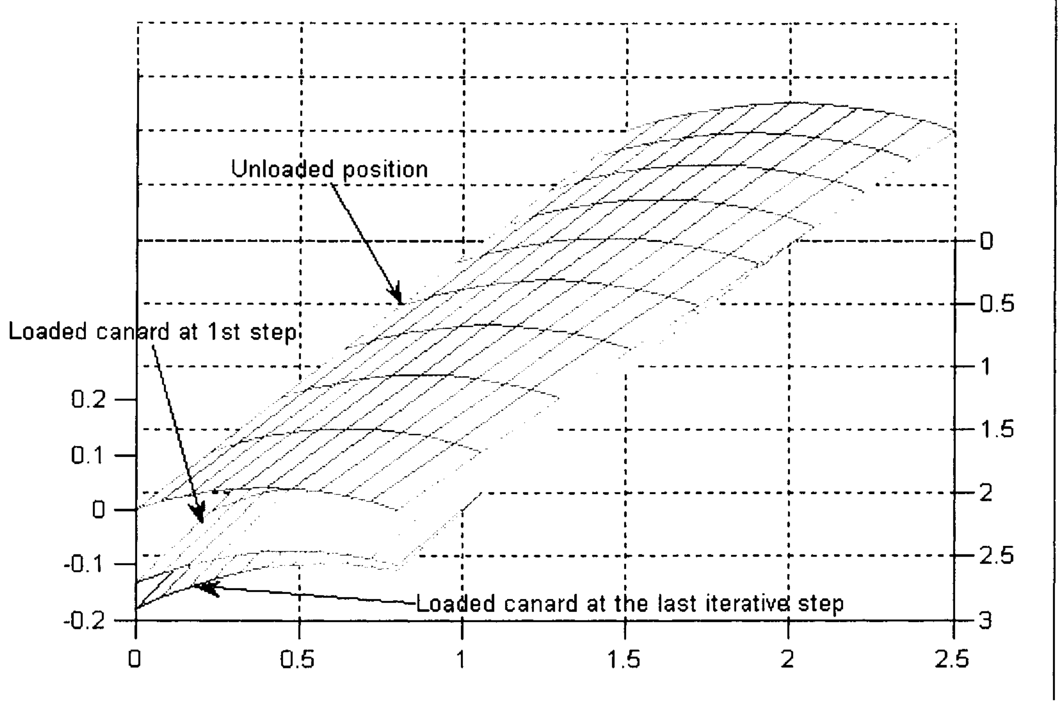

(b) Comparisons of positions of unloaded and loaded canards

Fig. 3.6: Deflections of loaded canard

The structural analysis also provided the off-axis stress components, σ_x, σ_y, σ_{yz}, σ_{xz}, and σ_{xy} on each element (transverse normal stress σ_z is negligible in FSDT) after the iterative process converged. Fig. 3.7 shows the stress components of an infinite element to help understand the stress analysis.

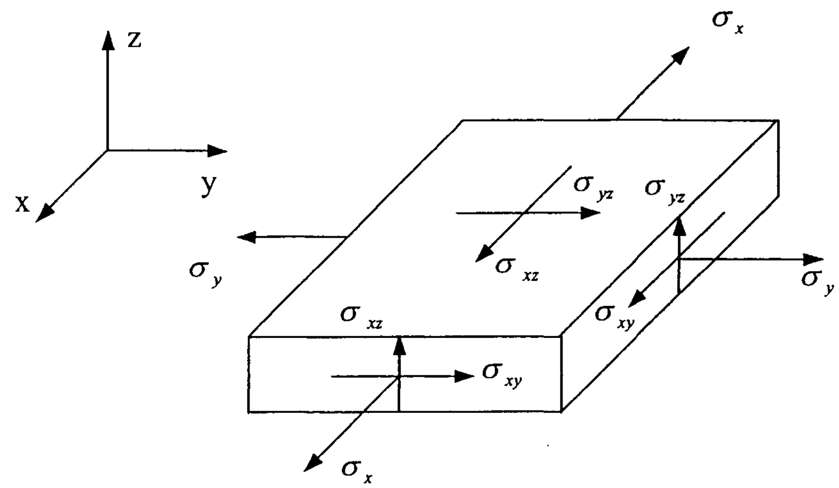

Fig. 3.7: Stress components of an infinitesimal element

Since distributed transverse pressure was the only loading applied on this panel, this section is concerned with the analysis of transverse deflections of laminated panel under transverse loading. Fig. 3.8 (a) to (e) give the contour plots for stress components. In these diagrams, the in-plane normal stresses σ_x, σ_y and shear stress σ_{xy} are very small, but transverse shear stresses σ_{yz} and σ_{xz} due to bending are much larger because the flexural stiffness is lower than extensional stiffness. Fig. 3.8 (c) and (d) shows that, the maximum transverse stress σ_{yz} 3523.0 MPa, is on the element at the fixed edge (Element 1), and the maximum transverse stress σ_{xz} 111.8 MPa, occurs on the bottom element at the fixed edge (Element 1). The distribution of transverse stresses across the thickness for Element 1 and Element 81 are presented in Fig. 3.9 (a) to (d). It can be seen that the transverse shear stresses produced by the transverse loading have a smooth variation in the thickness direction.

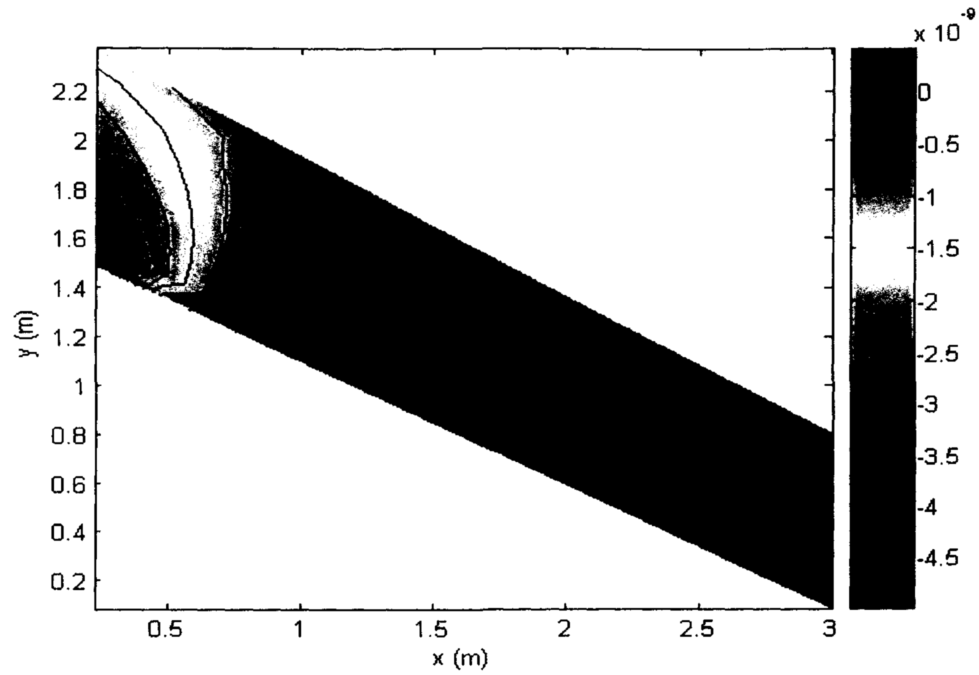

(a) Normal stress σ_x (Pa)

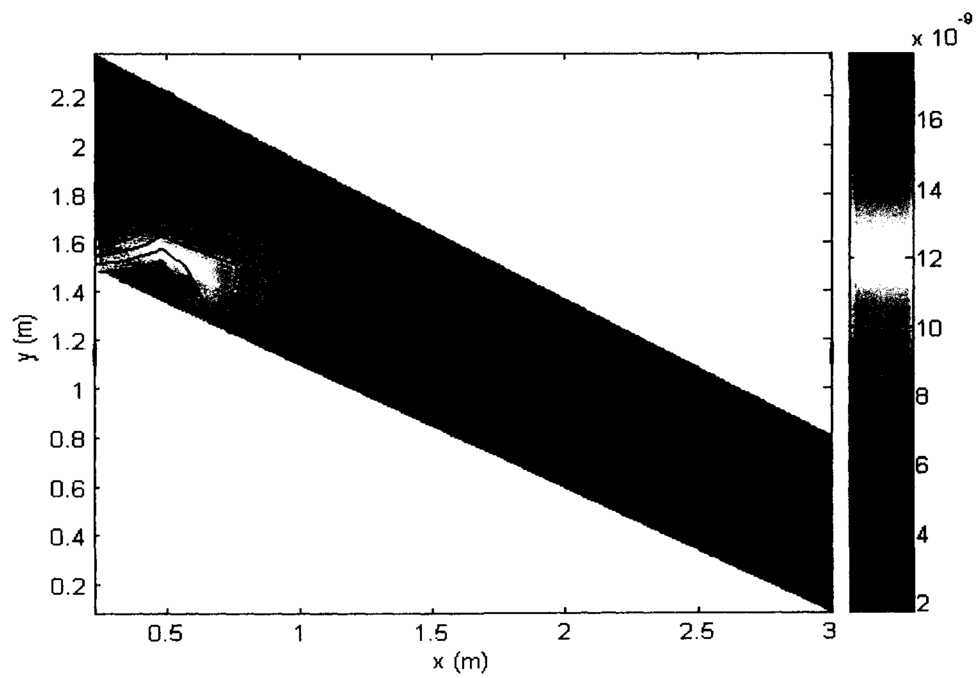

(b) Normal stress σ_y (Pa)

Fig. 3.8: Contour plots of stresses for Canard #1

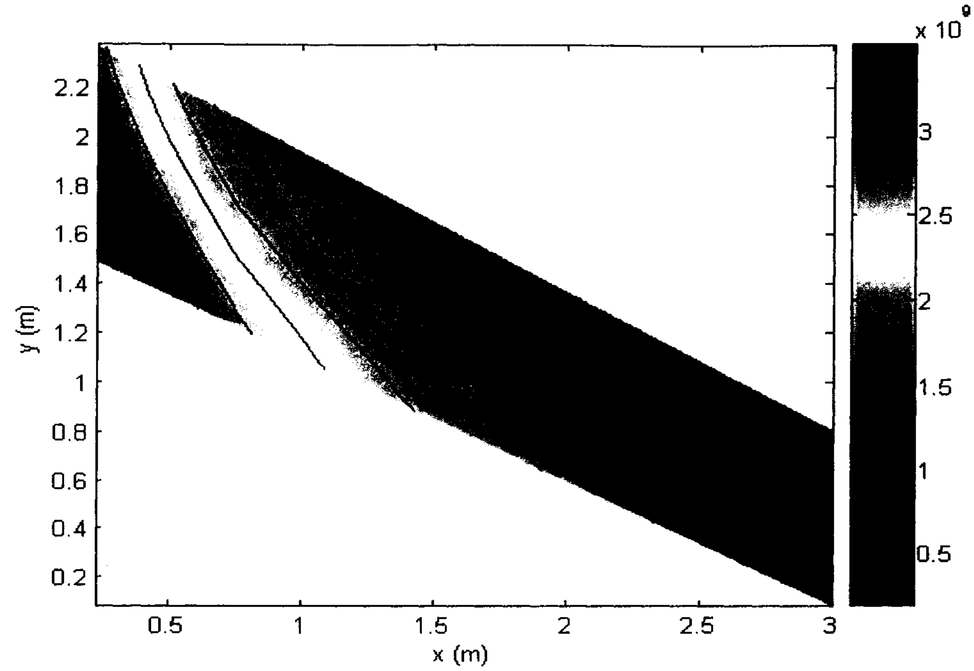

(c) Transverse shear stress σ_{yz} (Pa)

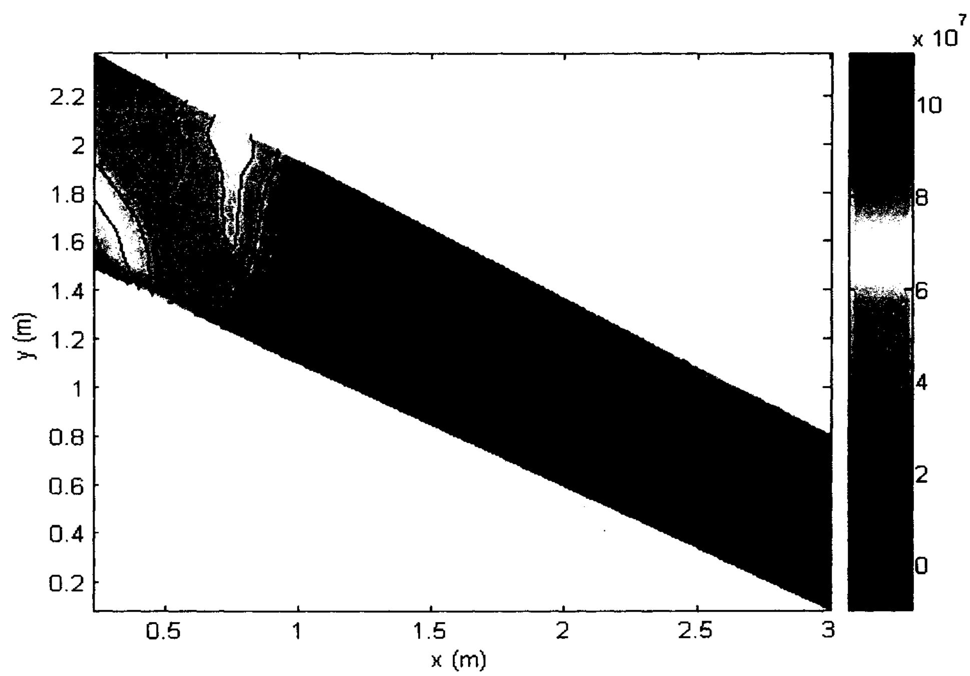

(d) Transverse shear stress σ_{xz} (Pa)

Fig. 3.8: (Continued)

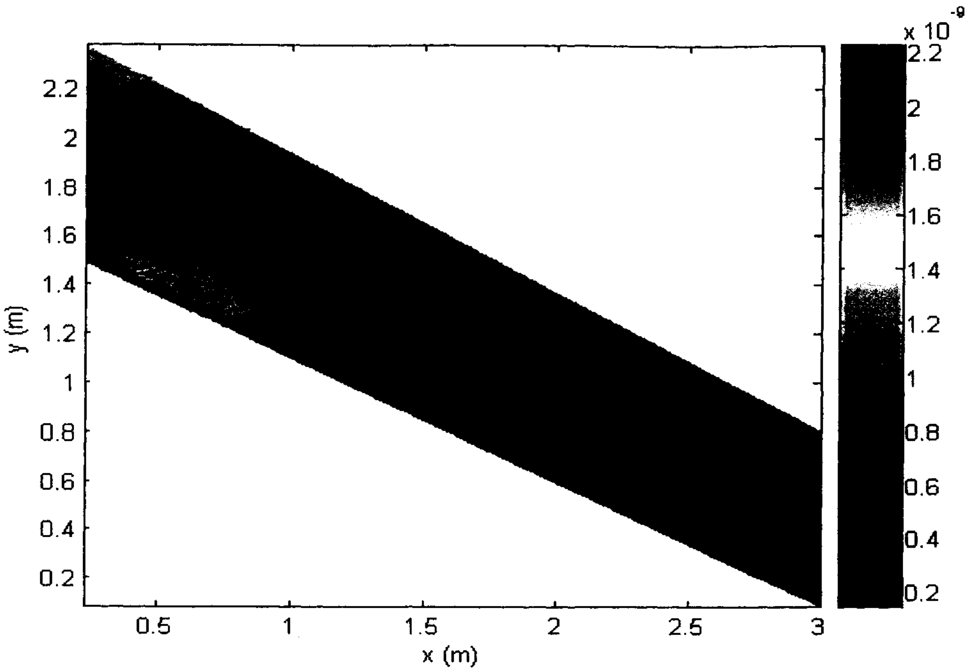

(e) Shear stress σ_{xy} (Pa)

Fig. 3.8: (Continued)

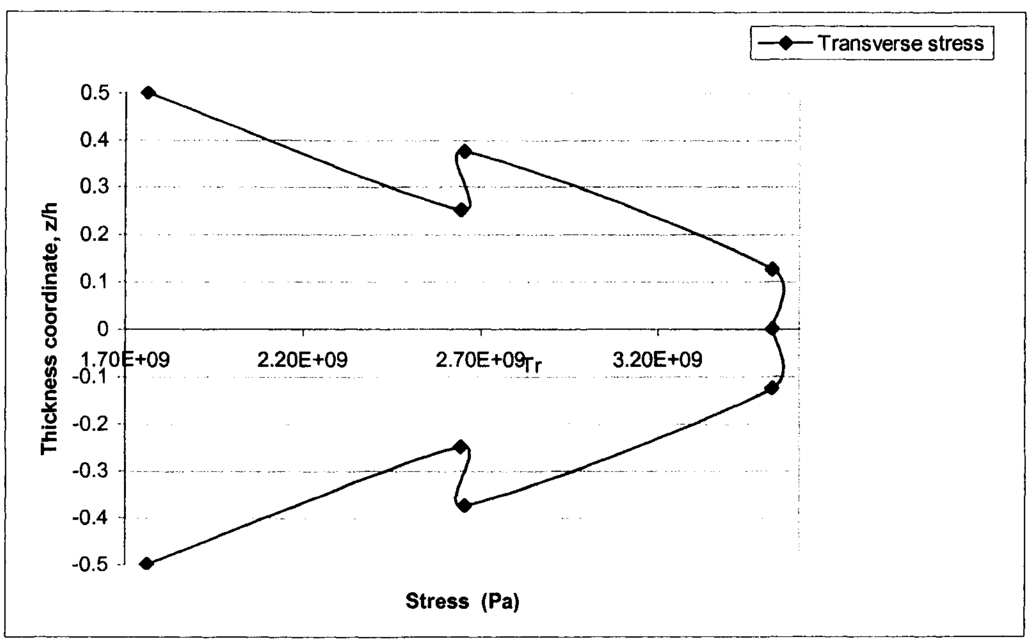

(a) Distributions of transverse shear stress σ_{yz} on Element 81

Fig. 3.9: Shear stress distributions in the element with the largest shear stress

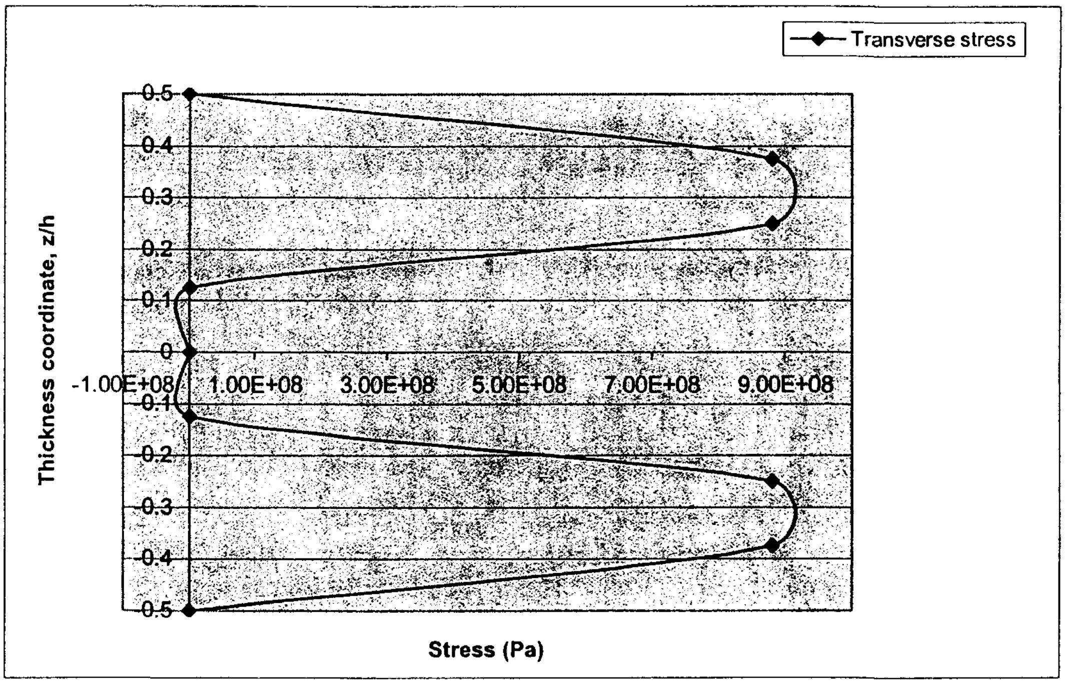

(b) Distributions of transverse shear stress σ_{xz} on Element 81

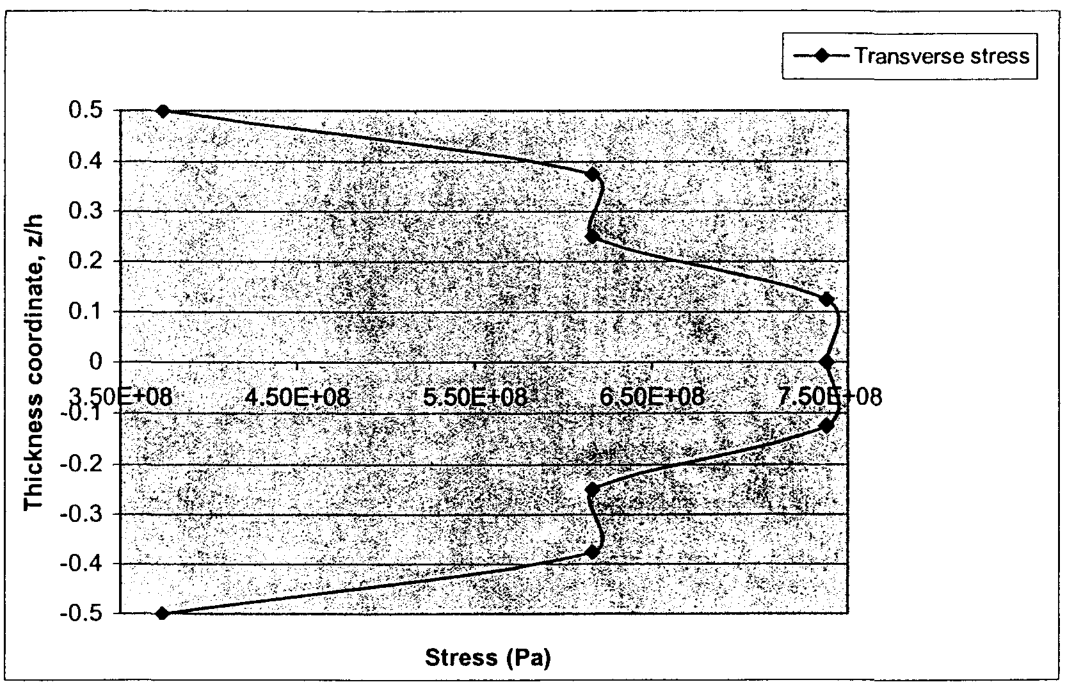

(c) Distributions of transverse shear stress σ_{yz} on Element 1

Fig. 3.9: (Continued)

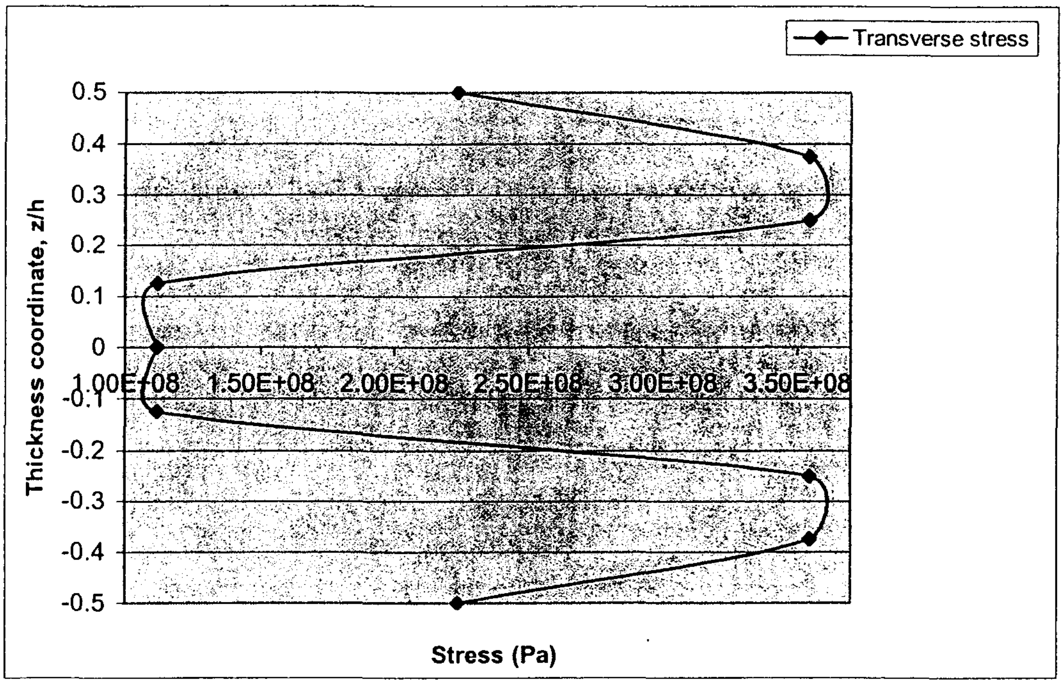

(d) Through-thickness distributions of transverse shear stress σ_{xz} on Element 1

Fig. 3.9: (Continued)

3.2.2 Effect of plate thickness

The effect of plate thickness on stiffness was investigated in this part. To carry out this investigation, the same stacking sequence and geometric dimensions are maintained as above and only the plate thickness is changed. A new set of results was obtained. The comparison on the maximum out-of-plane deflections of the plates with different thickness were made in Fig. 3.10, where (b) is the same plot as (a) but with a different scale to show the divergence. The negative signs of the deflections mean their directions are opposite to z direction. It can be seen in (a), as the plate thickness increases, the maximum out-of-plane deflection become smaller. This means that the plate stiffness is larger. Fig. 3.10 (b) shows that, when the length-to-thickness ratio is around 70, the plate is not strong enough to support the loads any more and the maximum displacement was very large. The structural divergence occurred at that time. The effect of the plate thickness on the plate stiffness is not surprising since for an isotropic plate the flexural rigidity is given by $D = \dfrac{Et^3}{12(1-\gamma^2)}$, where D is the stiffness and t is the thickness. Hence the stiffness of the plate is proportional to t^3.

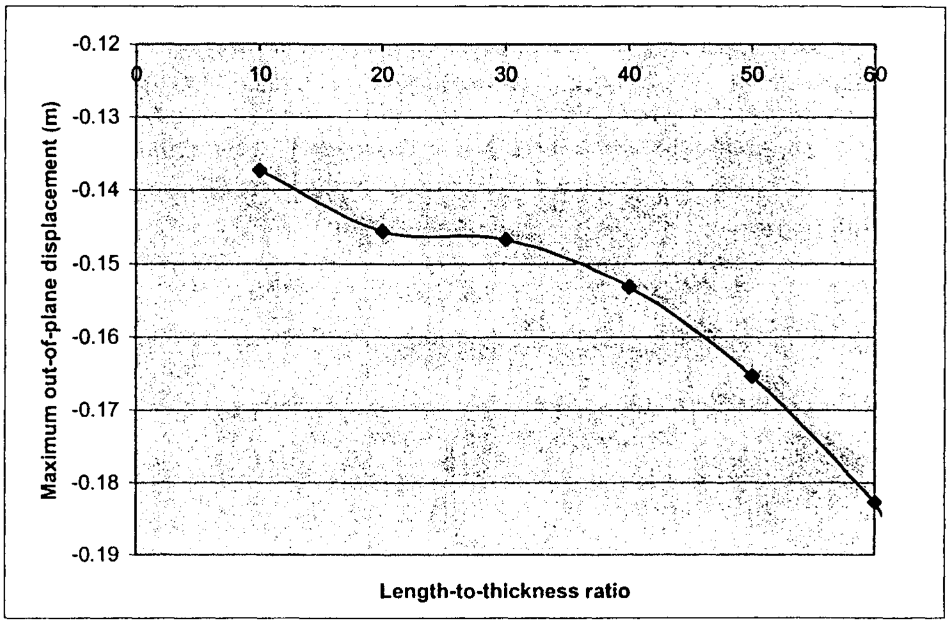

(a) Within stiffness bound

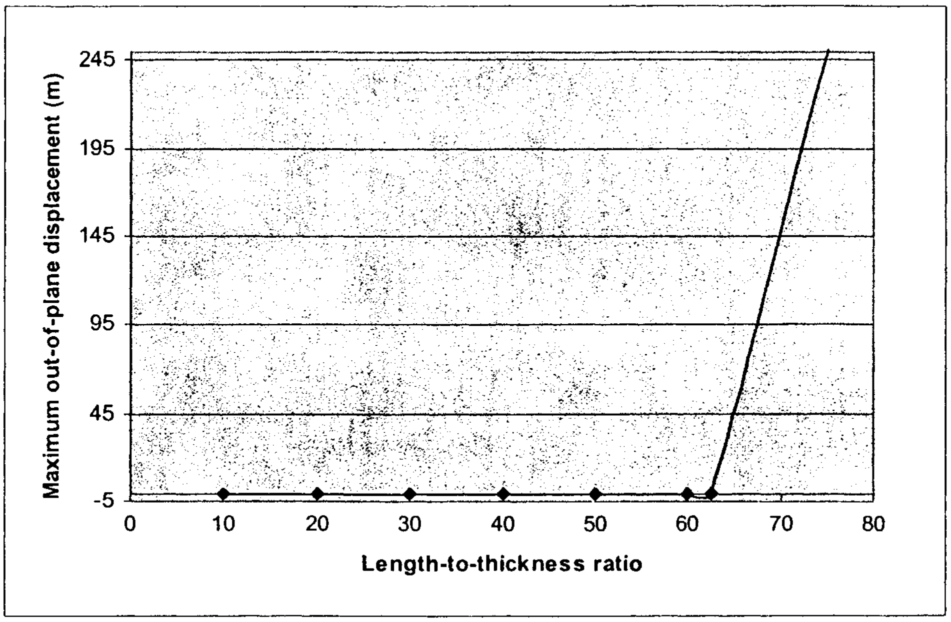

(b) Out of stiffness bound

Fig. 3.10: Thickness effect on out-of-plane displacement under aerodynamic loading

3.3.2 Effect of stacking sequence

The composite material is fundamentally different from a conventional isotropic material. The anisotropic nature of fiber reinforced composite provides the unique opportunity of tailoring such properties as the stacking sequence, fiber orientation, and thickness of laminate according to design requirement. The strength of composite materials is dependent on fiber direction and is better in that direction.

To observe the effect of the stacking sequence on the mechanical behaviors of the composite canard, two other similar stacking sequences were chosen with the same thickness of 0.05m,

$$[-45°/0°/45°/90°]_s$$

$$[90°/45°/0°/-45°]_s$$

Canard made with these stacking sequences is referred to as Canard #2 and Canard #3 respectively. The performances of panels made with different stacking sequences were compared to each other.

Improved FEMCOMP program. In order to make compatible comparisons of the mechanical behaviors among the designs with different stacking sequences, the final loads applied on each canard should be at the same value. Therefore, the angle of attack (AOA) in the aerodynamic subroutines was adjusted to meet this requirement. Instead of using the FEMCOMP code presented at the beginning of this chapter, an Improved version of FEMCOMP has been employed as shown in Fig. 3.11. After the structure-fluid iterative loop converged, another iterative loop is added to ensure that the final applied loads on the current design are the same as those on the original design of Canard #1. The checking-loading loop converges when the maximum difference between the subsequent pressure fields is within 1% of the previous load value.

Table 3.3 shows the comparisons of mechanical behaviors of Canard #1, #2, and #3. As can be seen, Canard #2 gives a better performance. Its maximum deflection was reduced to 0.1311 m at Node 100, which is an improvement of 28%. Compared to the other designs, Canard #3 behaved in the opposite way. The iterative calculation converged for this design, however, its stiffness provided by stacking sequence $[90°/45°/0°/-45°]_s$ was not adequate to support the aerodynamic pressures. Therefore, the structural divergence occurred.

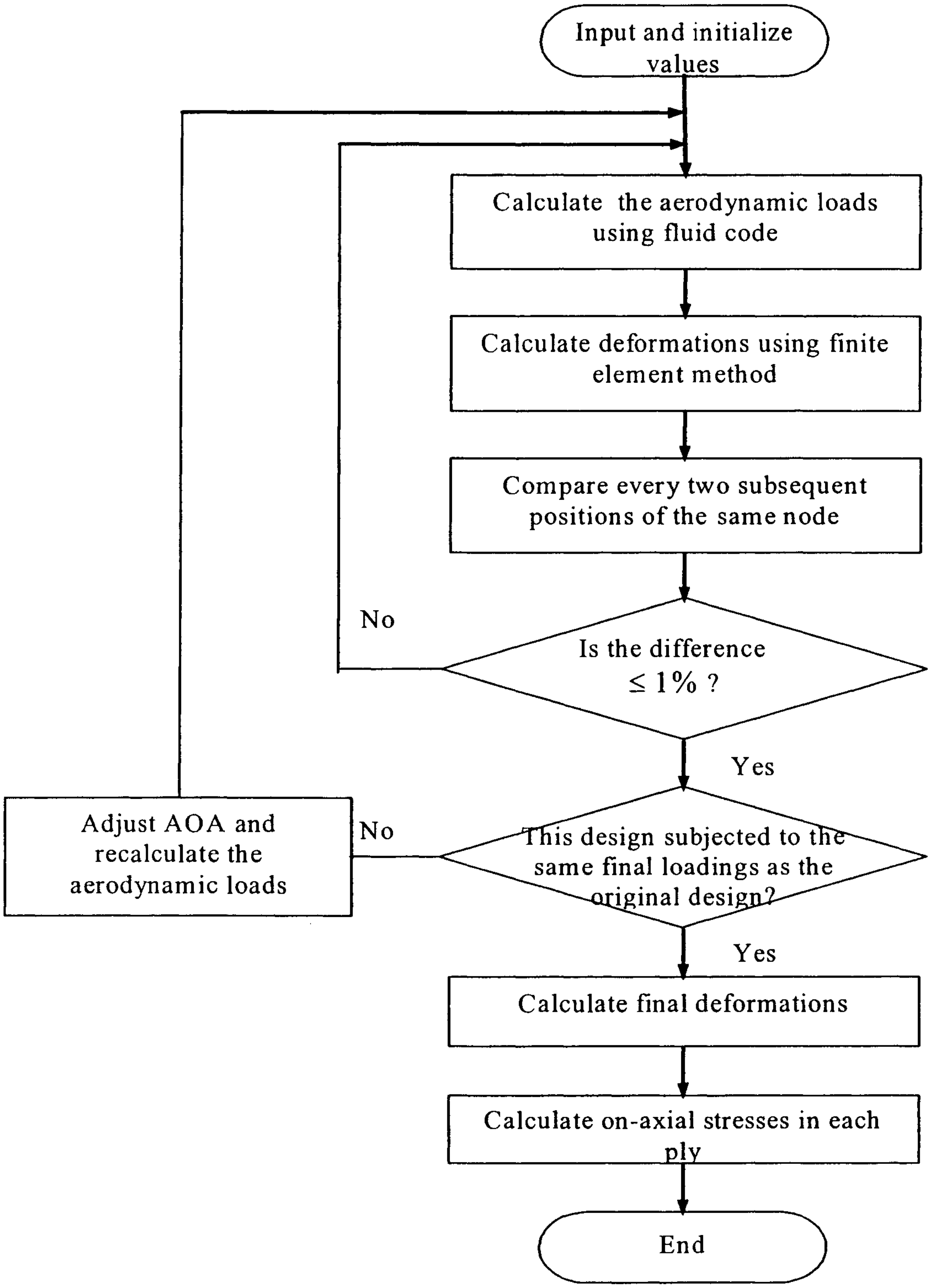

Fig. 3.11: Flowchart of improved FEMCOMP

Table 3.3: Comparisons of mechanical behaviors of laminated panels made with different stacking sequences

Canard	Stacking sequences	Maximum displacement (m)	Maximum σ_{yz} (MPa)	Maximum σ_{xz} (MPa)
#1	$[0°/45°/-45°/90°]_s$	-0.1829	3523.0	111.8
#2	$[-45°/0°/45°/90°]_s$	-0.1311	2095.0	100.0
#3	$[90°/45°/0°/-45°]_s$	Infinity	NA	NA

Fig. 3.12 presents the out-of-plane deflections of Canard #1 and #2 (the negative sign means the direction is opposite to z direction). Canard #2 shows a better stiffness performance compared to the design of Canard #1.

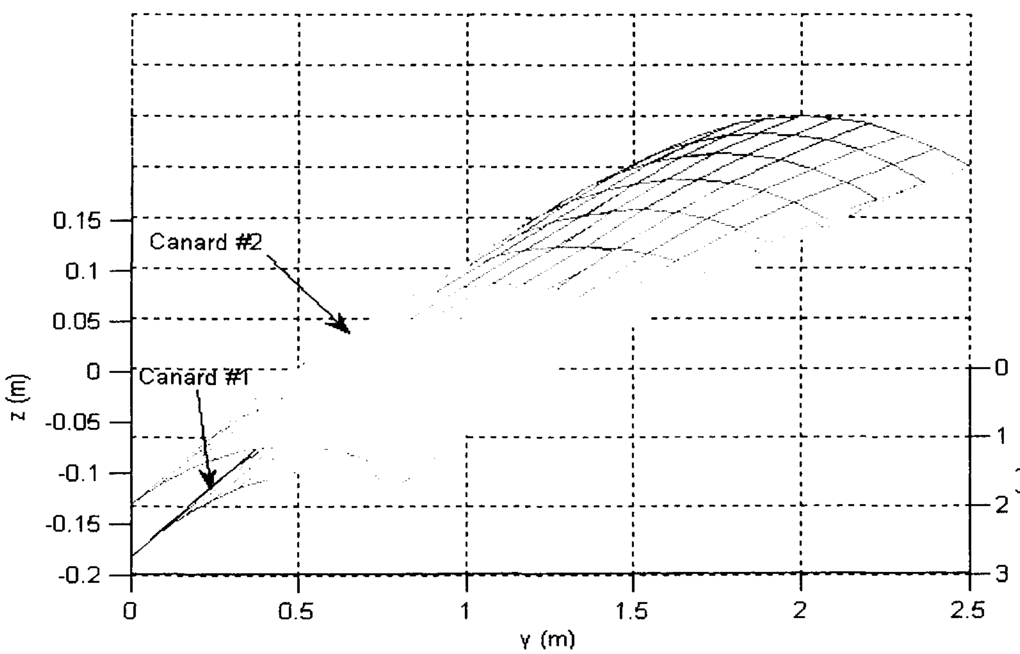

Fig. 3.12 Deflections of Canard #1 and Canard #2

The contour plots of stresses components for Canard #2 are presented in Fig. 3.13 (a) and (b). The maximum transverse stress σ_{yz} 2095.0 MPa, is located on Element 1 at the left bottom tip, and the maximum transverse stress σ_{xz} 100.0 MPa, is located on Element 1 on the fixed edge. The positions where the maximum transverse shear stresses occurred are the same as in Canard #1. Compared to the results of Canard #1, the maximum transverse stresses were reduced subject to the same loads.

Even though Canard #2 and Canard #3 are both quasi-isotropic laminates, their performances are quite different. Canard #2 made with the stacking sequence $[-45°/0°/45°/90°]_s$ has much better mechanical performance. This is consistent with the fact that the strength of composites is dependent on direction and is better in the fiber direction. Also, the bending behavior of composites depends on the stacking sequence. This provides us the opportunities to optimize the laminated composite structure.

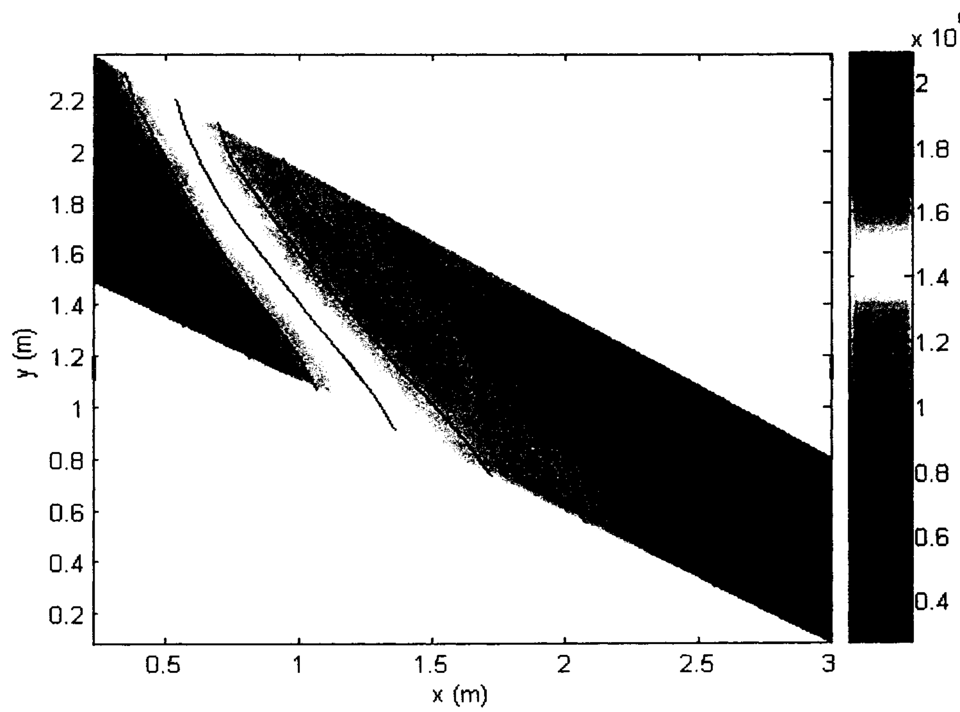

(a) Transverse shear stress σ_{yz} (Pa)

Fig. 3.13: Contour plots of stresses for Canard #2

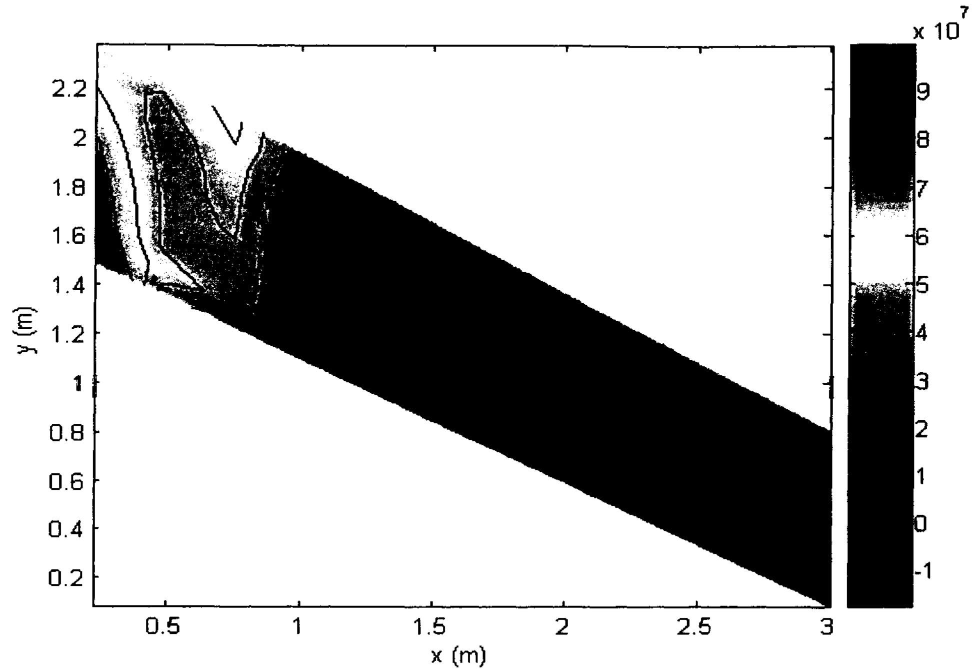

(b) Transverse shear stress σ_{xz} (Pa)

Fig. 3.13: (Continued)

Conclusions

1. A structure-fluid interaction problem has been discussed in this chapter. A structural analysis on the composite canard subjected to aerodynamic loading has been carried out.
2. The mechanical performances of canards made with different stacking sequences and thicknesses were compared to each other. The effect of the stacking sequence on performance of the canard shows the possibility to optimize the laminated composite structure.
3. A Fortran program FEMCOMP was employed in the structural analysis. FEMCOMP integrated the structural FEM code and the aerodynamic routine together in order to solve this specific interdisciplinary problem.

CHAPTER 4 OPTIMIZATION DESIGN USING GRADIENT-BASED ALGORITHM CONMIN

The structural analysis of the laminated canard has been performed in the previous chapter. It has been demonstrated that the original design of the canard can be improved by using composite materials. The anisotropic nature of fiber reinforced composite provides the unique opportunity of tailoring such properties as the stacking sequence, fiber orientation, and thickness of laminate according to design requirements. The stiffness and strength of composite materials are dependent on fiber direction, which makes it easy and possible to optimize the existing design. In order to best utilize the composite material, one must optimize the structure with proper fiber orientation [10, 11].

The aim of this work is to minimize the weight of the laminated composite canard by altering the ply orientations and thickness of layer subjected to the stiffness constraint. In this study three optimization approaches were employed to obtain the optimal design of the canard consisting of 8 plies subjected to the static aerodynamic loads: 1) gradient-based searching method; 2) genetic algorithms; and 3) a hybrid numerical optimization technique which combines gradient-based optimizer CONMIN and Genetic Algorithm. All three optimization methods were programmed in Fortran. The finite element mesh, material properties, and aerodynamic loading were kept the same as in the previous structural analysis.

In this chapter, the optimization problems are investigated by using the gradient-based method. Optimized results and relevant discussions are presented. Gradient-based optimizer CONMIN, which is coded in Fortran, is applied to optimize the design.

4.1 Overview of the gradient-based optimization method

To obtain the optimum design, the engineering structural optimization problems are usually converted into mathematical forms, and then numerical techniques are used to solve the problems. Gradient-based searching methods are a class of typical numerical optimization techniques, which compute the gradient of the objective function with respect to the parameters at the current search point and use this vector to define the next point in the search sequence.

Gradient-based algorithms use the iterative improvement technique; the technique is applied to a single point in the search space. During a single iteration, a new point is selected from the neighborhood of current point. If the new point provides a better value of the objective function, the new point becomes the current point. The method terminates if no further improvement is possible, i.e. the gradient becomes zero. There are two sub-problems for each major iteration: computing the search direction and finding the step length. The difference between the various types of gradient-based algorithms is the method that is used for computing the search direction.

In general, compared to non-gradient-based algorithms, gradient-based optimizers are capable of reaching an optimum design very quickly, which is the greatest advantage of gradient-based algorithms. However, engineering optimization problems have often to deal with non-smooth and/or non-convex design spaces and multiple local minima and saddle points often exist. Consequently, gradient-based optimization techniques converge to the nearest local optima. Since the optimum values provided by gradient-based algorithms depend on the selection of the starting point, in order to increase the chances of achieving global minima, gradient-based algorithms usually are executed for a number of different starting points.

4.1.1 General problem statement

The general constrained optimization problem can be stated mathematically as follows:

Minimize:	$F(X)$		objective function
Subject to:			
	$g_j(X) \le 0$	$j = 1, m$	inequality constraints
	$h_k(X) = 0$	$k = 1, l$	equality constraints
	$X_i^l \le X_i \le X_i^u$	$i = 1, n$	side constraints

where $X = \begin{Bmatrix} X_1 \\ X_2 \\ X_3 \\ \vdots \\ X_n \end{Bmatrix}$ design variables

The objective function F (X) and the constraint functions, g_j (X) and h_k (X) may be linear or nonlinear, explicit or implicit functions of X, but must be continuous and should have continuous first derivatives. m is the number of inequality constraints and n is the number of equality constraints. The limits on X_i are referred to as side constraints. Although they could be included in the general constraint set, it is usually convenient to treat them separately because they define the region of search for the optimum. X_i^l and X_i^u are lower and upper bounds respectively on the design variables. n is the number of design variables.

4.1.2 Iterative optimization procedure

The optimization process begins with an initial set of design variables, X^0. The design is updated iteratively from the starting point. The most common iterative procedure is of the form:

$$X^q = X^{q-1} + \alpha^* S^q$$

where q is the iteration number and S is a vector search direction in the design space. The scalar factor α^* defines the amount of change in X and q is the iteration number. For the q th iteration, a usable-feasible direction S^q, which will reduce the objective (usable direction) without violating the constraints (feasible direction), must be determined. Then, the iteration process becomes a one dimensional search problem for move parameter, α^*, which must be found to minimizes F(X) in S^q. Some new constraint or some currently active constraint is encountered. The process is repeated until the converged result is obtained.

Mathematically, if the scalar product of ∇F(X) with S is non-positive, direction S is usable; if the scalar product of ∇ g_j (X) with S is non-positive, direction S is feasible. The search direction required to be both usable and feasible is stated as

$\nabla F(X) \bullet S \leq 0$ usable direction

$\nabla g_j(X) \bullet S \leq 0$ feasible direction

Thus, the structure of a typical gradient based searching method is given as following,

1. Select starting point and convergence parameters;

2. Compute the gradient vector at current point (the direction of maximum decrease of the function at that point). If the result is converged, stop; otherwise, compute the normalized search direction;

3. Find the positive step length such that the evaluation function is minimized at this step;

4. Update the current point;

5. Evaluate the objective function. If the convergent condition is satisfied, then stop; otherwise, move to next point and return to step 2.

4.2 Gradient-based optimization process

In today's competitive world, the designer strives for least weight structures. This is critically true for aerospace structures. In the present study, attention has been focused on reducing the weight of the canard with adequate stiffness. The objective is to minimize the canard weight. This is generally compatible with other requirements, such as prescribed strength and stiffness. Therefore, the goal in designing a composite canard is to obtain the lightest canard by adjusting the ply orientations and thickness under the given constraint, the fixed range of out-of-plane deflection.

4.2.1 Formulation of the design model

The canard is a design of 8-ply symmetric and balanced laminate. The symmetry allows modeling of only half of the laminate, which helps reduce the design space and keep the computational time manageable. Therefore, the design variables include 4 ply angles and the plate thickness.

The optimization problem is formulated so as to find the proper ply orientations and the thickness of the laminated canard in order to minimize the mass of the canard with adequate stiffness. The requirements of the optimization design are declared as following

- *Objective function*

  Minimize the weight $W(t)$

- *Design variables*

  Plate thickness t, $0.03m \le t \le 0.05m$

  Ply orientations θ_i, $-90° \le \theta_i \le 90°$, $i = 1,2,3,4$

- *Design parameters*

  Geometric dimensions, design loading

- *Design constraint*

  Out-of-plane deflection $|d_i(t,\theta_i)| \le 0.15m$

where the constraint d represents a functional relationship between design objective minimum $W(t)$ and design variable t, which satisfies certain physical phenomenon and resource limitations. Canard #1 with the sequence $[0°/45°/-45°/90°]_s$ and Canard #2 with the sequence $[-45°/0°/45°/90°]_s$ are assigned as the initial designs and will be compared with the optimum designs.

4.2.2 Software implementation

The flowchart describing the procedure of optimizing the composite canard is shown in Fig. 4.1. The optimizer CONMIN and structural evaluation program FEMCOMP have been coupled together to carry out the task.

The design of Canard #1 is input to CONMIN as the starting point of the search. Then the objective function is evaluated by using FEMCOMP with respect to the parameters of the current point. The terminate condition of CONMIN is checked after each evaluation. If the design is not converged, another design (point) is chosen in the searching direction as the current design; otherwise, if the condition for convergence is satisfied, the search is completed with an optimal design. The iteration is repeated till the final optima are obtained.

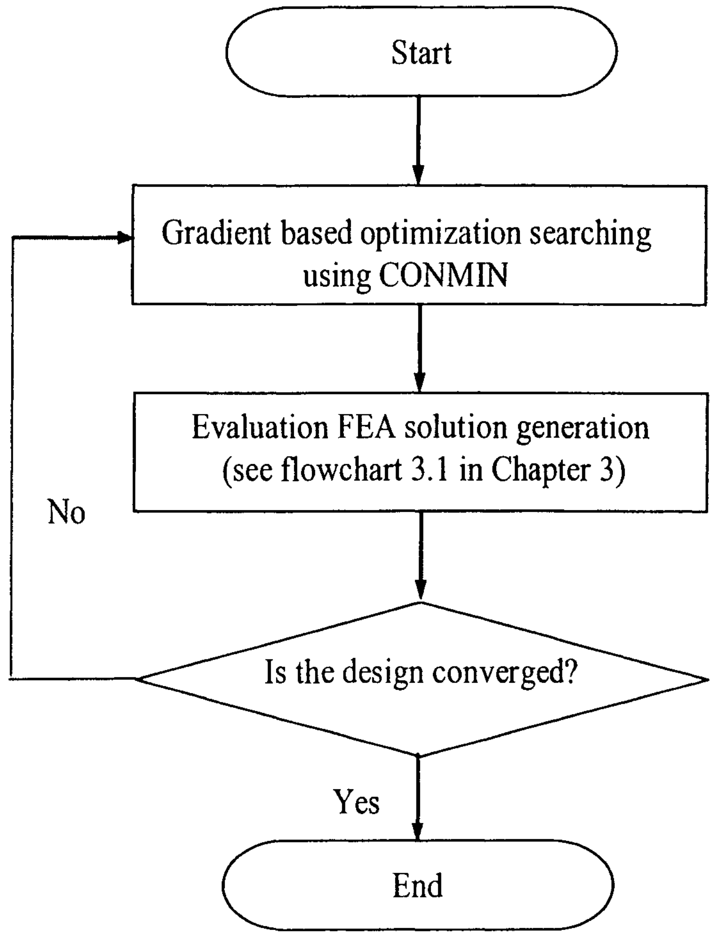

Fig. 4.1: Flow chart of gradient-based optimization

4.3 Results

4.3.1 Optimal results of Canard #1 $[0°/45°/-45°/90°]_s$

The calculations converged very quickly. The optimum design with the stacking sequence of $[-31.4°/74.1°/-58.8°/90°]_s$ is presented in Table 4.1. The weight of Canard #1 has been slightly reduced by 0.8%. The maximum deflection has been significantly reduced by 18% within the allowable constraint limit. It can be seen that by applying the proper ply angles, a lighter and stronger design of composite canard is obtained.

Table 4.1: Optimal results of Canard #1 using CONMIN

	Weight (Kg)	Deflection (m)	Weight reduction	Deflection reduction
Canard #1	217.87	0.1829	----	----
Optimized design	216.13	0.15	0.8%	18%

Table 4.1: (Continued)

	Thickness (m)	$\theta_1(^{\circ})$	$\theta_2(^{\circ})$	$\theta_3(^{\circ})$	$\theta_4(^{\circ})$	$\theta_5(^{\circ})$	$\theta_6(^{\circ})$	$\theta_7(^{\circ})$	$\theta_8(^{\circ})$
Canard #1	0.05	0	45	-45	90	90	-45	45	0
Optimized design	0.0496	-31.4	74.1	-58.8	90	90	-58.8	74.1	-31.4

By substituting those optimal ply angles back into FEMCOMP program, the stress distributions of this optimized canard are obtained. The comparisons of the resulting maximum transverse stresses σ_{yz} and σ_{xz} to initial design are provided in Table 4.2. It shows that both the maximum transverse stresses σ_{yz} and σ_{xz} were reduced.

Table 4.2: Comparisons of maximum σ_{yz} and σ_{xz} between optimal design and initial design of Canard #1

	Maximum σ_{yz} (MPa)	Maximum σ_{xz} (MPa)
Canard #1	3523.0	111.8
Optimized design	2451.8	105.4

Fig. 4.2 gives the detailed stress contour plots. It can be concluded from the present results that due to optimized ply angles, the strength and the stiffness are significantly improved as compared to the initial design of Canard #1.

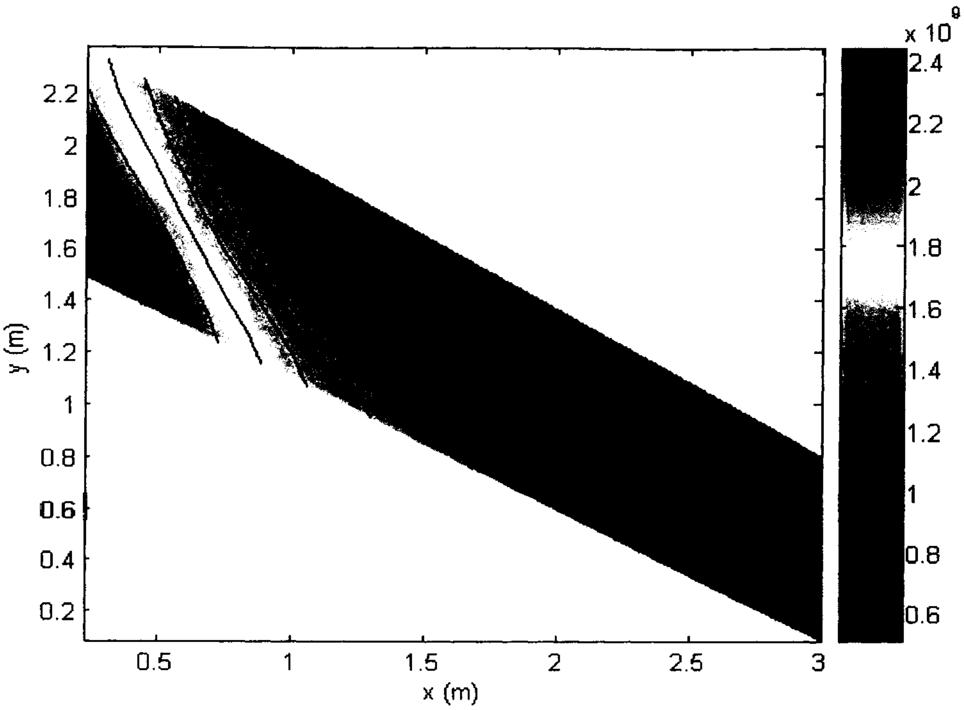

(a) Transverse shear stress σ_{yz} (Pa)

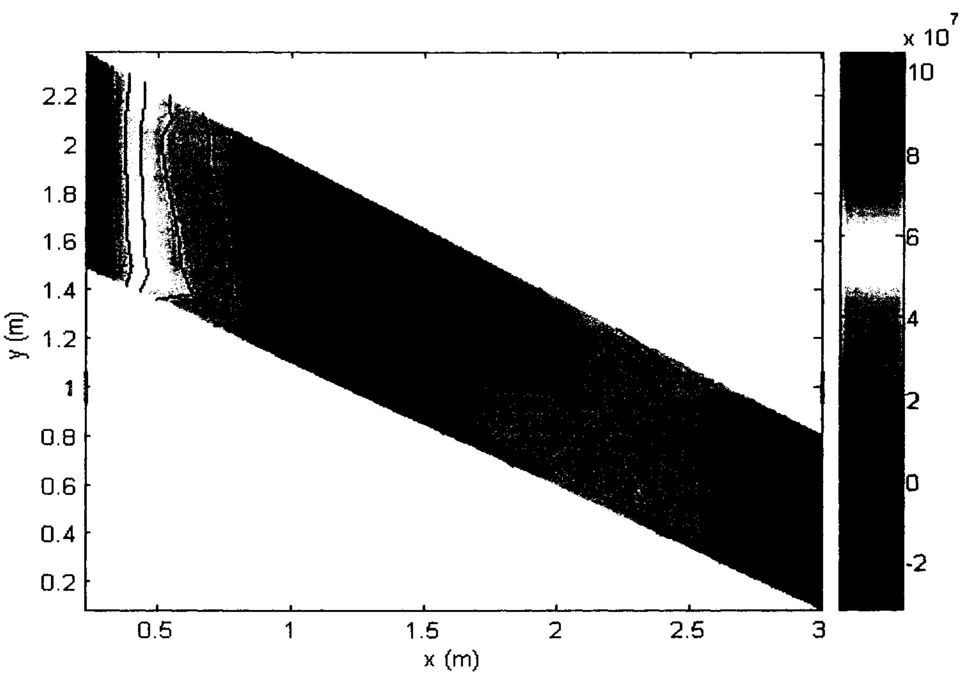

(b) Shear stress σ_{xz} (Pa)

Fig. 4.2: Contour plots of stresses for optimized design of Canard #1

4.3.2 Optimal results for Canard #2 $[-45^\circ/0^\circ/45^\circ/90^\circ]_s$

In this section, CONMIN program re-runs with a different initial design Canard #2 with stacking sequence $[-45^\circ/0^\circ/45^\circ/90^\circ]_s$. The optimal results are presented in Table 4.3. The stacking sequence of the optimized Canard #2 is $[-42.2^\circ/-6.4^\circ/45.2^\circ/90^\circ]_s$. The weight has been reduced by 10.5%, but the maximum deflection increased from 0.1311m to 0.1488m which is acceptable because it still meets the constraint requirement. Since weight is the premium consideration in this optimization problem, this design is better optimized than the optimized design of Canard #1.

Table 4.3: Optimal results of Canard #2 using CONMIN

	Weight (Kg)	Deflection (m)	Weight reduction	Deflection increment
Canard #2	217.87	0.1311	----	----
Optimized design	195.03	0.1488	10.5%	13.5%

Table 4.3: (Continued)

	Thickness (m)	$\theta_1(^\circ)$	$\theta_2(^\circ)$	$\theta_3(^\circ)$	$\theta_4(^\circ)$	$\theta_5(^\circ)$	$\theta_6(^\circ)$	$\theta_7(^\circ)$	$\theta_8(^\circ)$
Canard #2	0.05	-45	0	45	90	90	45	0	-45
Optimized design	0.0448	-42.2	-6.4	45.2	90	90	45.2	-6.4	-42.2

The stress distributions in this optimized design are obtained from the structural analysis. The comparisons of the resulting maximum transverse stresses σ_{yz} and σ_{xz} with initial design are provided in Table 4.4. It shows that both the maximum transverse stresses σ_{yz} and σ_{xz} were increased which is acceptable because the strength check provided positive feedback.

Table 4.4: Comparisons of maximum σ_{yz} and σ_{xz} between optimal design and initial design of Canard #2

	Maximum σ_{yz} (MPa)	Maximum σ_{xz} (MPa)
Canard #2	2095.0	100.0
Optimized design	2603.4	105.8

Fig. 4.3 gives the detailed stress contour plots. It can be concluded from the present results that the strength and stiffness are significantly improved as compared to the initial design due to optimized ply angles.

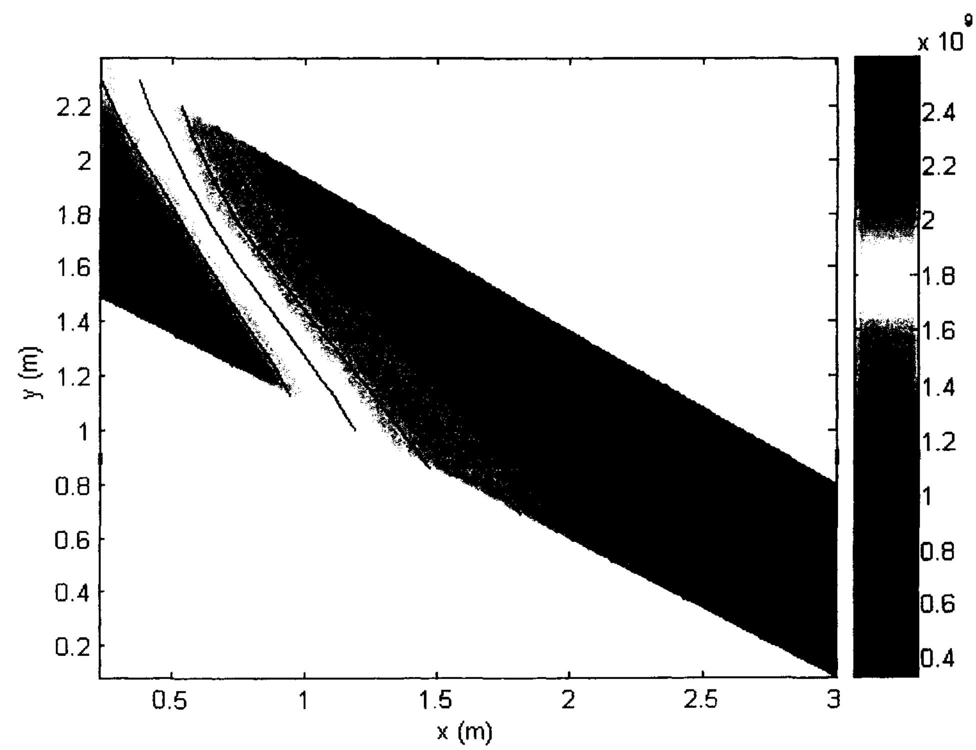

(a) Transverse shear stress σ_{yz} (Pa)

Fig. 4.3: Contour plots of stresses for optimized design of Canard #2

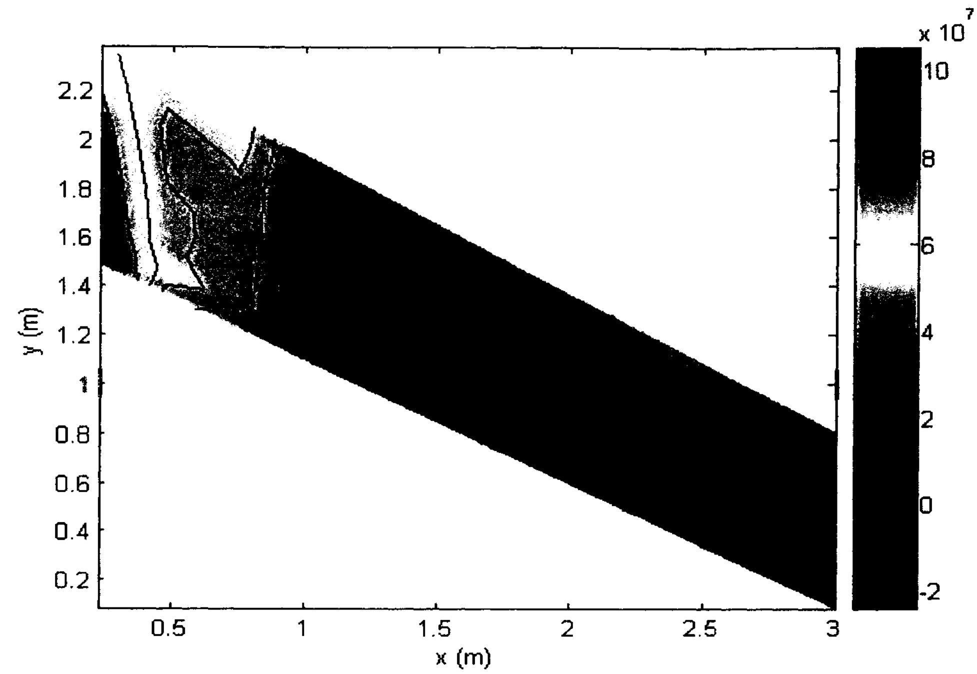

(b) Shear stress σ_{xz} (Pa)

Fig. 4.3: (Continued)

4.3.3 Comparisons of optimal results from different designs

Table 4.5 provides the comparisons of the optimized designs from the searches which started from Canard #1 and Canard #2 respectively. It shows that two different optimized designs have been reached during the gradient-based searching procedure with different initial designs. The optimal design obtained from Canard #2 shows the better performance than the one achieved from Canard #1. Previous structural analysis has shown that the design of Canard #2 provide better mechanical performance than the design of Canard #1. It can be concluded that in order to obtain a better optimized design from the gradient-based optimization, the starting point of the searching procedure plays an important role. The use of a gradient-based optimization is very sensitive to the choice of the initial guess and may often lead to various convergent solutions.

Table 4.5 Comparisons of improved designs of Canard #1 and #2

Starting point	Weight (Kg)	Deflection (m)	Ending point
Canard #1 $[0^\circ/45^\circ/-45^\circ/90^\circ]_s$	216.13	0.15	$[-31.4^\circ/74.1^\circ/-58.8^\circ/90^\circ]_s$
Canard #2 $[0^\circ/45^\circ/-45^\circ/90^\circ]_s$	195.03	0.1448	$[-42.2^\circ/-6.4^\circ/45.2^\circ/90^\circ]_s$

Gradient-based algorithms use the iterative improvement technique; the technique is applied to a single point in the search space. During a single iteration, a new point is selected from the neighborhood of current point. If the new point provides a better value of the objective function, the new point becomes the current point. The method terminates if no further improvement is possible. It can be concluded that the gradient-based algorithms provide local optimum values only and these values depend on the selection of the starting point. To increase the chances to succeed, gradient based algorithms usually are executed for a number of different starting points.

Conclusions

1. Optimized designs were achieved by applying gradient-based optimization program CONMIN. Both the weight and the stiffness of the canard have been improved by adjusting the ply angles and the thickness.
2. The optimized results are different as the starting points of the searches are various. It is clear that the use of gradient-based CONMIN is very sensitive to the choice of the initial design and may lead to a convergence failure. The accuracy of gradients thus obtained is not very high and gradient-based optimizer provides local optimum values only.

CHAPTER 5 OPTIMIZATION DESIGN USING GENETIC ALGORITHMS

The structural optimization using gradient-based optimizer CONMIN has been performed in Chapter 4. In this chapter, the non-gradient based searching methods, genetic algorithms (GAs), are applied to the optimization of the composite canard. The optimum design and relative discussion are presented. Compared to gradient based optimization, non-gradient based optimizers are allowed to perform the optimum search in a zone of design space significantly larger than in the gradient based optimization case. GAs maintain a population of potential solutions while other methods process a single point of the search space. Therefore, in general, the possibility of achieving the true global optimum is high [22].

5.1 Overview of genetic algorithms

Many important large-scale combinatorial optimization problems and highly constrained engineering problems can only be solved approximately on present day computers. GAs aim at such complex problems and belong to the class of probabilistic algorithms, yet they are very different from random algorithms as they combine elements of directed and stochastic search. Because of this, GAs are also more robust than existing directed search methods.

GAs are numerical search procedures derived from the concept of natural genetics and rely on the application of Darwin's principle of survival of the fittest. When a population of biological creatures is allowed to evolve over generations, individual characteristics that are useful for survival tend to be passed onto future generations.

GAs use a vocabulary borrowed from natural genetics. The individuals in a population are called strings or chromosomes. Chromosomes are made of units – genes – arranged in linear succession. Every gene controls the inheritance of one or several characters. Binary numbers are used for representing design information as bit strings. An evolution process run on a population of chromosomes corresponds to a search through a space of potential solution.

Since GAs work with a population of strings, the chances of obtaining global or near-global optima are increased. The risk of converging to a local optima is reduced by keeping many solution points that may have the potential of being close to local or global optima in the pool during the search process, rather than converging on a single point early in the process. There are more detailed discussions on their theoretical properties in Michalewicz's book [22]. First application of GAs to the structural design problem can be attributed to Goldberg. Gurdal, Haftka and Hajela discussed the applications of GAs to the design of structures made of composite materials in their book [43].

GAs are ideal for global optimization for non-linear systems with non-convex solution spaces. The notable feature of GAs is that it emulates the biological system's characteristics like self repair and reproduction. The actual differences between the GAs and other methods of optimization are briefly summarized below. GAs move through the solution space starting from a population of points and not from a single point as in gradient based algorithm. This is similar to the calculus based methods where the solutions are restarted from a number of points in order to ensure global convergence. GAs work with the objective function information directly and not with any other auxiliary information like derivatives. GAs use probabilistic rules and not deterministic rules.

5.1.1 Representation of the optimal problem

As we know, GAs use a genetic vocabulary and work with a population of strings, therefore, the representation of the problem is required before the operations of GAs can be applied to a search problem. The design variables and objective function are converted to chromosomes and fitness function. The representing procedure could be implemented in the following steps,

(1) Use binary vectors as chromosomes to represent real values of the design variables.

(2) A population of chromosomes is created and each chromosome is initialized randomly.

(3) Define an evaluation function for binary vectors, which is equivalent to the objective function f,

$$eval(v_1, v_2, v_3, v_4) = f(\bar{X}) \qquad (5.1)$$

where the chromosomes v_1, v_2, v_3, v_4 represent the real values $\bar{X}$. The evaluation function plays the role of the environment, potential solutions in terms of their fitness, which is defined on the basis of the numerical value of the objective function.

5.1.2 Genetic operators

The mechanics of natural genetics is based on operations that result in structured yet randomized exchange of genetic information between the chromosomal strings of the reproducing parents and consists of selection, crossover, occasional mutation, and permutation. Typically, two designs selected from a population are mated to create child designs. In order to ensure that good designs propagate to the child populations, a higher chance to be selected as parents is given to those designs that are better (having a higher fitness) than the rest of the population. The major genetic operators are listed below,

(1) Selection

The selection process simulate biology in giving more fit designs a higher chance to breed and pass their genes to future generations. GA use fitness in a procedure that selects pairs of parents that will be used to create child designs for future generations.

(2) Crossover

Once pairs of parents are selected, the mating of the pair also involves a random process called crossover. A cutoff point in each of the two strings is defined, which separates each into two substrings. Then the left part of the string of one parent and the right part of the string of the other parent are spliced together. One or both of the child designs are then selected for the next generation.

(3) Mutation

Mutation alters one or more genes (positions in a chromosome) at random with small probability equal to the mutation rate, which prevent the premature loss of important genetic information. Mutation is implemented by generating a random number between 0 and 1 and changing the value of a digit in the string if its value is smaller than the mutation rate.

During a single iteration, a genetic algorithm maintains a population of potential solutions (chromosomes). Each solution is evaluated to give some measure of its "fitness". Then, a new population is formed by selecting the more fit individuals. Some members of this new population undergo alterations by means of crossover and mutation, to form new solutions. Crossover combines the features of two parent chromosomes to form two similar offsprings by swapping corresponding segments of the parents. The intuition behind the applicability of the crossover operator is information exchange between different potential solutions. Mutation arbitrarily alters one or more genes of a selected chromosome, by a random change with a probability equal to the mutation rate. The intuition behind the mutation operator is the introduction of some extra variability into the population.

5.1.3 Constrained problem statement

For most engineering optimization problems, implementation of performance constraints is one of the most important factors in obtaining feasible solutions. In GAs, for unconstrained problems, the fitness of a design can be easily defined as the objective function; for constrained problems, the fitness must consider constraint violations or constraint margins. The search procedure of GAs does not directly consider constraints. To account for solution constraints, the constrained optimization problem is transformed into an unconstrained maximization problem using a penalty function approach.

Consider the standard formulation of an optimization problem, such as

Minimize $f(x)$, $\quad x \in X$

Such that $g_j(x) \leq 0$, $j = 1,\ldots,n_g$

where $g_j(x)$ are normalized constraints. The design margin of safety is defined by the most critical constraint $g_{\max} = \max_j(g_j)$. If $g_{\max}$ is positive, the design is infeasible, and a penalty will be added to the objective function to help the search move into the feasible design. If $g_{\max}$ is negative, a feasible design with a positive margin of safety will be obtained. Define an augmented objective function f^* as

$$f^{*}=\begin{cases} f\Phi, if(g_j > g_{\max}) \\ f-\varepsilon|g_{\max}|, otherwise \end{cases} \quad (5.2)$$

where, Φ is the penalty function; ε is the bonus parameter, which is needed to find the optimum design with the highest safety margin.

5.2 Optimization process of GAs

GAs perform a multi-directional search by maintaining a population of potential solutions and encourages information formation and exchange between these directions. The population undergoes a simulated evolution: at each generation the relatively "good" solutions reproduce, while the relatively "bad" solutions die. To distinguish between different solutions an evaluation function is employed which plays the role of an environment.

5.2.1 Formulating the optimization problem in GAs

The requirements of the optimization problem are the same as defined in gradient based optimization in Chapter 4 – finding the proper ply orientations and the thickness of the laminated canard to minimize the weight of the canard with adequate stiffness. The objective function and design variables are also kept the same as in the previous study. Constraint is augmented to the objective function using penalty functions.

The formulation of the optimization problem in GAs is provided below:

(1) Genetic representation for potential solutions (Encoding/decoding)

Usually GAs are used for discrete variables, but here the design variables are continuous. Ply angles and thickness are coded as binary numbers and mapped back to decimal numbers later. Chromosomes are defined as shown in Fig.5.1.

The length of the binary vector depends on the required precision, which, in this problem, is 3 places after the decimal point. For example, the range of the ply angles is $[0,\pi]$ which has length π; the precision requirement implies that the domain should be divided into at least $\pi \cdot 1000$ equal size ranges. This means that 9 bits are required as a binary chromosome:

$2048 = 2^{11} < 3142 < 2^{12} = 4096$.

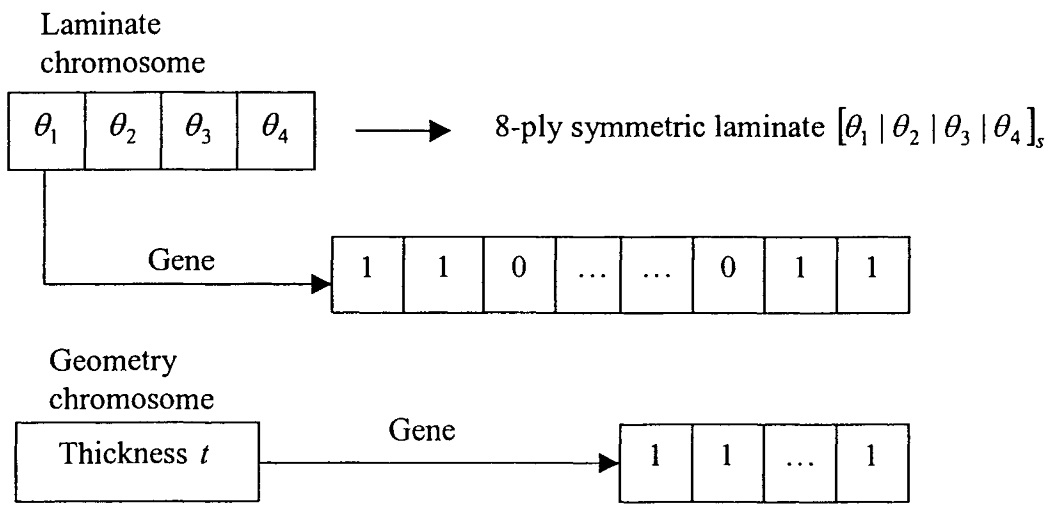

Fig. 5.1: Definition of chromosomes

Hence, there are four binary strings in laminate chromosomes: each of them consequently represents a ply angle by a 12 bits string. The range of the thickness is $[0.03, 0.05]$ and the required precision is 4 places after the decimal point. One binary string is in the geometry chromosome to represent the plate thickness, which is a 8 bits long binary number:

$$128 = 2^7 < 200 < 2^8 = 256.$$

The mapping from a binary string into a real number from the range is straightforward and is completed in two steps:

- Convert the binary string from the base 2 to base 10;

  For example, reverse the laminate chromosome back to real number, $(b_{12}b_{11}...b_1)_2 = (\sum_{i=1}^{12} b_i \cdot 2^i)_{10} = \theta_i^{'}$

- Find a corresponding real number θ_i.

$$\theta_i = LB + \theta_i^{'} \cdot \frac{UB}{2^{12} - 1},$$

Where LB is the lower boundary of the domain of θ_i and UB is the upper boundary.

(2) Creation of the initial population

In this work, the optimizer works with a fixed-size population, so the size of the initial population of designs determines the size of the population in all future generations as well. In general, the optimal size of the population increases with problem size. The design of a thin laminate will require a smaller population size than the design of a thicker laminate that must be represented by a longer string. The initial population is typically generated at random and distributed uniformly between 0 and 1.

(3) Fitness function

The weight of the canard is used as the fitness function, which is a function of the continuous design variables. The goal of the optimization is to find the lightest design that does not violate any of the imposed constraints.

Although constraints are usually classified as equality or inequality constraints, both types are handled identically in GAs. After performing the evaluation processor FEACOMP, it is possible to evaluate the objective function and to check the associated constraint. If no constraint is violated, then no penalty is assigned to that string; therefore, the values of the fitness function and its corresponding penalized fitness function are identical. In case that some constraints are violated, a penalty function is applied to the objective function. The value of the penalty is related to the degree in which the constraints are violated. The penalized objective function quantitatively demonstrates the extent of the violation of constraints and provides a relatively meaningful measurement on the performance of the string.

For the standard formulation,

$$\text{Minimize } W(t), \qquad x \in X$$

$$\text{Such that } d_i(t,\theta) \le d_{\max},\ i = 1,\dots,n_g$$

Where, W is the weight of the canard; d_i is the constraint of the problem; n_g is the number of constraints. The design margin of safety is defined by the critical constraint. If d_i is larger than $d_{\max}$ and then the design is out of the target range, side constraint is active and a penalty will be added to the objective function to help the search move into the feasible design range.

A Quadratic penalty function is applied to the objective function, which is defined as:

$$\Phi = 1 + p\left(\frac{d_i - d_{\max}}{d_{\max}}\right)^2 = 1 + p\left(\frac{d_i}{d_{\max}} - 1\right)^2 \tag{5.3}$$

where Φ is the penalty for the constraint, p is the penalty factor, d_i is the value of the constraint from a solution string, $d_{\max}$ is the maximum allowable value of the constraint.

The value of the penalty is related to the degree in which the constraint is violated. The penalized objective function of a particular solution string can be obtained by multiplying the fitness value (weight of the structure) by the corresponding penalty. Substitute Eq.(5.2) into Eq.(5.3), the fitness function with penalty function is obtained as below

$$W^* = \begin{cases} W\left[1 + p\left(\dfrac{d_i}{d_{\max}} - 1\right)\right]^2, if(d_i) > d_{\max} \\ W - \varepsilon\left|\dfrac{d_i}{d_{\max}}\right|, otherwise \end{cases} \tag{5.4}$$

where, p penalize infeasible design; ε is the bonus parameter, which is needed to find the optimum design with the highest safety margin.

(4) Genetic operators

The routine includes tournament selection, uniform crossover, creep mutation, and the jump mutation.

Selection operator. The selection scheme used here is *tournament selection* with a shuffling technique for choosing random pairs for mating. To run a tournament selection, a tournament size is chosen. The procedure is simply to randomly choose solutions from the population and select the one with the highest fitness. When using Tournament selection to create a mating population, the selected solution remains since the very good solutions would be chosen more than once.

Crossover operator. The crossover operator used here is *uniform crossover.* It decides with some probability, known as the mixing ratio, which parent will contribute each of the gene values in the offspring chromosomes. This allows the parent chromosomes to be mixed at the gene level rather than the segment level (as with one and two point crossover).

Mutation operator. Two mutation operators were used in this work. *Creep mutation* – the value of the gene is randomly changed by a small random quantity assuming a quadratic probability distribution functions centered on the current value. *Jump mutation* – the value of the gene is randomly reset to a value determined by assuming a uniform probability distribution functions with appropriate upper and lower bounds [22].

(5) Values of various parameters employed in GAs

Based on the precious discussion of GAs, the parameters used in the optimization procedure have been determined and listed in Table 5.1.

Table 5.1: GA parameters used in the optimization design

Parameter	Value
Number of generation	50
Population size	50
Laminate chromosome length	48
Geometry chromosome length	8
Probability of crossover (p_c)	0.01
Probability of mutation (p_m)	0.5
Crossover type	Uniform

The requirements of the optimization design using GAs are declared as following

- *Objective function*

  Minimize the weight $W(t)$

- *Design variables*

  Plate thickness t, $0.03m \le t \le 0.05m$

  Ply orientations θ_i, $-\dfrac{\pi}{2} \le \theta_i \le \dfrac{\pi}{2}$, $i = 1,2,3,4$

- *Design parameters*

  Geometric dimensions, design loading

- *Design constraint*

$$\|d(t,\theta_i)\| \le d_{\max} \quad \text{where } d_{\max} = 0.15m$$

- *Fitness function*

$$W^*(t) = \begin{cases} W\{1 + p[(\dfrac{d_i}{d_{\max}}) - 1]^2\}, if(d_i) > 0.15 \\ W - \varepsilon\left|\dfrac{d_i}{d_{\max}}\right|, otherwise \end{cases}$$

where the constraint d represents a functional relationship between design objective minimum $W(t)$ and design variable t, which satisfy certain physical phenomenon and resource limitations; the penalty factor $p = 100$, and the bonus parameter $\varepsilon = 1.0$.

5.2.2 Software implementation

A Fortran program GA originally coded by David Carroll [44, 45, 46] has been re-implemented and served as the function optimization engine in this work. This code initializes a random sample of individuals with different parameters to be optimized using the genetic algorithm approach. The finite element code FEMCOMP was used as a fitness function evaluator in conjunction with GA. The flow chart in Fig. 5.2 presents the optimization process using GA.

At the start of the optimization, a random choice of potential designs is created and put into a fitness function. The fitness of this potential design is then calculated. Next, the potential solutions are converted to binary strings from floating point numbers, which is called encoding. The collection of binary strings of potential designs is *chromosome* and each bit of the string is gene. The collection of chromosomes and corresponding fitness are called individual. The collection of individuals is called population. The initial set of individuals is called parents. After initializing the population, two "good" parents with good fits are selected, which is done by using the selection process. The selection process ensures that parents with good fits get to breed, and parents with bad fits don't. In the crossover part, two parents chosen in selection process are mated by taking some genes form each parent to create a new complete binary string, which is called child. Once a complete binary string is created, expose the children to a low mutation rate, flipping or switching a few bits randomly

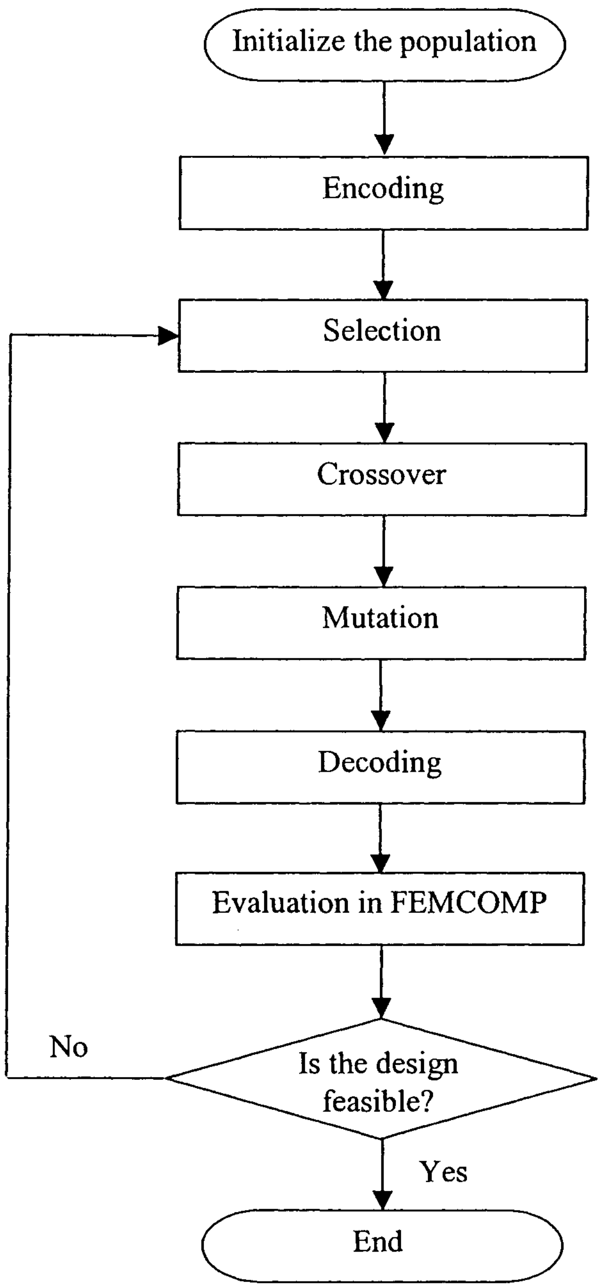

Fig. 5.2: Flowchart of GA optimization

which is mutation process. After the genetic operations, the binary strings are turned back into floating point numbers (decoding) and the fit of the set is calculated. This is the formulation of child. If this child is proved to be the best design, the optimization is finished, otherwise, transfer children array to the parent array and this is a new generation. The operations are repeated until the population converges. Here, the fitness value is defined as the objective function of the minimization instead of weight of the canard due to the constraint property.

5.3 Results

5.3.1 Discussion about the convergence of GA

For gradient-based optimizer CONMIN, the norm of the gradient can be used as a descent function and should decrease as the iterations progress and become very small at the local optimal point. However for GA, it is not possible to tell when the optimal point is reached particularly for engineering problems where the point is not known in advance. Since this structure-fluid problem consists of plenty of iterative loops, it is very difficult to determine a general converged situation (e.g. 80% of the population converge to same value) in GA. Thus, in the present study, there is no convergent condition applied on GA program and GA is required to run through 50 generations at each time due to the consideration of the computational cost.

On the other hand, GA is a randomized procedure. In order to prove the consistency in getting optimal solutions, 5 independent runs with the same GA parameters were conducted. Fig. 5.3 plots the variation of the best fitness vs. generations of the 5 random runs. It shows that each node achieving approximately the same performance after relatively few generations and converged around 25 generations. All 6 runs were converging to the same best fitness values within 50 generations. Run 3 converged a bit slower than other runs. Run 5 and 6 experienced the exact same convergence procedure.

The convergence curves of the random runs also demonstrate that initially the solution quality improved very rapidly and converged to a relative stable optimal value around 25 generations. Then no further significant improvement on the best fitness value has been made and the majority of the computation time was spent in the later part of the process in which very small improvement is obtained slowly. It indicates that GA faces difficulties in fine tuning. In general, local search techniques have the advantage of solving the problem quickly, though their results are very much dependent on the initial starting point; therefore they can easily be trapped in a local optimum. GA samples a large search space, climbs many peaks in parallel, and is likely to lead the search towards the most promising area. However, GA spends much time on comparing the similar peaks instead of catching a 'higher' one which causes the less efficiency of current standard GA.

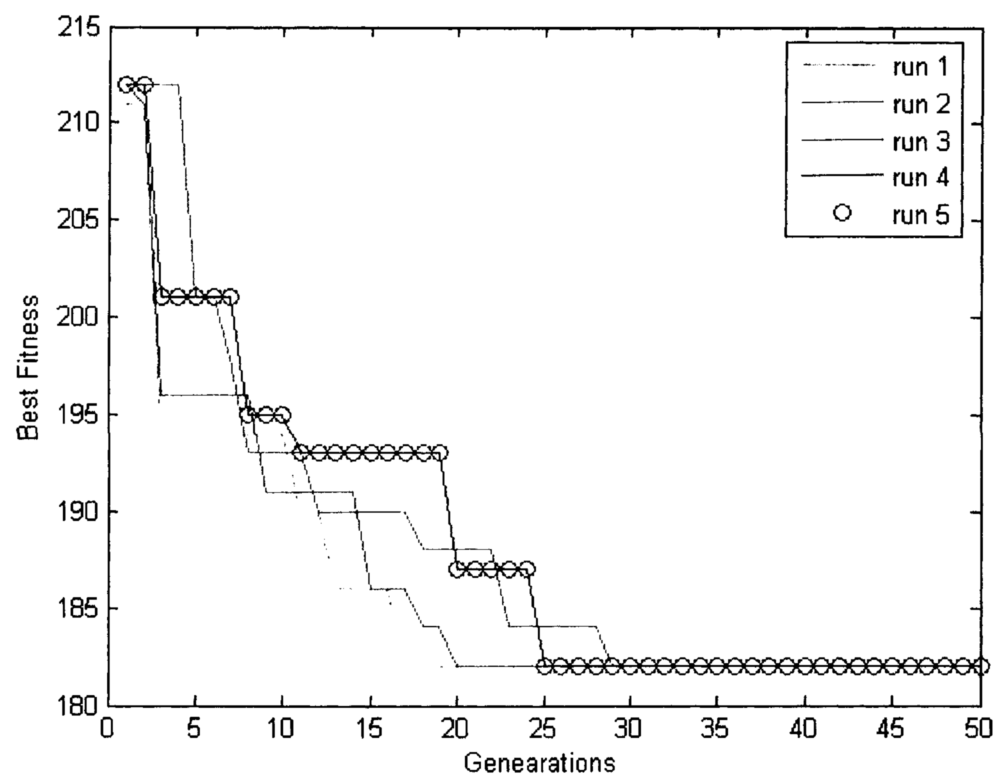

Fig.5.3: Convergence tendencies of GA

Table 5.2 presents the optimal results from 5 random runs shown above. As the objective function, the weight of the canard has been optimized to the same value 184.32 Kg from all runs. According to the various stacking sequences provided by GA, the deflections of those designs are slightly different. Since the result of run 5 has been repeated exactly in run 6 and performed better than others, the design with stacking sequence

$[-20.2°/-67.7°/-20.9°/-57.1°]_s$ and thickness 0.0423 m is considered as the converged design from GA.

Table 5.2: Results of 5 runs of GA

	Weight (Kg)	Deflection (m)	Thickness (m)	Optimized stacking sequence
Run 1	184.32	-0.1499	0.0423	$[-19.5°/-83.9°/-15.9°/-50.1°]_s$
Run 2	184.32	-0.1489	0.0423	$[-20.5°/-37.8°/-76.5°/-67.3°]_s$
Run 3	184.32	-0.1406	0.0423	$[-18.4°/79.6°/-29.3°/-52.6°]_s$
Run 4	184.32	-0.1373	0.0423	$[-20.2°/-67.7°/-20.9°/-57.1°]_s$
Run 5	184.32	-0.1373	0.0423	$[-20.2°/-67.7°/-20.9°/-57.1°]_s$

5.3.1 Optimal design from GA

Again, Canard #1 with the sequence $[0°/45°/-45°/90°]_s$ is assigned as the initial design and then is compared to the optimal design obtained from GA.

Both the optimum design with the stacking sequence of $[-20.2°/-67.7°/-20.9°/-57.1°]_s$ from GA and the design of Canard #1 are presented in Table 5.3. It demonstrated that the weight of the canard has been significantly reduced from 217.87 Kg to 184.32 Kg by 15.4%. The maximum displacement at the free end of the optimum laminate is 0.1373 m, which has been improved by 24.8%. Compared to the optimum designs obtained from CONMIN, the optimum design from GA has a much lighter weight and hugely improved mechanical performance. It is clear that GA helps reach the global optimum and gradient-based algorithm CONMIN provides local optimum only.

Table 5.3: Optimal results using GA

	Weight (Kg)	Deflection (m)	Weight reduction	Deflection decrement
Canard #1	217.87	-0.1827	----	----
Optimized design	184.32	-0.1373	15.4%	24.8%

Table 5.3: (Continued)

	Thickness (m)	$\theta_1(^{\circ})$	$\theta_2(^{\circ})$	$\theta_3(^{\circ})$	$\theta_4(^{\circ})$	$\theta_5(^{\circ})$	$\theta_6(^{\circ})$	$\theta_7(^{\circ})$	$\theta_8(^{\circ})$
Canard #1	0.05	0	45	-45	90	90	-45	45	0
Optimized design	0.0423	-20.2	-67.7	-20.9	-57.1	-57.1	-20.9	-67.7	-20.2

By substituting those optimal ply angles back into FEMCOMP program, the stress distributions of this optimized canard are obtained. The comparisons of the resulting maximum transverse stresses σ_{yz} and σ_{xz} to Canard #1 are provided in Table 4.2. It shows that the maximum transverse stress σ_{yz} was reduced significantly by the optimization while the value of maximum σ_{xz} increased. This design passed the strength check.

Table 5.4: Comparisons of maximum σ_{yz} and σ_{xz} between optimal design and initial design of Canard #1

	Maximum σ_{yz} (MPa)	Maximum σ_{xz} (MPa)
Canard #1	3523.0	111.8
Optimized design	1931.0	532.3

Fig. 5.4 gives the detailed stress contour plots. It can be concluded from the present results that due to the optimized ply angles, the weight and the stiffness are significantly improved as compared to the design of Canard #1.

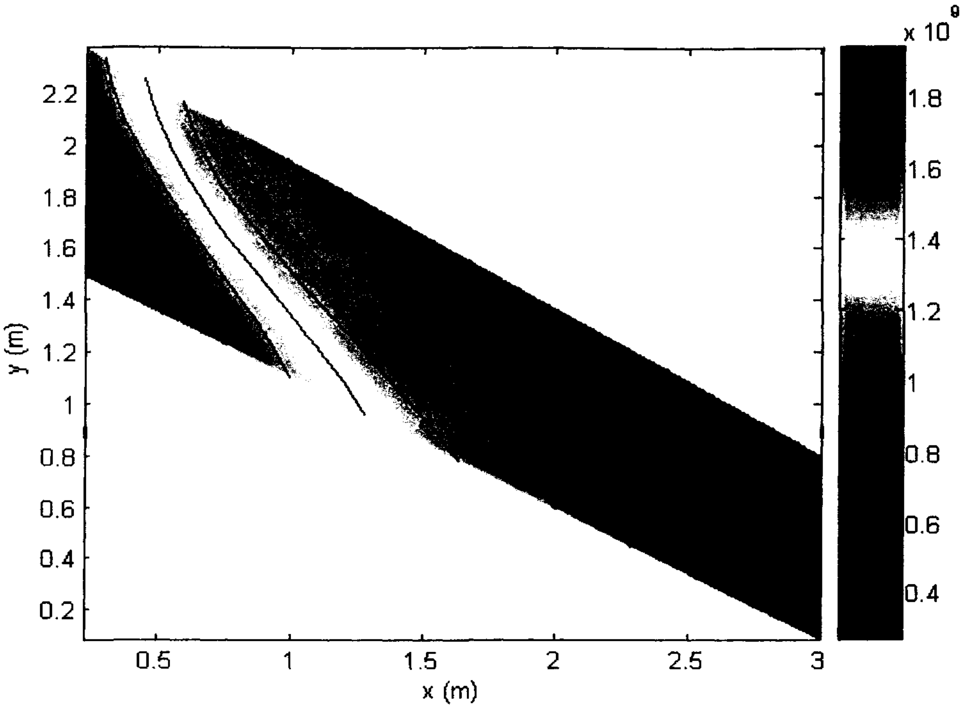

(a) Transverse shear stress σ_{yz} (Pa)

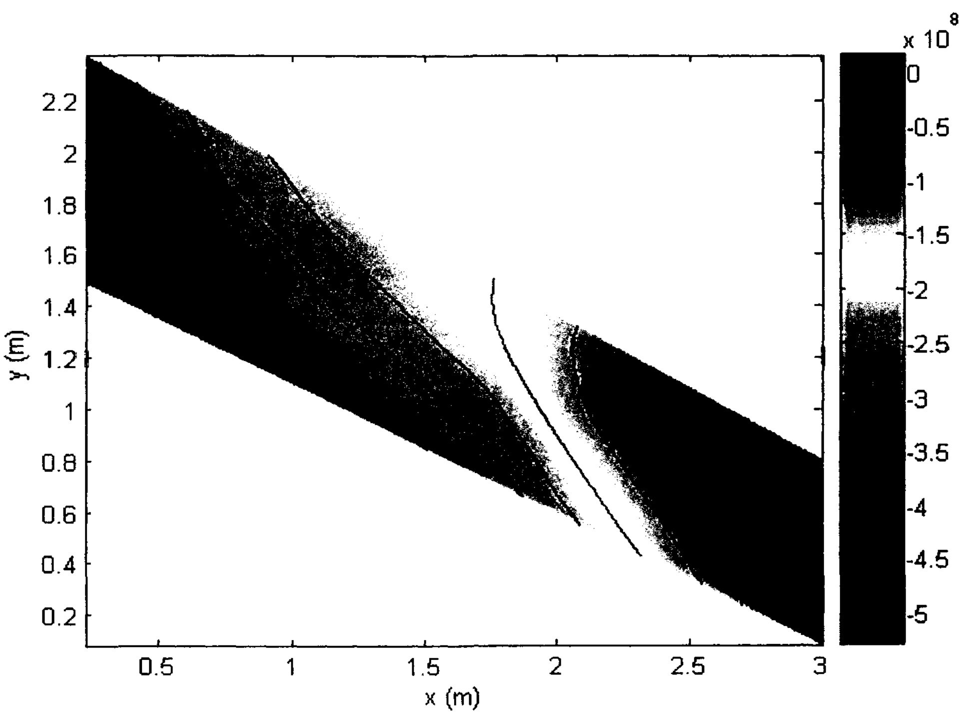

(b) Shear stress σ_{xz} (Pa)

Fig. 5.4: Contour plots of stresses of GA optimization

Conclusions

1. GA has been applied on the optimization of composite canard as a global optimizer in this chapter. An optimal design has been obtained which has much better mechanical performance than the original design of Canard #1 and the optimal designs obtained from CONMIN.
2. Despite the broad applications and superior searching abilities, GA has not demonstrated itself to be very efficient. GA is generally time-consuming because they needs much trial and huge search space. On the other hand, the use of GA doesn't guarantee convergence to global optima because of its poor exploitation capabilities. The other drawback of GA is the lack of a good convergence criterion.

CHAPTER 6 A HYBRID APPROACH OF GA AND CONMIN

The gradient based algorithms and GAs have been applied to the optimization design problems in the previous chapters. In this chapter, firstly, the optimization processes and optimal designs of the laminated canard by using CONMIN and GA are compared and the relative discussion is provided. Secondly, a hybrid method, which combined gradient based algorithms and GAs, is implemented. A program HYBRID coupled CONMIN and GA has been coded in Fortran to carry out the optimization design. It is demonstrated that the hybrid approach is a more accurate and efficient technique by comparing to CONMIN or GA alone. Results from HYBRID are presented next.

6.1 Comparisons of gradient-based algorithms and GAs

The optimization problem has been solved by analyzing the gradients of the objective function and constraints with respect to the independent design variables (CONMIN) and by performing a very large number of design evaluations (GA) separately. Table 6.1 gives the comparisons of the final optimal results and computational cost of CONMIN and GA. It can been seen that CONMIN converged to a local best value in reasonable computational time and GA typically required a large number of analyses during the optimization search to reach the global or near-global optimum with a high degree of confidence. Both methods were run on Pentium M 1.5 GHz computer.

Table 6.1: Comparisons of optimal results and computational cost

Solution method	Optimal weight (Kg)	Out-of-plane deflection (m)	Computational time (hour)
CONMIN	216.13	-0.15	0.2
GA	182.58	-0.1373	20~25

Engineering optimization problems have often to deal with non-smooth and/or non-convex design spaces. Consequently, many optimization methods may become unattractive since they get stuck in local optima. In general, gradient-based optimizers are capable of reaching an optimum design rather quickly but there is no guarantee if the attained design is global optimized. A typical feature of such problems is that the generation of starting points, that are used to perform the search with conventional optimization methods, is a basic point to guarantee the success of the optimization procedure. The use of a gradient based optimization is very sensitive to the choice of the initial guess and may often lead to a convergence failure. It has been demonstrated that the accuracy of gradients thus obtained is not very high. But gradient information is calculated in a fast and easy manner.

On the other hand, for non-gradient based optimizers, such as GAs, the optimum search is performed in a zone of design space significantly larger than in the gradient based optimization case, which increases the chances to reach the global and near-global optimum. However, the main problem of GAs is that it consumes significant time, especially for solving complicated problems, which is because that GAs sample a large search space and climb many peaks in parallel to lead the search towards the most promising area. GAs are considered too time-consuming in an optimization cycle. Due to high cost of computation it is unaffordable. Recently, methods to improve the performance of standard GAs have attracted the attention of researchers. In a typical GA convergence curve, initially the solution quality improves very rapidly. However, obtaining further improvements soon becomes very difficult, and the majority of the computational time is spent in the later part of the process in which very small improvement is achieved and that too slowly. Local search techniques have the advantage of solving the problem quickly, though their results might not be the global optima.

GAs have another drawbacks such as premature convergence which occurs because of the loss of diversity in the population and it is a commonly encountered problem when the search goes on for several generations [24, 31]. Numerical experiments are also needed to properly select the size of the starting population, crossover probability, mutation probability, and the maximum number of generations. One more shortcoming of GAs is the lack of a good convergence criterion. For gradient-based optimization methods, the norm of the gradient can be used as a descent function and would decrease as the iterations progress and become very small at the local optimal point. For GAs, it is not possible to tell when the optimal point is reached particularly for engineering problems where the point is not known in advance. Hence, most of the engineering software use gradient-based methods which offer a clear optimal point.

As a summery of the comparisons of gradient-based optimization methods and non-gradient-based GAs, Table 6.2 lists the advantages and disadvantages of local searching and direct search methods. In order to improve the optimization algorithms both effectively and efficiently, a reasonable compromise is to use GAs to explore large fractions of design space and uses gradient information to speed up the design process.

Table 6.2: Comparisons of gradient-based algorithms and GAs

Optimization method	Advantage	Disadvantage
Gradient-based algorithms	Quick convergence	Local optima
GAs	Global or near-global optima, robustness	Time-consuming, lack of clear convergence criteria, premature convergence

6.2 Integration of gradient based algorithms and GAs

Despite the superior search ability of GAs, they fail to meet the high expectation that theory predicts for the quality and efficiency of the solution. It has been widely accepted that a standard GA is only capable of identifying the high performance region at an affordable time and display inherent difficulties in performing local search for numerical applications [29, 30]. Michaelewicz suggested that GAs should be used as a preprocessor to perform the initial search [22], once the high performance regions of the search space are identified by GAs, it may be useful to invoke a local search routine to optimize the members of the final population. To the direct search method such as GAs, a large number of design evaluations required, and the problem of premature convergence, are the main disadvantages identified for this type of optimization. As opposed to gradient-based methods, there is no guarantee that the optimum is attained, or even that it will be found at all. On the other hand, the method is likely to locate the global optimum instead of converging on a local one. The Robustness of the method, unless premature convergence occurs, is higher that that for gradient-based methods.

6.2.1 Automated hybrid approach

GAs are often hybridized using a local optimization algorithm to improve its performance as a global optimization technique while overcoming the limitations of poor convergence and weak exploitation capabilities. Several methods of hybridization have been proposed to improve the reliability and efficiency of GAs, such as, pre-hybridization [47, 48] where the local optimization algorithms are applied to reduce the solution space of GA; organic-hybridization [49, 50, 51, 52] where a local optimization method is used as one of the operators of GA for improving each member of the population in each generation; and post-hybridization [33, 35, 53] where GA is used to provide an optimal design for local optimization method. However, the application of the hybridization of GAs on the optimization of composite structures has not gained enough attention yet. On the other hand, to run the hybrid procedure in one scheme is also a huge challenge.

A contribution to improve GAs by developing an automated hybridization method which provides increased performance when compared to a GA or local search along has been presented. A combined optimization algorithm based on the successive use of a genetic algorithm and of a classical gradient-based method is proposed. Instead of running the GA and CONMIN in two separate schemes, an automated hybrid approach is developed. Then, a single run of the algorithm will give a global optima in most cases irrespective of the characteristics of the optimization function. In the automated scheme, GA is used to perform a preliminary search in the solution space for locating the neighborhood of the solution. Once the feasibility condition in the first phase is achieved, the gradient-based optimizer CONMIN is applied to refine the best solution field provided by GA and quickly converge towards the exact optimum. In this way, the good characteristics of gradient-based method (efficiency, exactness) and global search methods (global optimum, robustness) are combined.

6.2.2 Software implementation

To overcome the limitations and obtain a compromise between the computational expense and the accuracy of the solution, an automated approach HYBRID based on the hybridization of GA and gradient-based CONMIN has been developed here. In HYBRID, in the first phase the conventional GA is applied for the initial search and CONMIN with a proper starting point (the best individual of GA search) has been used to refine the search in the second phase. The proposed hybrid technique is applied to optimize the design of the laminated canard. The results achieved are compared with results from GA and CONMIN seperately. The flowchart of HYBRID is shown in Fig. 6.1. The scheme of HYBRID is expected to take advantage of the strength of each algorithm. The basic operations involve GA developed in the previous study (encoding with binary representation of real values, evaluation function) for the first phase search to find the optimal region very quickly and in the second phase, CONMIN is applied to speed up the searching process.

Feasibility condition for GA. One of the key components of the automated hybridization algorithm is the feasibility condition in the first phase which is used to stop the GA runs and obtain the best solution field for the local searching run by CONMIN. The gradient-based local searching should be applied as early as possible to reduce computational time. However, if it is started too early, the results from GA may not be close enough to the best individual field because the sample points are few. Thus, the local search becomes nonsense and the calculation of local optima is wasted. Hence, the appropriate time for beginning local improvement must be carefully determined. The feasibility plays a very important role in the automated hybridization process.

The first phase of HYBRID stops if the following pre-set termination condition of Eq. (6-1) becomes true: for the best fitness value at generation j, $BestFit(j)$, and at generation $j-1$, $BestFit(j-1)$,

$$\frac{|BestFit(j)-BestFit(j-1)|}{|BestFit(j)|}\le\delta \tag{6-1}$$

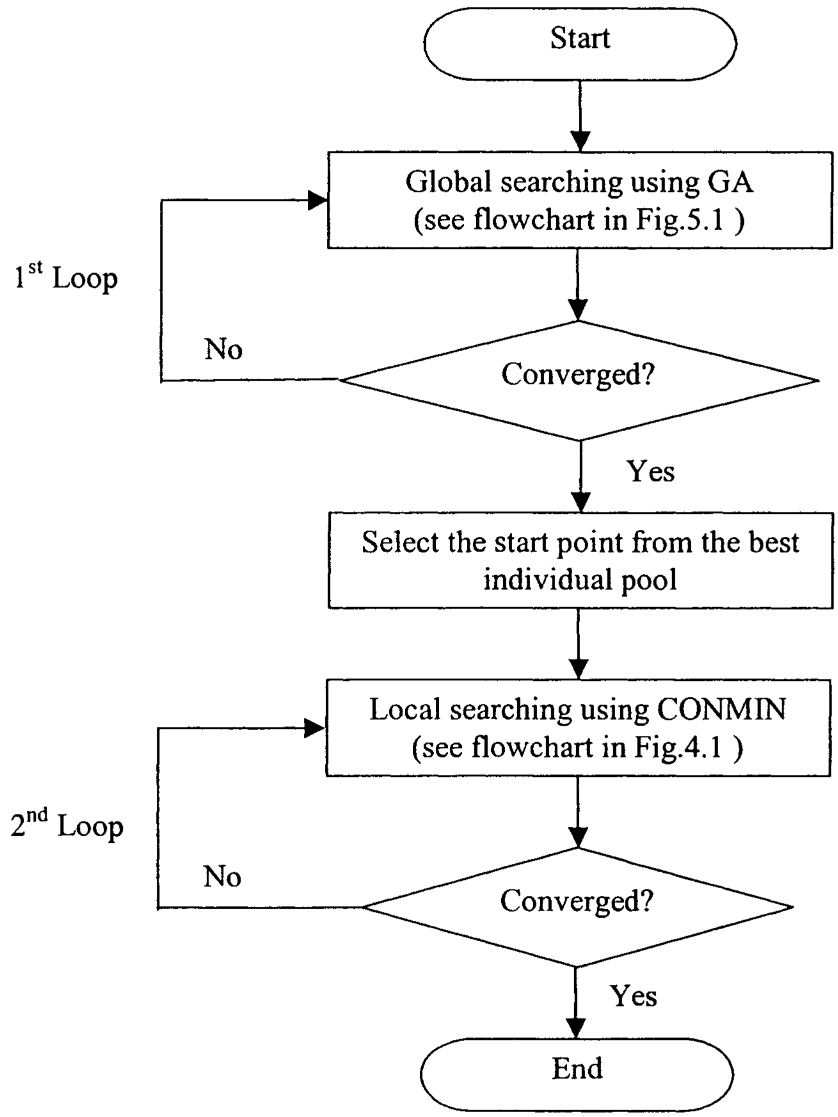

Fig. 6.1: Flowchart of the hybrid optimization method

for successive 10 generations; where, δ is a sufficiently small positive value, which is taken as 0.001. Once GA converges, an optimal region in the form of best vector $BestFit(10)$ is achieved. For each generation, there is a set of design solutions for $BestFit$, such as, θ_1^i, θ_2^i, θ_3^i, θ_4^i, and t^i for $BestFit(i)$, which is the solution set at the ith counted generation.

After the optimal field is obtained, optimization by CONMIN is next employed. The results obtained from GA are used as the initial conditions for CONMIN. The optimization procedure based on gradient-based search in searching region is found effective in solving various problems in the field of non-linear programming. The most attractive feature is the speed in obtaining the optimum and reliability of the results.

Selection of the starting point for CONMIN. The selection of starting point from the optimal region obtained from GA is the other key component of the automated process.

The best vector *BestFit* from GA is used as the optimal field for CONMIN. The design with the minimum weight and deflection is taken as the best design in *BestFit* and will be fed to CONMIN as its initial estimate. Also, the searching bound of the second phase is defined according to the range of the optimal field from GA. The minimum value of the thickness solution in vector *BestFit* are taken as the upper searching bound of the design variables in CONMIN; the upper and lower searching boundaries of ply angles are not necessarily to follow the bounds of designs in vector *BestFit* because CONMIN, as a gradient-based searching method, is more sensitive to the starting point than the constraint bounds. Thus, the searching bounds have been given below in Eq. (6-2),

$$\begin{aligned} & t \le t^*_{\min} \\ & -\frac{\pi}{2} \le \theta_i \le \frac{\pi}{2}, \qquad i = 1,\ldots,4 \end{aligned} \tag{6-2}$$

where, $t^*_{\min}$ is the thickness of the best design $BestFit_{\min}$.

Usually, an improved design will be obtained from the local search of the second phase. But sometimes it can not be achieved even though the starting point is the best design from GA due to the limitation of CONMIN. Thus a correction factor is applied to help the local search reach the global optimum. In general, the correction factor is taken as 0.5% because the best design from GA is very close to the global optimum or might be the global optimum and there is no space to make a big shift. For example, if the design from the second loop is not improved, then the thickness and the relative search bounds will be reduced by 0.5% and the local search runs based on the adjusted parameters. If the design keeps unchanged after this operation, then it is assured that the best design from GA is the global optimum. Fig.6.2 gives the flow chart of the process with adjustment on objective value.

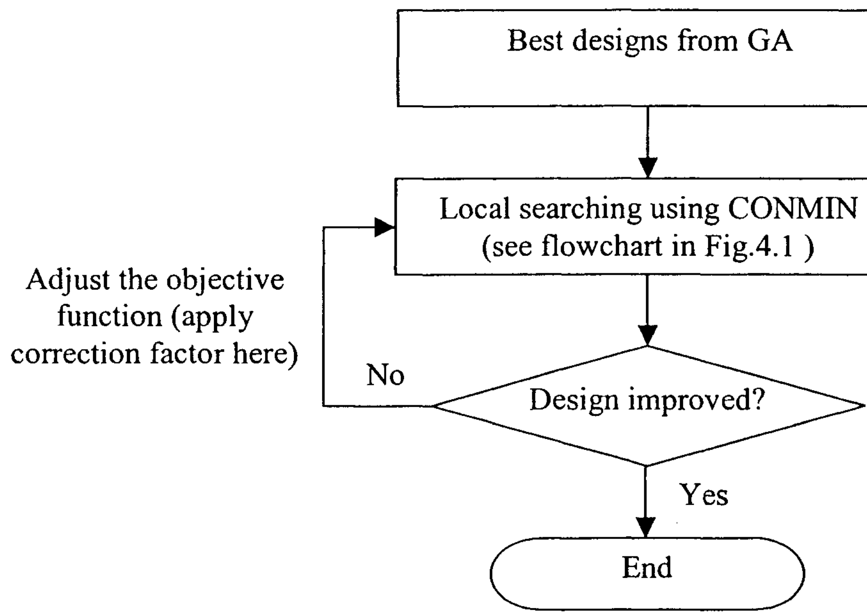

Fig.6.2: Flowchart of the second search phase with correction factor

The main reason for the success of the second algorithm is that lies in its local search ability. Since the values for the variables are always chosen around the best point determined in the previous iteration, there is a more likelihood of convergence to the optimum solution. In contrast, GA spends most of the time competing between different hills, rather than improving the solution along a single hill that the optimal point locates.

6.3 Results

As defined in previous chapters, Canard #1 with the sequence $[0°/45°/-45°/90°]_s$ is assigned as the initial design. In order to evaluate the performance of automated hybridization process HYBRID, the computational study is performed here. The HYBRID was applied on the optimization problem. The optimal design of laminated composite canard has been provided. The performances of CONMIN, GA, and HYBRID have been compared and discussed.

6.3.1 Optimized design of laminated canard from HYBRID

Fig. 6.3 shows the convergence characteristic curve of a random HYBRID run which is referred to as run 1 in the following study. It can be seen that GA run as the first phase of the hybridization and stopped at generation 34 when a stable optimum field has been obtained. Then the best design of this global optimum field was fed to CONMIN as its initial estimate. CONMIN took over the process from this global or near-global optima provided by GA. After 5 iterations of gradient-based local search, a further improved design was achieved. It also demonstrates the effectiveness of CONMIN in fine local tuning. The optimum solution is achieved within 300 more iterations.

5 independent runs of HYBRID were conducted in order to prove the consistency in getting optimal solutions. The results of the 5 random runs are shown in Table 6.4. It can be observed that the optimums from HYBRID are quite consistent. Run 1 and 5 obtained the same results which show better performance than other designs. Initially the best designs of GA were not improved after the local search in run 2 and 4. Thus the 0.5% correction factor was applied. Then the thicknesses were reduced from 0.0423 m to 0.0420 m and 0.0421 m respectively. Table 6.4 indicates that the local search using CONMIN in the second phase did improve the near-global design from GA. The weight in each run has been reduced with adequate stiffness. Instead of running GA through 100 more generations to obtain the similar level improvement, running of CONMIN provides great computation efficiency.

In the present discussion, the best result from run 1 with the final optimized stacking sequence of $[-19.6°/-67.7°/-20.9°/-57.1°]_s$ is selected as the representative optimum from HYBRID and will be compared with other designs in the following sections.

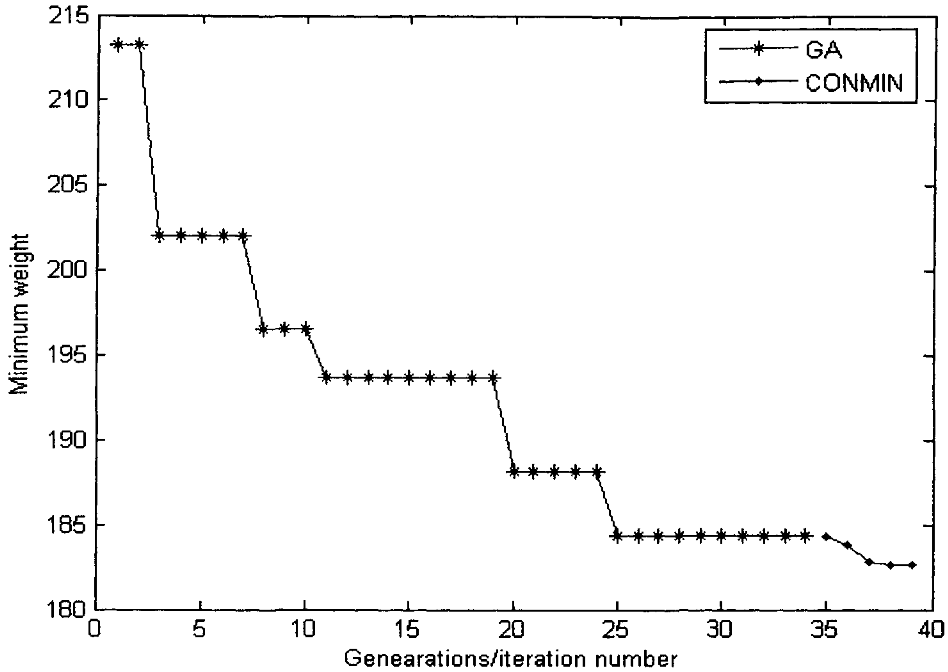

Fig. 6.3: Convergence tendency of HYBRID

Table 6.4: Results of 5 runs of HYBRID

	Best thickness of 1^{st} phase (m)	Best thickness of 2^{nd} phase (m)	Deflection of 1^{st} phase (m)	Deflection of 2^{nd} phase (m)	Weight reduction in 2^{nd} phase	Deflection reduction in 2^{nd} phase
Run 1	0.0423	0.04193	-0.1373	-0.1411	0.87%	-2.8%
Run 2	0.0423	0.04200	-0.1406	-0.1474	0.71%	-4.8%
Run 3	0.0423	0.04200	-0.1499	-0.1416	0.71%	5.5%
Run 4	0.0423	0.04210	-0.1489	-0.1496	0.47%	-0.47%
Run 5	0.0423	0.04193	-0.1373	-0.1411	0.87%	-2.8%

Table 6.4: (Continued)

	Starting stacking sequence of CONMIN	Final optimized stacking sequence
Run 1	$[-20.2°/-67.7°/-20.9°/-57.1°]_s$	$[-19.6°/-67.7°/-20.9°/-57.1°]_s$
Run 2	$[-18.4°/79.6°/-29.3°/-52.6°]_s$	$[-20.2°/-67.7°/-20.9°/-57.1°]_s$
Run 3	$[-19.5°/-83.8°/-15.9°/-50.0°]_s$	$[-21.9°/-82.8°/-16.4°/-49.7°]_s$
Run 4	$[-20.5°/-37.8°/-76.5°/-67.3°]$	$[-20.5°/-37.8°/-76.5°/-67.3°]_s$
Run 5	$[-20.2°/-67.7°/-20.9°/-57.1°]_s$	$[-19.6°/-67.7°/-20.9°/-57.1°]_s$

Table 6.5 summarizes the mechanical performance of the optimum design. The weight of the optimized design from HYBRID is 182.58 Kg, which is reduced by 16.2% compared to the initial design of Canard #1. The maximum displacement at the free end decreased significantly from 0.1827 m to 0.1479 m by 29.5%.

Table 6.5: Comparisons of optimal design from HYBRID and the initial design of Canard #1

Solution method	Weight (Kg)	Deflection (m)	Weight reduction	Deflection increment
Canard #1	217.87	0.1827	----	----
HYBRID	182.58	0.1411	16.2%	29.5%

Table 6.5: (Continued)

Solution method	Thickness (m)	$\theta_1(°)$	$\theta_2(°)$	$\theta_3(°)$	$\theta_4(°)$	$\theta_5(°)$	$\theta_6(°)$	$\theta_7(°)$	$\theta_8(°)$
Canard #1	0.05	0	45	-45	90	90	-45	45	0
HYBRID	0.0419	-19.6	-67.7	-20.9	-57.1	-57.1	-20.9	-67.7	-19.6

By substituting those optimal ply angles back into FEMCOMP program, the stress distributions of this optimized canard are obtained. The comparisons of the resulting maximum transverse stresses σ_{yz} and σ_{xz} to initial design are provided in Table 6.6. It shows that the maximum transverse stress σ_{yz} significantly reduced but the maximum σ_{xz} increased.

Table 6.6: Comparisons of maximum σ_{yz} and σ_{xz} of optimal design and initial design of Canard #1

	Maximum σ_{yz} (MPa)	Maximum σ_{xz} (MPa)
Canard #1	3523.0	111.8
Optimized design	2040.8	558.4

Fig.6.4 presents the contour plots of the transverse shear stresses distributions inside the composite canard. Both of the peak stresses occurred at the fixed end.

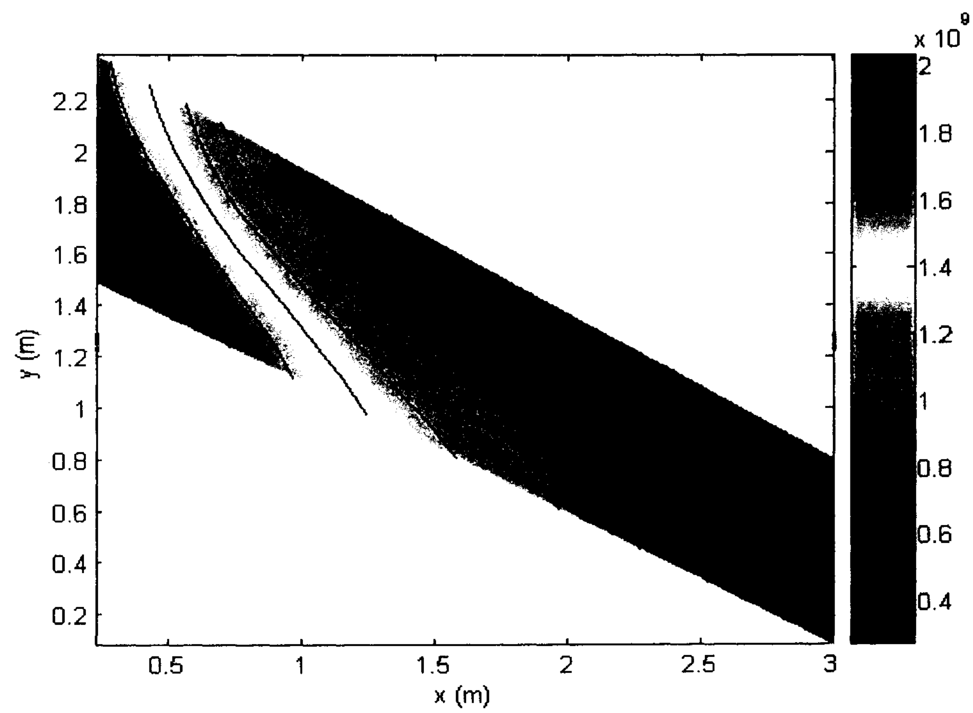

(a) Transverse shear stress σ_{yz} (Pa)

Fig. 6.4: Contour plots of stresses for constrained optimized design

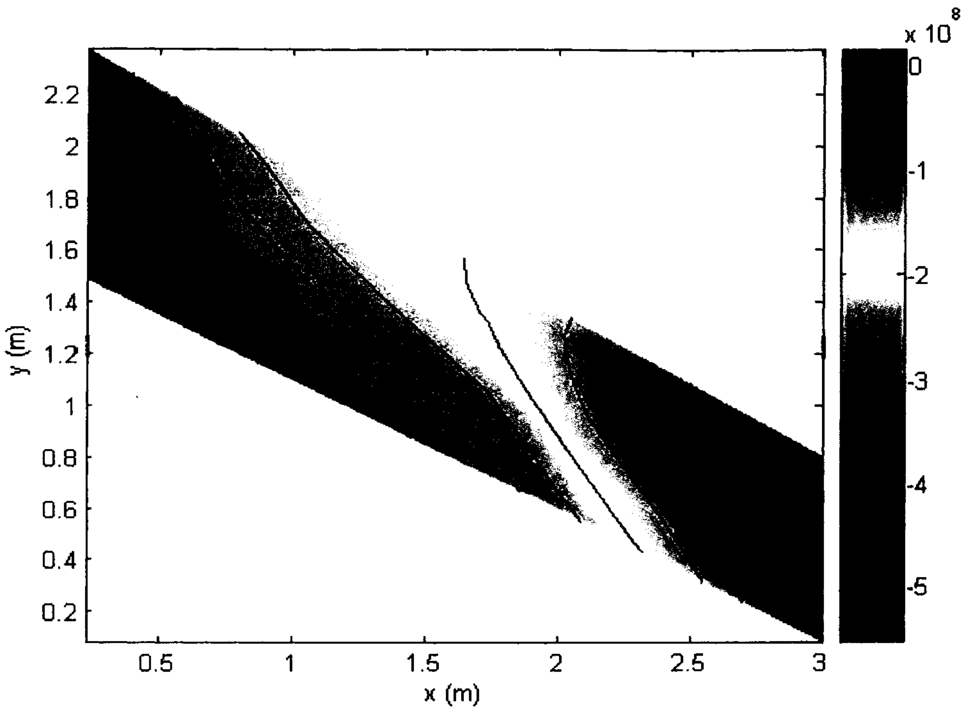

(b) Transverse shear stress σ_{xz} (Pa)

Fig. 6.4: (Continued)

6.3.2 Comparison of CONMIN, GA, and HYBRID

The optimum results from CONMIN (including two results from different starting points), GA, and HYBRID are listed in Table 6.7. Based on the comparisons of the optimum designs, it is very clear that GA and HYBRID were able to reach the best solutions but gradient-based optimizer CONMIN failed to provide global optimum result. The use of gradient-based CONMIN is very sensitive to the choice of the initial estimate and may lead to a convergence failure. However, it can be observed that CONMIN has much better computational efficiency than heuristic optimization technique GA. The latter spends most of the time competing between different hills, rather than improving the solution along a single hill that the optimal point locates and thus has difficulty in fine local searching.

Table 6.7: Comparisons of optimal results of CONMIN, GA, and HYBRID

Solution method	Weight (Kg)	Deflection (m)	Stacking sequence	Cmpt. time (hr.)
CONMIN (1)	216.13	0.15	$[-31.4°/74.1°/-58.8°/90°]_s$	0.2
CONMIN (2)	195.03	0.1488	$[-42.2°/-6.4°/45.2°/90°]_s$	0.5
GA	184.32	0.1373	$[-20.2°/-67.7°/-20.9°/-57.1°]_s$	20~25
HYBRID	182.58	0.1411	$[-19.6°/-67.7°/-20.9°/-57.1°]_s$	10~15

Even though the gradient-based searching technique CONMIN is not able to reach the global optimum alone due to its characteristic drawback, CONMIN plays an important role in the hybridization process. One of the major contributions of CONMIN is to significantly accelerate the optimization procedure based on the best solution field provided by GA. And also, CONMIN provides a clear convergence criterion which helps to reach a certain design optima instead of a best solution field.

Next, the discussion about the computational study will be focused on the performances of GA and the hybridized GA – HYBRID. Table 6.8 lists the results of a random run of GA from previous chapter. It demonstrates that the fitness values obtained after generation 25 are unchanged, which means that there is no significant improvement in the solution vector even after spending very large amount of computation time. This table also shows the difficulty faced by the GA in fine local search. GA spends most of the time competing between different hills, rather that improving the solution along a single hill that the optimal point locates.

Fig. 6.5 shows the convergence tendencies of CONMIN (index '1' means that the search starts from the design of Canard #1; index '2' means that the search starts from the design of 'Canard #2'), GA (a random GA run whose running size has been extended to 80 generations), and HYBRID.

Table 6.8: Results of first 50 generations of GA

Generation number	Best fitness value	Thickness (m)	Deflection (m)
1~2	212.44	0.0494	0.1163
3~7	201.25	0.0468	0.1221
8~10	195.49	0.0455	0.1493
11~19	192.79	0.0448	0.1365
20~24	187.19	0.0435	0.1414
25~50	181.64	0.0423	0.1373

It can be observed very clearly that gradient-based optimizer CONMIN is capable to reach an optimum design rather quickly but there is no guarantee on that attained design is global optimized. The convergence curves of CONMIN (1) and (2) also show that the initial estimate has huge influence on gradient-based search method. CONMIN (2), which started from a better performing point, was able to find much further improved optima than CONMIN (1). The starting guess is a basic point to guarantee the success of the optimization procedure. The use of a gradient-based optimization is very sensitive to the choice of the initial guess and may often lead to a convergence failure. To increase the chances to succeed, gradient based algorithms usually are executed for a number of different starting points.

In order to compare the performances of those optimization methods clearly, GA process shown in Fig. 6.5 has been extended to 80 generations. The convergence tendency shows that the non-gradient based optimizer GA allows to perform the optimum search in a zone of design space significantly larger than the gradient-based optimization case which provides the possibility to find the global or near-global optimum, but this is unaffordable at a computational cost. GA provided a much better improved solution field compared to CONMIN. However, the optimum designs have not been upgraded since generation 24 which demonstrates the inefficiency of the standard GA in the fine tuning. It can be concluded that if GA is employed for the entire search, there would be a mere wastage of computation time without any change in fitness function value. The other drawback of GA is that GA is only capable to provide a best design field but not a converged design because of its ambiguity in the definition of convergence criterion.

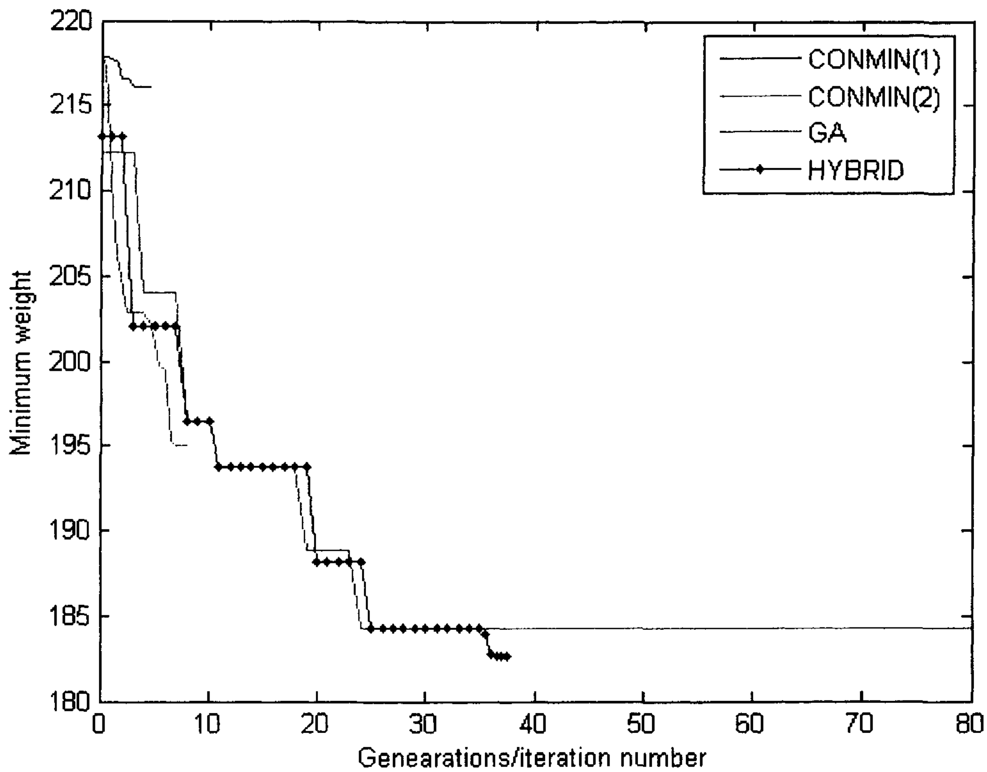

Fig. 6.5: Convergence tendencies of CONMIN, GA , and HYBRID

The discussion on the performances of CONMIN and GA indicates that a reasonable compromise is to use an optimization algorithm, which explores large fractions of design space but also uses gradient information in order to speed up the design process. The effectiveness of automated hybridization process HYBRID in obtaining global optimum with relatively low computational cost compared to standard GA has been demonstrated in Fig. 6.5. A further improved design based on the global optimum searching field provided by GA has been achieved by CONMIN. HYBRID has obtained a compromise between the computational expense and the accuracy of the solution. In HYBRID, the good characteristics of gradient-based method (efficiency, exactness) and global search methods (global optimum, robustness) are combined.

Conclusions

1. An automated hybridization process HYBRID has been implemented so that a single run of the algorithm will give a global optimum in most cases irrespective of the characteristics of the optimization methods. The outcome of the study clearly demonstrates the effectiveness, exactness, and robustness that a hybridized genetic algorithm HYBRID can obtain over a GA or CONMIN alone. To evaluate the performance of HYBRID, the comparison of the performances of gradient-based optimizer CONMIN, standard GA, and HYBRID has been made.
2. A global optimized design of laminated composite canard has been obtained from HYBRID. The comparisons of the mechanical performances of the optimal designs from CONMIN, GA, and HYBRID have been conducted.

CHAPTER 7 MORPHING DESIGN

Morphing wings are adaptable to the fluid flow around them structurally and geometrically, thereby changing the wing structural parameters in order to provide the best performance under any flight conditions. Adaptive wings use induced light weight strain actuators to change aerodynamic shape instead of using heavy hydraulic systems. Wing morphing can increases the payloads and flight range. Some researchers have started applying the morphing design on adaptive composite structures. They modeled the composite laminate with embedded piezoelectric actuator/sensor patches and developed corresponding finite element models [54, 55]. Most of the works have focused on the aspects of dynamic structural performance. However, the mechanical energy requirement which severely affects the performance of the adaptive structure also need to be considered carefully. Besides, the high mechanical energy losses have huge influence on the delamination of the composite laminate structure.

Thus, the primary objective of the present study is to reduce the energy requirement which affect the performance of the adaptive structure by minimizing the strain energy produced in the deformed adaptive canard based on the optimized model obtained in Chapter 6. The gradient-based optimizer CONMIN is used to optimize the design of composite canard further.

7.1 Introduction to adaptive structures

Many aerospace engineers are exploring innovative technologies that will determine the future of flight, which may have the capability to respond to changes in speed or environmental conditions by altering or morphing their shape. Structures using distributed induced sensors and strain actuators through closed loop control systems to change shapes are termed adaptive/smart structures. For example, adaptive aircraft wing have the capability to respond to vibration reduction, flutter suppression, and gust alleviation by altering the system characteristics (stiffness and/or damping) as well as the system response (strain or shape) in a controlled manner.

7.1.1 Adaptive structures

An adaptive structure involves distributed actuators and sensors and one or more microprocessors that analyze the responses from the sensors and use integrated control theory to command the actuators to apply localized strains/displacements to alter system response [37]. It has the capability to respond to a changing external environment as well as to a changing internal environment. Applications of adaptive structures to aerospace systems are expanding rapidly. An adaptive structural system includes four key elements: actuators, sensors, control strategies, and power conditioning electronics. Sensors convert strain or displacement into an electric field; actuators undergo the deflections when electric field is applied; microprocessors analyze the responses from the sensors and command the actuators to apply localized strains/displacements to alter system responses. The working principle of adaptive structures is shown in Fig. 7.1.

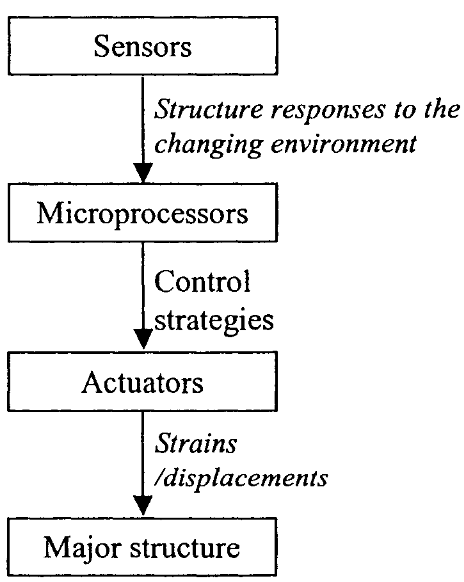

Fig. 7.1: Working procedure of adaptive structures

Numerous applications of adaptive structures technology to aerospace system are evolving, such as aeroelactic stability, stress distribution, and shape control of large flexible wing structures. For instance, embedded or surface mounted smart actuators on an airplane wing or a helicopter blade can induce airfoil twist/camber change that in turn causes a variation of lift distribution and can help to control static and dynamic aeroelastic problems.

7.1.2 Smart material actuators

Smart materials describe a group of material compounds with unique properties. These properties usually relate to a large strain deformation when the smart material is subjected to electrical/thermal/magnetic fields, which allows changing the shape of wing in flight.

Smart materials which deform under an electric field are termed piezoelectric. Piezoelectrics are the most popular smart materials which can deform in both compression or elongation. They undergo strain/deformation to when an electric field is applied across them, and conversely produce voltage when strain is applied. Hence, piezoelectric can be used both as actuators and sensors. Piezoelectric materials are relatively linear and bipolar, but exhibit hysteretic. The most widely used piezoceramics are in the form of thin sheets. These sheets generate isotropic strains on the surface and a non-Poisson strain across the thickness. They can be readily bonded or embedded in composite materials and work as sensors or actuators for high performance structural applications.

In a piezoelectric material, when an electric field is applied, the dipoles of the material try to orient themselves along the field causing strain in the material. When the piezoelement is exposed to a high electric field or large strain produced, piezoelectric actuator loses its piezoelectric property, accompanied by more dielectric losses and lower efficiency, which results in a permanent deformation. At high vibration frequencies, energy from mechanical losses can generate large self-heating that can severely affect the performance of the actuator and losing its characteristic behavior.

The total strain in the actuator is assumed to be the sum of the mechanical strain caused by the stress and the induced strain caused by the electric field. The strain in the host structure is obtained by establishing the displacement compatibility between the host material and the actuator. The induced strain is treated like thermal strain.

7.1.3 Laminated composite panel with induced actuators

The adaptive composite structures have enhanced the possibility of carring out shape control, vibration isolation and control, and noise reduction as described in [38]. Laminated composite plate with induced actuators is one of the basic elements of adaptive structures. Sheet actuators are embedded or bonded to composite laminate for the high performance structural applications. With a laminated plate, induced strain actuation can control its extension, bending, and twisting. Composite plate with distributed induced strain actuators can be used to change aerodynamic shape for vibration reduction, flutter suppression, and gust alleviation. As an example, a laminated composite plate with two rows of surface-mounted actuators on both top and bottom surface is shown in Fig. 7.2.

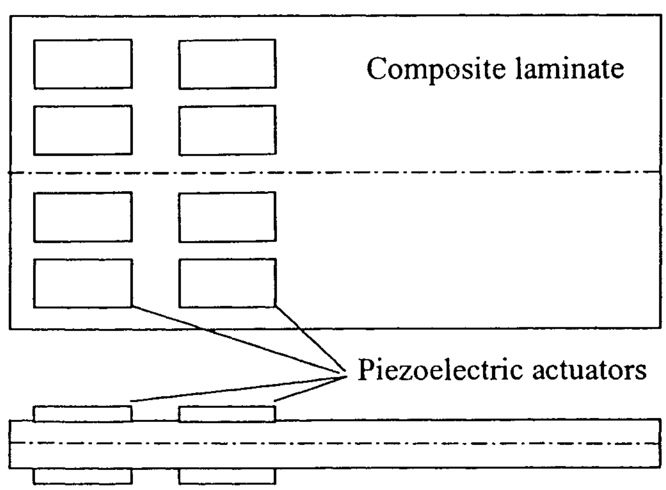

Fig. 7.2: Laminated composite plate with surface-mounted piezoelectric actuators

Efficient computational tools are needed to represent and predict the behavior of laminated composite panel with induced actuators. Several plate theories have been developed to predict flexural response of laminated plates with surface-bonded or embedded induced strain actuators, such as CLPT, FSDT, and High order shear deformable Theory

(HSDT). All of these theories assume that the actuators and substrate are integrated as plies of a laminated panel undergoing consistent deformation. FSDT has been applied to the previous structural analysis and will be used here as the modeling theory. FSDT is based on the Reissner-Mindlin plate model and is quite similar to Timoshenko's beam theory. Transverse shear strains are assumed uniform through the thickness of the plate. Shear correction factors are applied to compensate for nonzero shear strain at free lateral surfaces.

7.1.4 Strain and Strain energy of laminated composite panel with induced actuators

The total strain in the actuator is assumed to be the sum of the mechanical strain caused by the stress and the induced strain caused by the electric field, $\varepsilon = \varepsilon_{mechanical} + \varepsilon_{induced}$. The strain in the host structure is obtained by establishing the displacement compatibility between the host material and the actuator.

Chopra [37] defined the strain energy of the adaptive system as following,

$$U = \frac{1}{2}\iint_A \begin{Bmatrix} \varepsilon^{0T} & \kappa^T \end{Bmatrix} \begin{bmatrix} A & B \\ C & D \end{bmatrix} \begin{Bmatrix} \varepsilon^0 \\ \kappa \end{Bmatrix} dA - \iint_A \begin{bmatrix} N_\Lambda & M_\Lambda \end{bmatrix} \begin{Bmatrix} \varepsilon^0 \\ \kappa \end{Bmatrix} dA \tag{7.1}$$

where N_Λ and M_Λ are the actuator forces and moments; ε^0 is the midplane strain and κ is the bending curvature of composite panel.

Strain energy of the host structure is shown as,

$$U = \frac{1}{2}\int_{vol} (\sigma_{xx}\varepsilon_{xx} + \sigma_{yy}\varepsilon_{yy} + \sigma_{xy}\varepsilon_{xy} + \sigma_{xz}\varepsilon_{xz} + \sigma_{yz}\varepsilon_{yz}) dvol \tag{7.2}$$

Since the strain energy from mechanical losses can generated enough 'self-heating' that can severely affect the performance of the actuator, the energy reduction becomes a major issue. On the other hand, minimization of the strain energy also helps avoid the delamination of the composite laminate structure.

7.2 Formulation of morphing design

The composite canard with lighter weight and higher stiffness has been achieved in structural optimizations. This morphing design will be carried out based on the results from the previous optimizations in order to obtain the advanced composite canard with high structural efficiency and maneuverability. The optimized variables from the Chapter 6 will be imported to the morphing design as initial values.

7.2.1 Development of design model

In this study, the laminated composite canard with surface-induced and embedded piezoelectric sheet actuators which can control its extension, bending, and twisting, is taken as the multi-functional adaptive structure. It can sense and adapt to their environment and self-repair when damaged.

This morphing design mainly focused on the improvement of the structural maneuverability. In order to achieve the advanced composite canard design, the morphing design is performed based on the structural optimization and the host structure is defined as the design model. Therefore, the functionalities of the actuators are not included in the modeling of the adaptive composite structure. The energy reduction of the host structure is considered as the objective of the morphing optimization. The minimization of the strain energy of the composite canard helps to reduce the 'self-heating' which can severely affect the performance of the actuator. And also, delamination of the composite structure due to high mechanical energy losses could be avoided.

Since the morphing design is performed based on the optimized structural design, thickness of the composite panel is kept the same and the ply orientations are adjusted to minimize the strain energy of the host structure.

The statement of this morphing design is declared as following

- *Objective function*

  Minimize the strain energy of the host composite structure, U

- *Design variables*

  Ply orientations, θ_i, $-90^\circ \le \theta_i \le 90^\circ$, $i = 1,2,3,4$

- *Design parameters*

  Geometric dimensions, design loading

- *Design constraint*

Deflection of the free end, $\|d\| \le d_{opt}$, where $d_{opt} = 0.15m$

where, d_{opt} is the maximum displacement of the optimal design from the study in Chapter 6. The weight of the canard is unchanged and the stiffness might be improved while the strain energy is reduced .

7.2.2 Software implementation

Since the good structural characteristics need to be kept in the advance composite canard design, the optimizer CONMIN is applied on the minimization design due to its good capability on local search. According to the requirements of the morphing design, the optimizing objective is defined as the strain energy instead of weight and ply angles are modified to obtain the optimum. Figure 7.3 gives the flow chart of the procedure of morphing design. The composite panel with optimized structural efficiency is imported as the initial design. CONMIN starts from this point and keep updating the ply angles. FEMCOMP is used to evaluate the strain energy and the mechanical performance of the composite canard. The optimum is achieved once the terminate condition is satisfied.

7.3 Results

This morphing design mainly focused on the improvement of the maneuverability of a laminated composite canard which has very good structural efficiency. In order to achieve the advance composite canard design, the morphing design is performed only on the host structure, the composite laminated canard which has been optimized in Chapter 6 and has high structural efficiency. Gradient-based optimizer CONMIN was employed to carry out the optimization on maneuverability. The laminated composite design with stacking sequence $[-19.6° / -67.7° / -20.9° / -57.1°]_s$ and optimized thickness, 0.04193 m is taken as the starting point of CONMIN.

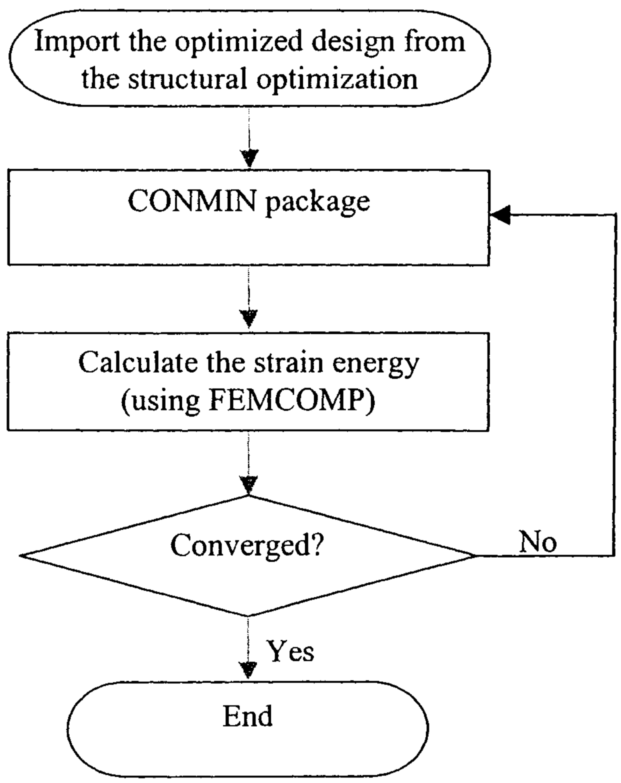

Fig. 7.3: Flow chart of the minimization of strain energy.

Table 7.1 lists the results of morphing design. A laminated composite panel with stacking sequence $[-19.2°/-67.6°/-20.8°/-57.2°]_s$ was obtained, which is considered as the advanced design of the laminated canard with high structural efficiency and improved maneuverability. Compared to the structural efficient design from HYBRID, the maximum deflection of the advanced design has been reduced to 0.1356 m which means the stiffness of the laminated canard has been improved and correspondingly the strain energy of the host structure has been reduced by 10.7%. The stacking sequence of the advanced design has only been modified slightly. However, the slight rearrangement on the ply angles has huge effect on the reduction of strain energy. It indicates that the adaptive laminated composite structures have enhanced the possibility to carry out the morphing performance due to its special characteristic feature that laminate is stronger in fiber direction. Laminated composite offers excellent design flexibilities.

Table 7.1: Results of morphing design

	Strain Energy (J)	Deflection (m)	Strain energy reduction
HYBRID	1.673×10^{7}	-0.1411	–
Morphing	1.494×10^{7}	-0.1356	10.7%

Table 7.1: (Continued)

	Stacking Sequence
HYBRID	$[-19.6°/-67.7°/-20.9°/-57.1°]_s$
Morphing	$[-19.2°/-67.6°/-20.8°/-57.2°]_s$

Fig. 7.3 gives the contour plots of the strain energy of structural optimized design from previous chapter and the design with improved maneuverability. It can be observed that the large strain energy occurred inside the elements close to the fixed end. The distributions of the strain energy are unchanged. The reduction of strain energy of the host structure helps eliminate the mechanical energy loss, reduce the self-heating and assure the performance of the embedded or bonded actuators/sensors.

Table 7.2 shows the comparison of the transverse shear stresses between the structurally optimized design and the advanced design. Both of the maximum shear stresses have been reduced so that the resulting strain energy was reduced too.

Table 7.2: Comparisons of maximum σ_{yz} and σ_{xz} from HYBRID and morphing design

	Maximum σ_{yz} (MPa)	Maximum σ_{xz} (MPa)
HYBRID	2040.8	558.4
Morphing	1914.9	522.6

Fig. 7.4 provides the contour plots of the transverse shear stresses σ_{yz} and σ_{xz}. Both of the maximum transverse stresses occurred at the fixed end.

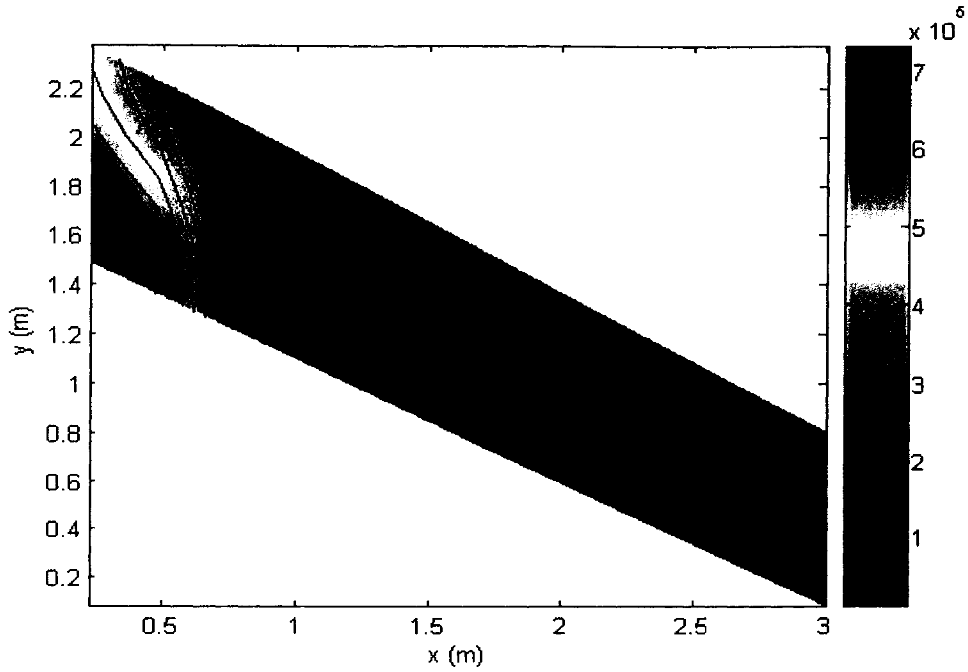

(a) Strain energy of structural optimized design from HYBRID

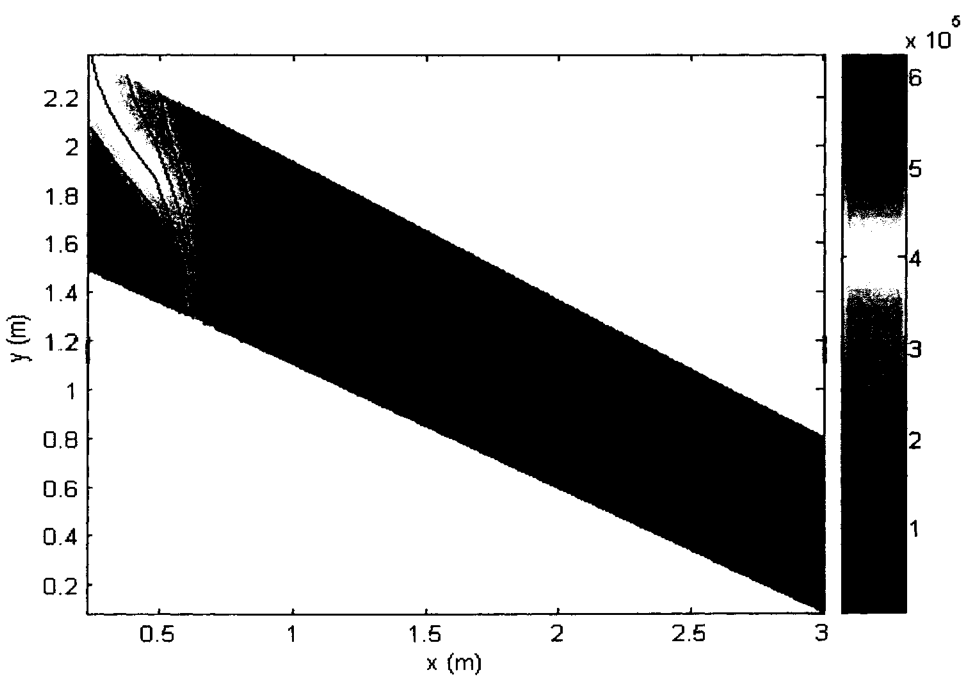

(b) Stain energy of the advanced design

Fig. 7.3: Contour plots of strain energy

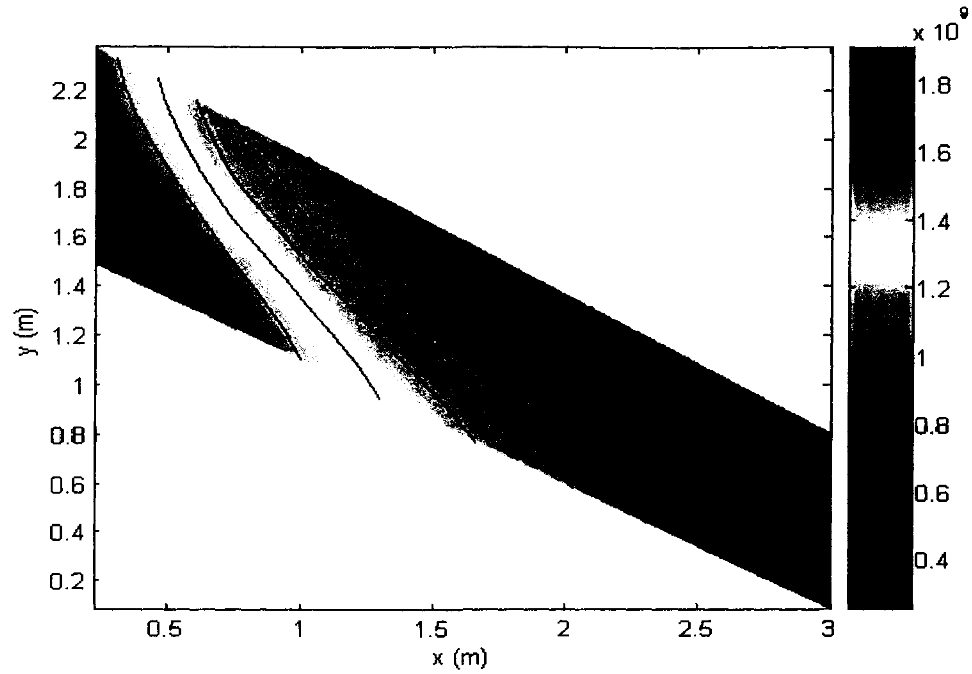

(a) Transverse shear stress σ_{yz} (Pa)

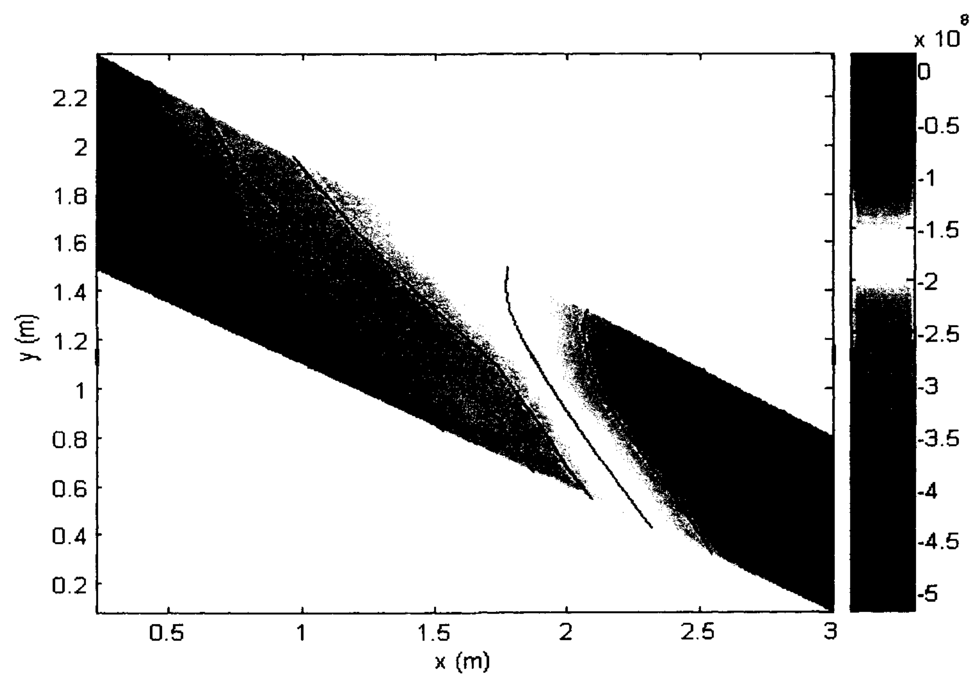

(b) Shear stress σ_{xz} (Pa)

Fig. 7.4: Contour plots of stresses of optimized design

Conclusions

1. An advanced laminated composite design with high structural efficiency and good maneuverability has been obtained by the gradient-based search. The strain energy of the host structure has been reduced significantly which helps eliminate the mechanical energy loss and assure the performance of the embedded or bonded actuators/sensors.
2. The improved mechanical performance of the advanced design indicates that the adaptive laminated composite structures enhance the possibility of achieving a multi-functional structure for high performance structural applications.

CHAPTER 8 CONCLUSIONS

Mechanical performance of a composite canard subject to static aerodynamic loads was numerically studied. The canard was modeled as a symmetrically laminated curved panel consisting of 8 plies of T300/5208 graphite/epoxy composite laminae. The modeling of this structure-fluid interaction system involves the coupling of two formulations: the solid classically treated in FEM formulation, and the fluid described by potential panel method in CFD. The coupling between the structure and flow requires taking into account the changes of aerodynamic forces due to the deflection of the loaded canard. The structural deflections and stresses caused by the aerodynamics loads were calculated through a FEM procedure. The finite element model of the canard was updated after each aerodynamic analysis to include the changes in pressure loads acting on the structural surface. Then the changes of the nodal deflections were taken into account when the aerodynamics loads were recalculated. Structural deformations and resulting distributed loads were repeatedly calculated till equilibrium between deformation and load was achieved.

A Fortran 90 program FEMCOMP which was implemented based on FEM, FSDT, CFD potential flow method, and the Mechanics of Laminated Composites, was employed to carry out the numerical study. A structure-fluid iterative loop was included to simulate the relationship between the deformed aircraft wing and aerodynamic load which is one of the attractions of this present study when calculating the loads on the panel. A suitable failure criterion was applied at the end of each structural analysis to maintain the appropriate margin of safe.

It can be observed from the results of the structural analysis that the values of the transverse shear stress components are significantly larger than in-plane stress components. The effects of thickness and stacking sequence on the laminated panel stiffness were also studied. Generally speaking, it was found that the ply orientation had marked influence on the mechanical behaviors of the composite laminates which indicates the great possibility to optimize the laminated composite structures.

After the basic structural analysis on the composite laminated canard, a few optimization approaches have been attempted to improve the existing design. Composite laminated canard was chosen as the subject of the present research on the optimization due to its excellent design flexibilities with respect to ply angles and layer thickness. Three numerical optimization techniques incorporated with FEMCOMP, which served as the evaluator of the objective function, were performed respectively. Since the ply orientation and thickness have a significant effect on the performance of the laminated composite canard, various design objectives can be achieved just by selecting the proper arrangement of ply orientation and thickness. The weight of the canard was considered as the objective function with respect to the ply orientations and plate thickness. This structural optimization aims at achieving the best structural performance and material efficiency while satisfying certain constraints.

Firstly, the gradient-based optimizer CONMIN was applied on the optimization problem to achieve the optimal designs of the laminated canard. Optimized designs were achieved in the gradient-based search and both the weight and the stiffness of the canard were improved by adjusting the ply angles and the thickness. The influence of the starting point on CONMIN has also been studied. Two initial estimates were taken as the starting points for CONMIN. The mechanical performances of the optima from those two starting points were hugely different. It demonstrated that CONMIN was capable of reaching an optimum design very quickly which is one of the greatest advantages of gradient based algorithms. However gradient-based optimization techniques get stuck in local optima easily, especially if the problem has a non-smooth and/or non-convex design space. It can be concluded that the gradient-based algorithms provide local optimum values only and these values depend on the selection of the starting point. To increase the chances of success, gradient-based algorithms usually are executed for a number of different starting points.

Compared to gradient-based optimization, non-gradient-based optimizers usually allow performing the optimum search in a zone of design space significantly larger than in the gradient-based optimization case. To obtain the global or near-global optimums, non-gradient-based technique GA in conjunction with Fortran 90 program FEMCOMP was applied on this layout optimization problem for the laminated composite panel as a global optimizer. An optimal design has been obtained which has much better mechanical performance than the initial design and even the optimal designs obtained from CONMIN. The weight of this design was reduced by 15.4% and the out-of-plane deflection decreased by 24.8%. Despite the broad applications and superior searching abilities, GA has not demonstrated itself to be very efficient. In the convergence procedure of GA, initially the solution quality was improved very quickly. But then it was very difficult to obtain further improvement soon. GA is generally time-consuming because it needs much trial and huge search space. The use of GA doesn't guarantee convergence to global optima because of its poor exploitation capabilities and lack of a good convergence criterion.

The discussion on the performances of CONMIN and GA indicates that a reasonable compromise is to use an optimization algorithm, which explores large fractions of design space but uses also gradient information in order to speed up the design process. An automated hybridization process HYBRID has been implemented so that a single run of the algorithm gives a global optimum in most cases irrespective of the characteristics of the optimization methods. In HYBRID, the global search uses the exact analysis in which all redundant iterative loops are omitted and the gradient-based search only focuses on the reduced design space containing the optimum as obtained from the global search. A further improved design of laminated composite canard based on the global optimum search field provided by GA has been obtained from HYBRID in relatively low computational cost compared to standard GA. Compared to the initial design, the weight of the canard was dropped by 16.2% and the stiffness improved by 29.5%. The outcome of the study showed that the hybridization process has obtained a compromise between the computational expense and the accuracy of the solution over a GA or CONMIN along. The good characteristics of gradient-based method (efficiency, exactness) and global search methods (global optimum, robustness) are combined in HYBRID.

The optimized design of composite canard with lighter weight and higher stiffness has been achieved in the structural optimization. In order to obtain the advanced composite canard with high structural efficiency and maneuverability, a morphing design was performed on the structurally efficient composite panel which is the host structure of the adaptive composite laminated canard. The gradient-based optimizer CONMIN was used to slightly modify the structural optimized design. The strain energy reduction of the host structure was considered as the objective function of the morphing optimization in the present work. An advanced design of composite canard with high structural efficiency and good maneuverability has been obtained by adjusting the ply angles. The strain energy of the host structure was reduced by 10.7% which helps reduce the mechanical energy loss and assure the performance of the embedded or bonded actuators/sensors. The improved mechanical performance of the advanced design indicates that the adaptive laminated composite structures enhance the possibility of achieving a multi-functional structure for high performance structural applications.

In conclusion, this dissertation studied the design problem on a composite canard in an integrated structure-fluid phenomenon. The mechanical performances of various designs have been analyzed. The structural analysis indicated the huge possibility to perform the optimization design on the laminated canard. The characteristic features of gradient-based optimization method CONMIN and non-gradient-based GA have been compared to evaluate the proposal of a hybridization process. The major contribution of this work is the development of an automated numerical hybridization optimization process HYBRID, which specially deals with the structure-fluid phenomenon and composite aircraft wing design. Finally, an advanced composite canard design with high structural efficiency and excellent maneuverability has been obtained from the structural optimization and morphing design.

BIBLIOGRAPHY

1. Taylor J. W., *Jane's all the world's aircraft 1988-89*, Jane's Information Group Limited, Coulsdon, UK, 1988

2. Beckert A., *Coupling fluid (CFD) and structural (FE) models using finite interpolation elements*, Aerospace Science and Technology, 4:13-22, 2000

3. Girodroux-Lavigne P., Grisval J.P., Guillemot S., Henshaw M., Karlsson A., Selmin V., Smith J., Teupootahiti E., Winzell B., *Comparison of static and dynamic fluid-structure interaction solutions in the case of a highly flexible modern transport aircraft wing*, Aerospace Science and Technology, 7: 121-33, 2003

4. Zienkiewicz O. C., *The finite element method*, 3^{rd}, Tata McGraw-Hill Publishing Company, London, UK, 1977

5. Reddy J. N., Krishnamoorthy C. S., Seetharamu K. N., *Finite element analysis for engineering design*, Springer-Verlag, Berlin, Germany, 1988

6. Rao S. S., *The finite element method in engineering*, 2^{nd}, Pergamon Press, New York, NY, 1989

7. Reddy J.N., *Mechanics of laminated composite plates and shells*, 2^{nd}, CRC Press, Florida, 2004

8. Tsai S.W., Hahn, H. T., *Introduction to composite materials*, Technomic Publishing Company, Lancaster, PA, 1980

9. Gibson R. F., *Principles of composite material mechanics*, McGraw-Hill, New York, NY, 1994

10. Halpin J. C., *Primer on composite material: analysis*, Technomic Publishing Company, Lancaster, PA, 1984

11. Reddy J.N., *Energy and variational methods in applied mechanics*, John Wiley & Sons, Inc., New York, 1984

12. Rolfes R., Noack J., Taeschner M., *High performance 3D-analysis of thermo-mechanically loaded composite structures*, Composite Structures, 46: 367-79, 1999

13. Ferreira A.J.M., Roque C.M.C., Martins P.A.L.S., *Radial basis functions and higher-order shear deformation theories in the analysis of laminated composite beams and plates*, Composite Structures, 66:287-93, 2004

14. Rolfes R., Rohwer K., Ballerstaedt M., *Efficient linear transverse normal stress analysis of layered composite plates,* Computers and Structures, 68:643-52, 1998

15. Noor A.K., Burton W.S., *Assessment of shear deformation theories for multilayered composite plates,* Applied Mechanics Review, 42:1-12, 1989

16. Pagano N.J., *Exact solution for rectangular bidirectional composites and sandwich plates*, Journal of Composite Materials, 4:931-3, 1970

17. Kim C.W., Hwang W., Park H.C., Han K.S., *Stacking sequence optimization of laminated plates*, Composite Structures, 39:283-8, 1997

18. Kam T.Y., Chang R.R., *Optimum layup of thick laminated composite plates for maximum stiffness*, Engineering Optimization, 19:237-49, 1992

19. Kim T-U., Sin H-C., *Optimal design of composite laminated plates with the discreteness in ply angles and uncertainty in material properties considered*, Computers and Structures, 79:2501-09, 2001

20. Vanderplaats G. N., *Numerical optimization techniques for engineering design with applications*, McGraw-Hill Book Company, New York, NY, 1984.

21. Vanderplaats G. N., *CONMIN- A Fortran program for constrained function minimization*, NASA TM X-62, 282, 1973

22. Michalewicz Z., *Genetic Algorithms + Data Structures = Evolution Programs, third edition,* Springer, New York, US, 1996

23. Holland J.H., *Adaptation in natural and artificial system*, the University of Michigan Press, Ann Arbor, MI, 1976

24. Goldberg D.E., *Genetic algorithms in search, optimization, and machine learning*, Addison-Wesley, Reading, MA, 1989

25. Le Riche R., Haftka R.T., *Optimization of laminate stacking sequence for Buckling load maximization by Genetic Algorithm*, AIAA Journal, 31(5):951-56, 1993

26. Le Riche R., Haftka R.T., *Improved genetic algorithm for minimum thickness composite laminate design*, Proceedings of International Conf. on Composite Engineering, New Orleans, LA, 1994

27. Muc A., Gurba W., *Genetic algorithms and finite element analysis in optimization of composite structures*, Composite Structures, 54:275-81, 2001

28. McMahon M.T., Watson L.T., Soremekun G.A., Gurdal Z., Haftka, R.T., *A Fortran 90 Genetic algorithm module for composite laminate structure design*, Engineering with Computers, 14:260-73, 1998

29. Gen M., Cheng R., *Genetic algorithms and engineering design*, John Wiley & Sons, INC., New York, US, 1997

30. Davis L., *A hand book of genetic algorithms*, New York, 1990

31. Chelouah R., Siarry P., *A continuous genetic algorithm designed for the global optimization of multimodal functions*, Journal of Heuristics, 6:191-213, 2000

32. Kim J-H, Myung H., *Evolutionary programming techniques for constrained optimization problems*, IEEE Trans Evolution Computation, 1(2):129-40, 1997

33. Baskar S., Subbaraj P., Rao M.V.C., *Hybrid real coded genetic algorithm solution to economic dispatch problem*, Computers and Electrical Engineering, 29:407-19, 2003

34. Lin C-C., Lee Y-J., *Stacking sequence optimization of laminated composite structures using genetic algorithm with local improvement*, Composite Structures, 63: 339-45, 2004

35. Chelouah R., Siarry P., *Genetic and Nelder-Mead algorithm hybridized for a more accurate global optimization of continuous multiminima functions*, European Journal of Operational Research, 148:335-48, 2003

36. Wlezien R.W., Horner G.C., McGowan A.R., Padula S.L., Scott M.A., Silcox R.J., Simpson J.O., *The aircraft morphing program*, AIAA-98-1927, 1998

37. Chopra I., *Review of state of art of smart structures and integrated system*, AIAA Journal, 40(11), 2002

38. Crawley E.F., de Luis J., *Use of piezoelectric actuators as elements of intelligent structures*, AIAA Journal, 25(10):1373-85, 1987

39. Saravanos D.A., *Mixed laminated theory and finite element for smart poezolectric composite shell structures*, AIAA Journal, 35(8):1327-33, 1997

40. Kulkarni S.A., Bajoria KM., *Finite elment modeling of smart plates/shells using higher order shear deformation theory*, Composite Structures, 62:41-50, 2003

41. Dano M.L., Hyer M.W., *SMA-induced snap-through of unsymmetric fiber-reinforced composite laminates,* International Journal of Solids and Structures, 40:5949-72, 2003

42. Chaudhuri R.A., *Analysis of laminated shear-flexible angle-ply plates,* Composite Structures, 67:71-84, 2005

43. Gurdal Z., Haftka R. T., Hajela P., *Design and optimization of laminated composite materials*, John Wiley & Sons, INC., New York, US, 1999

44. Yang G., Reinstein L.E., Pai S., Xu Z., Carroll D.L., *A new genetic algorithm technique in optimization of permanent 125-I prostate implants*, Medical Physics, 25(12):2308-15, 1998

45. Carroll D.L., *Chemical laser modeling with genetic algorithms*, AIAA Journal, 34(2):338-46, 1996

46. Carroll D.L., *Genetic algorithms and optimizing chemical oxygen-Iodine lasers*, Developments in Theoretical and Applied Mechanics, XVIII:411-24, 1996

47. Lee Y.H., Lee M.H., *A shape based block layout approach to facility layout problems using hybrid genetic algorithm*, Computers and Industrial Engineering, 42:237-48, 2002

48. Chen R.S., Lu K.Y., Yu S.C., *A hybrid genetic algorithm approach on multi-objective of assembly planning problem*, Engineering Applications of Artificial Intelligence, 15:447-57, 2002

49. Wang H.F, Wu K.Y., *Hybrid genetic algorithm for optimization problems with permutation property*, Computers and Operation Research, 30:2175-89, 2003

50. Park T.Y., Gilbert F.F., *A hybrid genetic algorithm for the estimation of parameters in detailed kinetics models*, Computers and Chemical Engineering, 22:S103-10, 1998

51. Kigoso N., Watson L.T., Gurdal Z., Haftka R.T., *Genetic algorithms with local improvement for composite laminate design*, Structure Optimization, 7:207-18, 1994

52. Seront G., Bersini H., *A new GA-local search hybrid for optimization based on multi level single linkage clustering*, Genetic and Evolutionary Computation Conference (GeCCO-2000), Las Vegas, NV, 2000

53. Gantovnik V.B., Anderson-Cook C.M., Gurdal Z., Watson, L.T., *A genetic algorithm with memory for mixed discrete-continuous design optimization*, Computers and Structures, 81:2003-9, 2003

54. Pinto Correia I.F., Mota Soares C.M., Mota Soares C.A., Herskovits J., *Analysis of adaptive shell structures using a refined laminated model,* Composite Structures, 66:261-68, 2004

55. Pletner B., Abramovich H., *Consistent methodology for the modeling of piezolaminated shells,* AIAA Journal, 35(8):1316-26, 1997

ACKNOWLEDGEMENTS

Acknowledgements go out to all who have helped to make the completion of this thesis possible. I would like to thank my major professor, Dr. Vinay Dayal, for his guidance, patience, support, and contributions to my personal and professional growth. I am greatful to Dr. Jerry Vogel for providing all possible help in the study of aerodynamics. I am thankful to Dr. Thomas McDaniel, Dr. James Bernard, and Dr. Adrian Sannier for their invaluable advice. Their gifts as teachers have been immense.

Special thanks and appreciation go out to my parents and my family for their supports and understanding. My gratitude also goes to my fiancé, Mr. Dmitry Yarushkin, for his love and support. Finally, I would like to thank all my dear friends for their friendships and supports.